Ministry of Higher Education and Scientific Research

Hassiba Benbouali University of Chlef
Faculty of Technology
Process Engineering Department

Thesis

Presented for graduation from

MASTER 2

Field: Process Engineering

Option: Pharmaceutical Process Engineering

Theme :

Computational investigation of natural products against P2XR, P2X7 and cullin neddylation NEDD8 processing as potential multi-target Inhibitors.

Presented by: Meziane Hassiba
Dahmane Rahima

In front of the jury composed of:

Mr. DJAFER Abd el rahmane	Professor	University of Chlef	President
Mr. BENDRISS Houari	MAA	University of Chlef	Examiner
Mr. OTMANINE Khaled	MCB	University of Chlef	Supervisor

Academic year: 2023-2024

Gratitude

Above all, we would like to thank the almighty Allah for giving us the courage, the will and the patience to complete this work.

Our heartfelt thanks and our deep gratitude goes to our supervisor ***OTMANINE KHALED****, his invaluable advice and help throughout the work period. For the orientation, the confidence of the patience* ***Dr.HAMOUDI MOUNIR*** *his requirement and his encouragement, by sharing his experience and his scientific knowledge with us, during the realization of this thesis*

We address our warm and sincere thanks to the members of the jury for having done us the honor of evaluating this modest work

Finally, we thank all those who have helped us from near or far, that they find here all our sympathy and our deep gratitude

Dedication

First of all I want to thank Allah the Almighty for giving me health, patience, will and for giving me his blessing

I dedicate this work to the closest to my heart

To my dear parents ***Abd el kader*** *and* ***Ben sehaila Houria****, to whom I owe this pride and who have supported me and helped me a lot*

To my sisters: ***Fatim****,* ***Hafidha****,* ***Soumia****,* ***Marwa***

To My brother-in-law ***Zidani Hadi*** *for the support and the help*

For all my friends without exceptions ***Ber909****a,* ***Narimane****,* ***Charifa, kawther***

To my colleagues who shared this journey with her difficulties and joys ***Rahima, Douaa, Ikram, Hanaa***

Last but not least

"I want to thank me for believing in me, I want to thank me for doing all this hard work. I wanna thank me for having no days off. I wanna thank me for never quitting. I wanna thank me for always being a giver and trying to give more than I receive. I wanna thank me for trying to do more right than wrong. I wanna thank me for being me at all times.

Meziane Hassiba

Dedication

First of all I want to thank Allah the Almighty for giving me health, patience, will and for giving me his blessing

I dedicate this work to the closest to my heart

To my dear parents ***A'mhammed*** *and* ***fatima****, to whom I owe this pride and who have supported me and helped me a lot*

To my sisters : ***Fati*** *and* ***Djimi*** *and my brothers and my sisters-in-law without forgetting all my cute nieces and nephews.*

My partner: ***Meziane hassiba*** *for her understanding and sincerity in difficult times throughout this project.*

For all my friends who shared me this journey

Ikram,Douaa,Hana,cherifa

God bless you all.

Dahmane Rahima

Abstract

Alzheimer's disease and Esophageal cancer are among the most common diseases in the world. Treating these two diseases by targeting two specific proteins using molecules from different plants will be a promising potential process. The object of this study is to inhibit the P2X7 receptor and NEDD8 protein which are responsible for these two diseases respectively. After screening of more than **20** plants original from chlef State, Algeria. We selected the *Salvia officinalis, Trigonella foenum-graecum* and *Phoenix dactylifera L* seeds. The ethanolic extracts of Sage have the best inhibitory activity against *Staphylococcu saurous* ATCC6538 (Gram positive) with D=19mm. All the plants have antioxidant activity: $IC_{50(sage)}$=0.191mg/ml , $IC_{50(Fenugreek)}$=0.143mg/ml, $IC_{50(dateseed)}$=0.193mg/ml .GC-MS analysis indicated several components in extracts. The study conducted a pharmacoinformatics analysis “in silico” of **6** compounds from 75 bioactive compounds. In silico studies reveal that the inhibitor ligand Tricin interacts with NAE1, forming 9 amino acid bonds with ΔG = -7.8 kcal/mol and 7,4’-Dihydroxyflavone interacts with P2X7 forming 7 amino acid bonds with ΔG = -6.8 kcal/mol . We finished our work with a new formulation which is Emulsuspension.

Key words: Alzheimer's disease, Esophageal cancer, P2X7, NEDD8, pharmacoinformatics, Emulsuspension

الملخص :

الزهايمر و سرطان المرئ من بين أكثر الأمراض شيوعاً في العالم. و علاج هذين المرضين باستهداف بروتينين محددين باستخدام جزيئات من نباتات مختلفة عملية محتملة واعدة.الهدف من هذه الدراسة هو تثبيط مستقبل P2X7 وبروتينNEDD8 المسؤول عن هذين المرضين على التوالي, بعد فحص أكثر من 20 نبتة اصلية من ولاية الشلف, الجزائر قمنا باختيار الحلبة، والمريمية، و نواة التمر. المستخلصات الإيثانولية لنبتة المريمية لديها أفضل نشاط مانع ضد *Staphylococcu saurous* ATCC6538بقطر 19 ملم . اثبتت الدراسة ان جميع النباتات لديها نشاط مضاد للأكسدة بقيم $IC_{50(sage)}$=0.191mg/ml $IC_{50(Fenugreek)}$=0.143mg/ml, $IC_{50(dateseed)}$=0.193mg/ml. وبيّن تحليل قياس الطيف الكتلي للكروماتوغرافيا الغازية أن هناك عدة مركبات في المستخلصات. وأجرت الدراسة المعلوماتية الصيدلانية في "ان سيليكو" لستة مركبات من اصل 75 مركباً حيويا من هذه النبتات . في دراسات ان سيليكو اثبتت أن هناك تلاحم مثبط لمركب Tricin مع NAE1 مشكلا 9 روابط لاحماض امنية بطاقة ترابط تقدر ΔG = -7.8 kcal/mol . اما مركب7,4’-Dihydroxyflavone فقد تفاعل مع بروتين P2X7 مشكلا روابط ب 7 احماض امنية و بطاقة ترابط تقدر ب ΔG = -6.8 kcal/mol. أنهينا عملنا بصيغة دواء جديدة وهي Emulsuspension.

الكلمات المفتاحية:مرض الزهايمر, سرطان المرىء ,NEDD8, P2X7, المعلوماتية الصيدلانية

Sommary

Table list

Table list

Figure list

Figure list

Figures list

Abbreviation list

P2X7: Purinergic receptor

NEDD8: Neural precursor cell expressed developmentally down-regulated protein 8

CULS: Cullin protein

CRLS: Cullin ring E3 ligases

NAE1: NEDD8 activating enzyme E1

AD: Alzheimer disease

EC: Esophageal cancer

R: Yeild

UV: Ultraviolet radiation

LogP: Water/octanol partition coefficient

3D: Three dimension

2D: Two dimension

A^0: Angstrom

ADME: Absorption distribution metabolism excertion

PDBQT: Protein data bank partial charge atom type format

MD: Molecular docking

HA: Hydrogen acceptor

HD: Hydrogen donor

SDF: Spatial data file

Abs: Absorption

pH: Potential hydrogen

IC50: Inhibitory concentration

DPPH: 2, 2-Diphel-1-picrylhydrazul

General Introduction

Introduction

Herbal medical products are those made from the study or application of medicinal herbs with the purpose of preventing, treating, or enhancing health and healing. Plants are the source of these chemicals, which have multiple applications such as treating and preventing illnesses **[1].**Natural goods are becoming more widely acknowledged in the realm of human health as beneficial supportive medicines for ailments like cancer, neurological illnesses, and cardiovascular disease **[2].**

Alzheimer's disease (AD) is the most common neurodegenerative disease affecting the elderly and the primary cause of dementia **[2].** Research has indicated that the P2X7 receptor regulates the neuroinflammation linked to Alzheimer's disease, suggesting a possible treatment approach to address the condition. **[3]**

Esophageal cancer is a significant global health concern, with squamous cell carcinoma (SCC) and adenocarcinoma (AC) being the two main histologic types. While SCC is more prevalent worldwide, the incidence of AC has risen in Western countries due to factors like obesity and gastro-esophageal reflux disease. **[4]** This cancer that develops in the esophagus, which is the tube that connects the throat to the stomach. It is a significant health concern globally, with high mortality rates and limited treatment options. **[5]**

The P2X7 is a transmembrane receptor that was first expressed by lymphocytes and macrophages, among other immune system cell types. Researchers subsequently showed that P2X7R was extensively distributed in a variety of tissues, organs, and neuronal cells. **[6]** Recent studies have revealed that the central nervous system's (CNS) microglial cells are the primary source of P2X7R expression. **[7].**

The P2X7 receptor is implicated in Alzheimer's disease through its involvement in chronic neuroinflammation, which can contribute to neurodegeneration **[8]**

Developmentally downregulated protein 8, or NEDD8, is expressed by neural precursor cells and is essential for several biological functions **[9].** Moreover, NEDD8 participates in neddylation, a process in which it conjugates to target proteins, influencing pathways for antigen presentation and protein degradation **[10] [11].** Targeting NEDD8 in cancer treatment offers therapeutic potential, as demonstrated by the encouraging anti-tumor effects observed in multiple myeloma models when NEDD8-activating enzymes are inhibited **[12].**

Salvia officinalis, commonly known as *sage*, has shown promising potential in the treatment of Alzheimer's disease and esophageal cancer. Research has highlighted the neurobiological

effects of *Salvia officinalis* on the central nervous system, indicating its role in memory enhancement, neuroprotection, and anti-addictive properties **[13].**

Fenugreek shows promising potential in the management of Alzheimer's disease (AD) due to its neuroprotective properties. Studies have demonstrated that *fenugreek seed* extract can improve memory, reduce depression, enhance quality of life, and regulate blood pressure in AD patients and protect against this disease**.[14]**

Date palm seeds have been extensively studied for their nutritional value and potential health benefits, including cytotoxic properties against cancer cells. **[15]**

In the first part of our work we will study the proteins P2X7 and NEDD8, their structure , activation and the diseases caused by their hyperactivation. We have focused on the Alzheimer disease and Esophageal cancer, finished with the medicinal herbs to treat this two diseases by the inhibition of this receptors.

In the second part we will see in vitro the evaluation Antioxidant and antibacterial activities of bioactive compounds of plants "*Sage*", "*Fenugreek*" and "*Date seeds*", Extracted using a polarizing solvent (ethanol)Various microbiological and technical methods were used during this search. In silico study will prove the interaction between the molecules selected and the targets.

In this study we use AI and Pharmacoinformatics as new process in phytochemicals screening leading to the development and discovering of new drugs.Any process lead to development or discovering of drugs is pharmaceutical process engineering.

General introduction

1-Critical review

After studying many scientific articles on the receptors related to our research, we noticed that there is a lack of commercial drugs that treat Alzheimer's disease (AD) and esophageal cancer (EC) by direct inhibition of the **P2X7** and **NEDD8** receptors.

In addition, there are no studies that develop drugs using molecules extracted from medicinal plants to inhibit the studied receptors **[16]**. Moreover, some articles did not use in silico studies to support the results obtained **[17].** In our research, we studied these proteins and their inhibition using molecules extracted from medicinal herbs.

We also did in silico to find out how much the molecules inhibit the proteins. We have also developed a drug from the medicinal herbs fenugreek, sage and date seeds to treat Alzheimer's disease and esophageal cancer by inhibiting these receptors.

2-Problematic

By inhibiting the **NEDD8** and **P2X7** proteins, can we completely cure esophageal cancer and Alzheimer's disease, or just prevent them, or minimize their side effects? Does artificial intelligence succeed in minimizing the reliance on Experimental side?

3-Purpose

This research primarily aims to treat Alzheimer's disease and prevent esophageal cancer using medicinal plants indigenous to Chlef, Algeria, using Pharmacoinformatics and Artificial Intelligence.

What is new in the research is the initiative to adopt a completely new technique that has never been used before: the development of a 2-in-1 biomedical product to treat two intractable diseases at the same time, by using the principle of selectively targeting and inhibiting proteins on the surface of diseased cells that have malfunctioned and caused the transmission of pathogenic cellular signals, resulting in the achievement of a strategic medical goal, such as Alzheimer's disease. This results in a strategic medical goal of significantly reducing treatment costs and minimizing the serious side effects caused by the consumption of several drugs at the same time, which may lead to the development of other, more complex diseases.

Bibliographic Study

1. Introduction

Receptors have become the central focus of investigation of drug effects and their mechanisms of action (pharmacodynamics). The receptor concept, extended to endocrinology, immunology, and molecular biology, has proved essential for explaining many aspects of biologic regulation. Many drug receptors have been isolated and characterized in detail, thus opening the way to precise understanding of the molecular basis of drug action. **[1]**

Medicinal plants are herbs used in medicine for the treatment of several diseases thanks to their richness in bioactive compounds. They are used in the prevention and treatment of diseases to reduce the use of chemical components. **[2]**

We will discuss the importance of the proteins under investigation in this section of the study, as well as how abnormal activity, or hyperactivity of proteins, might negatively impact the human health. We will also talk about one of the most significant illnesses caused by each protein's hyperactivity and the medicinal herbs which inhibit it.

2. Proteins

2.1. P2X7 receptor

2.1.1. Structure and activation

The P2x receptor family comprises ligand-gated, calcium-permeable cationic channels that are extensively distributed. They are exclusively triggered by extracellular adenosine triphosphate (ATP) within the body**.[2]** The activation of P2X receptors, which are ligand-gated ion channels in the plasma membrane, results in the selective inflow of minor cations (Na+, Ca2+), as well as the outflow of K+ from cells**.[3]**

The seventh receptor in this family P2X7 is a transmembrane receptor (see fig 1) that was first expressed by lymphocytes and macrophages, among other immune system cell types. Researchers subsequently showed that P2X7R was extensively distributed in a variety of tissues, organs, and neuronal cells**. [4]** Recent studies have revealed that the central nervous system's (CNS) microglial cells are the primary source of P2X7R expression**. [5]**

The largest monomeric component for the receptors found in humans, rats, mice, dogs, and is P2X7, which has a length of 595 amino acids**.[6]** Each subunit is distinguished by two hydrophobic membrane-spanning segments (transmembrane domains) separated by a long glycosylated extracellular ATP-binding domain, and by comparatively short and long

intracellular amino and carboxyl (C) termini, respectively. Atomic computer simulation supports the trimeric architectures of the P2X7 receptors in humans**. [7]**

Small cations, such as Ca2+, Na+, **[8]** and K+, can flow through the plasma membrane when P2X7 is activated by extracellular ATP. Nonetheless, in certain cellular lineages, prolonged activation of P2X7R by high ATP concentrations may result in necrosis or death. **[9]**

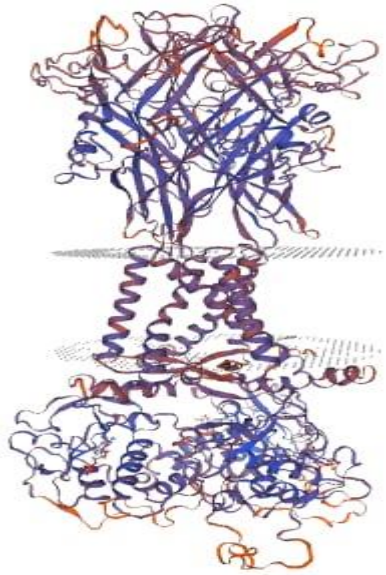

Figure 1: Structure of P2X7 receptor **[10]**

During inflammation, tissue damage, or T-cell activation occur, significant amounts of extracellular nucleotides are produced, activating P2X7 receptors (P2X7R), which are ligand-gated, non-selective cation channels (see fig 2). **[11] [12]** and are widely expressed in immune cells, especially those that belong to the myeloid lineage**. [13]** P2X7Rs have primarily been found in glial cells in the central nervous system, and opinions on P2X7Rs' expression in neurons are divided **[14].** P2X7Rs are activated by ATP and control the oxidation of nitric oxide derivatives and the synthesis and release of inflammatory mediators such PGE2, TNFα, and IL-1β **[15]** [**16].** P2X7Rs have been suggested as therapeutic targets for a variety of inflammatory and neurological disorders **[13] [15] [17-19],** as well as for autism-like behavior in mice with maternal immunological activation, due to their proinflammatory action **[20–22].**

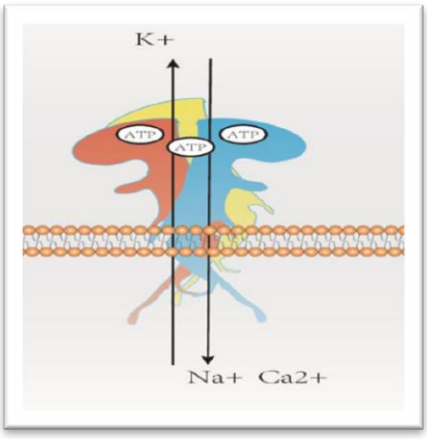

Figure 2: P2X7 Receptor: an Emerging Target in Alzheimer's disease**. [23]**

2.1.2. Distribution of the P2X7 Receptor

P2X7 is found abundantly in the body of mammals **[24].** The hematopoietic lineages, which comprise osteoclasts, mast cells, eosinophils, dendritic cells, monocytes, lymphocytes, and erythrocytes, were initially believed to be the only cell types that this receptor could be found in. Nevertheless, it is now clear that P2X7 is found on various lineages of cells, such as fibroblasts, osteoblasts, endothelial cells, and epithelial cells. Moreover, P2X7 is found on Schwann cells, oligodendrocytes, astrocytes, microglia, and other cells in the central and peripheral nervous systems **[25]**. Furthermore, P2X7 has been reported to be present on a few different neuronal populations, including those from the substantia nigra, cerebellum, spinal cord, and hypothalamus.

2.1.3. The P2X7 Receptor in Health and Disease

The altered expression and/or function of human P2X7 receptors has been related to pathologies including chronic pain conditions**[26][27],**osteoporosis and bone fracture **[28] [29],**rheumatoid arthritis **[30],** affective mood disorders**[31],[32],[33],** and cancers**[34]** including chronic lymphocytic leukaemia **[35],** Because of the connection to these debilitating diseases and the appeal of ion channels as pharmaceutical targets, these receptors have come under scrutiny as having potential for drug development. In vivo studies of P2X7 inhibitors in rodents have shown great promise, and pharmacological inhibition of this receptor has been demonstrated to attenuate neuropathic and inflammatory pain **[36],** reduce inflammation in models of rheumatoid arthritis **[37]** and to be neuroprotective and to significantly reduce the number of amyloid plaques in the brain in mice models of Alzheimer's disease**[38], [39].**

2.1.4 Alzheimer's disease

The most prevalent type of dementia in the senior population is Alzheimer's disease **[40] [41]**, which pose a significant public health risk. According to recent estimates, there are 50 million AD sufferers globally, and by 2050, there will be 132 million **[42].** Decades before the emergence of dementia symptoms, processes that cause AD can begin **[43] [44].** This emphasizes the significance of sensitive diagnostic techniques for more successful treatment approaches.

Alzheimer's disease, also called dementia (AD) is a neurological illness linked to age-related cognitive decline, particularly memory loss. Neurofibrillary lesions and amyloid plaques are found in the brain of AD patients, which results in synaptic impairments. After the amyloid precursor protein (APP) is sequentially proteolyzed by β and γ secretases, extracellular aggregates of β-amyloid (Aβ) peptides accumulate to form amyloid plaques. Unlike Aβ peptides, α-secretase-produced soluble fragment of APP (sAPPα) seems to have neurotrophic and neuroprotective qualities **[45].** Intraneuronal fibrillar aggregates of hyperphosphorylated and aberrantly phosphorylated Tau proteins are the basis of neurofibrillary lesions. Tau is a microtubule-associated protein that is essential for maintaining the microtubule network's stability and promoting material transfer across axons. According to Braak phases, the development of tau pathology in the brain coincides with cognitive deficits in AD patients **[46]**, indicating a crucial role in underlying synaptic dysfunctions (see fig 3).

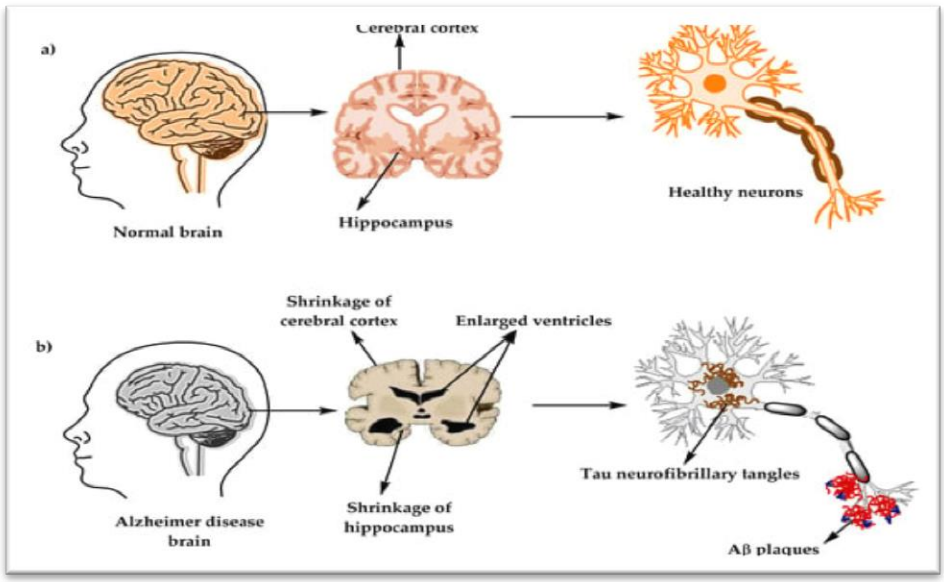

Figure 3: The physiological structure of the brain and neurons in (**a**) healthy brain and (**b**) Alzheimer's disease (AD) brain. **[47]**

2.1.5. The P2X7 Purinergic Receptor and AD

The P2X7 receptor is implicated in Alzheimer's disease through its involvement in chronic neuroinflammation, which can contribute to neurodegeneration (see fig 4). Studies have shown that the regulation of neuroinflammation associated with Alzheimer's disease by the P2X7 receptor may offer a potential therapeutic strategy to combat the disorder. Pharmacological blockade or knockout of the P2X7 receptor in Alzheimer's disease mouse models has demonstrated positive effects by reducing neuroinflammation. In vivo inhibition of the P2X7 receptor has been linked to attenuating inflammatory responses, diminishing blood-brain barrier leakiness, preventing spatial memory impairment, cognitive deficiency, microglial activation, and neuronal damage associated with Alzheimer's disease. Therefore, the P2X7 receptor's role in provoking Alzheimer's disease lies in its contribution to chronic neuroinflammation and subsequent neurodegenerative processes **[48]**

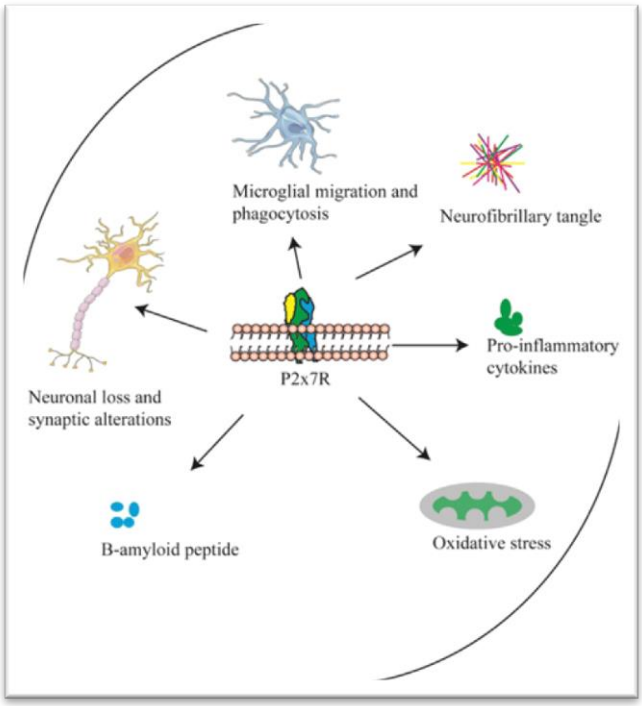

Figure 4: P2X7 Receptor: an Emerging Target in Alzheimer’s disease. **[48]**

This figure suggests that P2X7R is involved in different physiopathological processes in Alzheimer’s disease. As the figure demonstrates, P2X7R regulates the processing of amyloid APP, promotes Tau phosphorylation, and is also involved in synaptic changes, ROS, microglia activation, and promotes inflammatory factor release which are all processes that contribute to AD progression

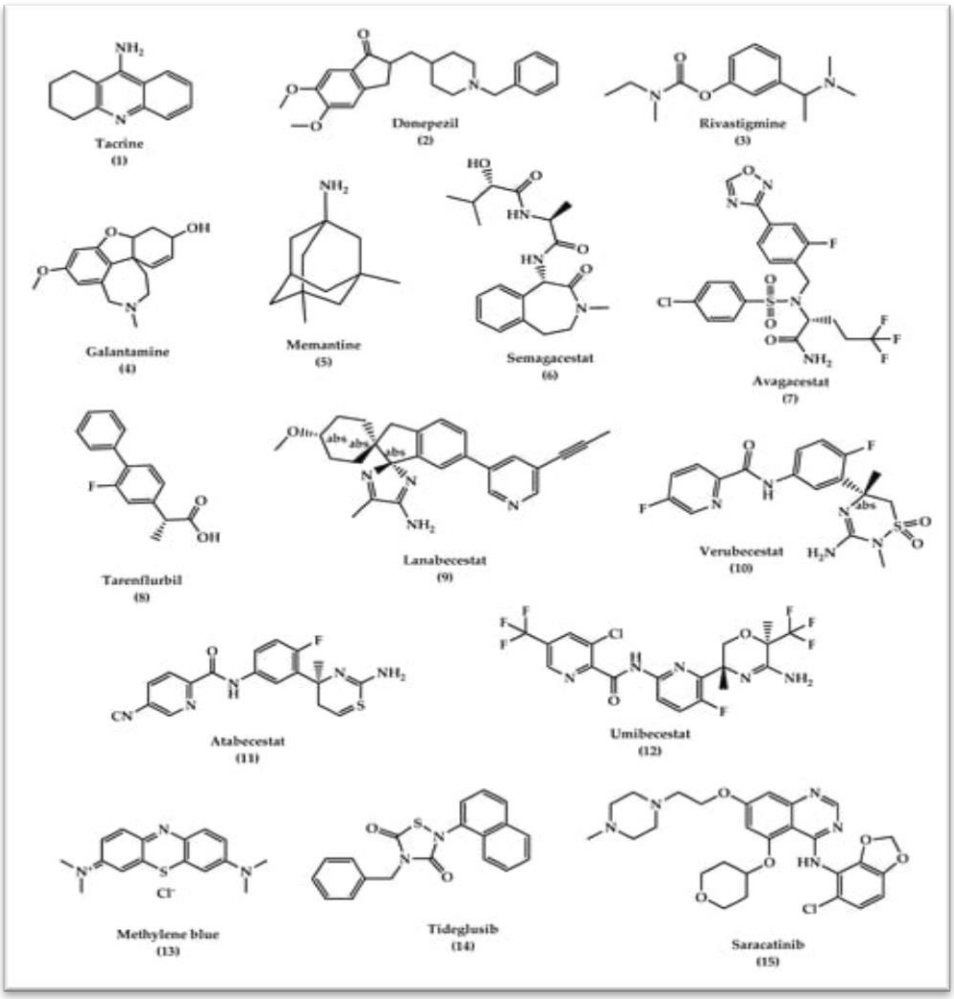

Figure 5: The chemical structures of approved drugs for symptomatic treatment of AD (tacrine 1, donepezil 2, rivastigmine 3, galantamine 4, and memantine 5) and disease-modifying compounds that entered clinical trials (semagacestat 6, avagacestat 7, tarenflurbil 8, lanabecestat 9, verubecestat 10, atabecestat 11, umibecestat 12, methylene blue 13, tideglusib 14, and saracatinibin 15). **[47]**

2.2. NEDD8 protein

2.2.1. Neddylation

Neddylation, a post-translational modification that adds an ubiquitin-like protein NEDD8 (neuronal precursor cell-expressed developmentally down-regulated protein 8) to substrate proteins, modulates many important biological processes. This process is a process of conjugating NEDD8, an ubiquitin-like molecule, to targeted protein substrates via enzymatic cascades involving NEDD8-activating enzyme E1, NEDD8-conjuagating enzyme E2 and substrate-specific NEDD8-E3 ligases **[48].** Neddylation is an important biochemical process that regulates protein function. The best-characterized substrates of neddylation are the cullin subunits of Cullin-RING ligases (CRLs). **[49]**

2.2.2. Cullin proteins (CULs)

Neddylation that involve ubiquitin is crucially impacted by cullin proteins, which act as molecular scaffolds. The cullin protein family of mammals includes eight members (cullin-1, cullin-2, cullin-3, cullin-4 A, cullin-4B, cullin-5, cullin-7, and the p53-associated parkin-like cytoplasmic protein (PARC)) each of which is identified by a cullin homology domain. **[50]** Cullins (CULs) are a core component of cullin-RING E3 ubiquitin ligases (CRLs), which regulate the degradation, function, and subcellular trafficking of proteins, CULs are post-translationally regulated through neddylation, a process that conjugates the ubiquitin-like modifier protein neural precursor cell expressed developmentally downregulated protein 8 (NEDD8) to target cullins **.[51]**

2.2.3. Cullin Neddylation:

Cullin neddylation is a critical post-translational modification that activates cullin- RING ligases (CRLs), the largest family of E3 ubiquitin ligases **[52]** .This process involves chemical bonding between the ubiquitin-like protein NEDD8 and a specific lysine residue on the cullin subunit of CRLs. **[53]**

2.2.4. Cullin-Ring E3 Ligases (CRLs)

The largest E3 superfamily consists of the multisubunit Cullin-RING ligases (CRLs). CRLs are nucleated by an extended cullin scaffold interacting with a catalytic RING- containing protein, either RBX1 or RBX2 **[54].** Structural studies revealed an overall common assembly for the best-studied cullins encoded by the human genome (CUL1, CUL2, CUL3, CUL4A, CUL4B, and CUL5), which form 300 distinct CRL complexes in different subfamilies (CRL1 containing CUL1, CRL2 containing CUL2, etc.) **[55].** Briefly, CRLs adopt an elongated architecture, with the substrate-binding site and E2-binding RING at opposite ends **[56].**

A cullin's N-terminal domain (NTD) binds a substrate receptor (SR) either directly or indirectly via an adaptor protein. Each cullin has its own large family of dedicated SRs, which bind a substrate's 'degron' motif. A cullin's C-terminal domain (CTD) binds the RBX RING protein. The RING domain recruits an E2ubiquitin intermediate, and promotes ubiquitin transfer from the E2 active site directly to the substrate associated with the SR. **[57, 58]**(see fig6).

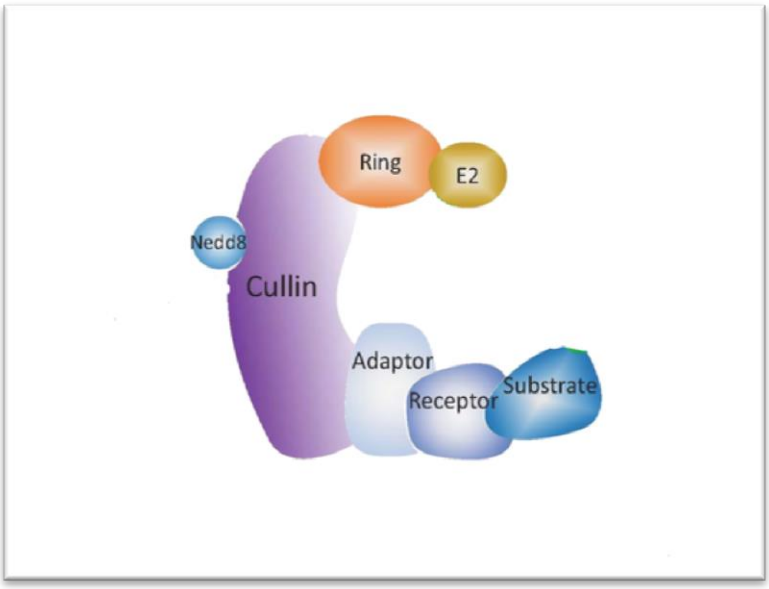

Figure 6: Structure of Cullin-Ring E3 Ligase **[59]**

2.2.5. The enzymatic cascade of Cullin Neddylation

The neddylation cascade begins with NEDD8 maturation. The reaction of mature NEDD8 synthesis is catalyzed by two enzymes ubiquitin C-terminal hydrolase isozyme 3 (UCHL3), and NEDD8-specifc protease 1 (NEDP1) also called human de-neddylase 1 (DEN1) or SUMO-1**[60]** .The C-terminal 5-amino acid residues of NEDD8 are removed by these enzymes to convert the precursor form into the mature form **[61].**The NEDD8 after becoming matured is activated by NAE, a heterodimer that comprises amyloid-β precursor protein- binding protein 1 (APPBP1) and ubiquitin-activating enzyme 3 (UBA3) **[62]** ,the activation of NEDD8 via NAE requires ATP and forms the NEDD8-AMP molecule before transferring NEDD8 to cysteine of NAE through the thioester bond. The NAE-NEDD8 complex then transfers NEDD8 to the E2 enzyme, which has two forms which are UBE2M and UBE2F, respectively **[63]** An interaction between NEDD8-charged NAE and its homologous E2s that promotes the production of NEDD8-E2 thioesters is responsible for the unique specificity of the NEDD8 pathway.

A combination of the ionic interactions and conformational flexibility of this specific hydrophobic interaction allows NAE to recognize its two distinct E2s and thus integrates further specificity concerning CRLs modification, as UBC12 and UBE2F have been found to neddylate different CRLs **[64]** .The last step includes the interaction of the E2 enzyme with the E3 enzyme to attach NEDD8 with the lysine residue of the substrate (CRLs) protein molecule **[65].** The shift of NEDD8 from UBC12 or UBE2F towards the relevant CRLs may need a ligase-like activity, including the five defectives in cullin neddylation 1 protein (DCN1) and similar proteins being hypothesized to operate as facilitators of particular cullin neddylation **[66**](see fig7)**.**

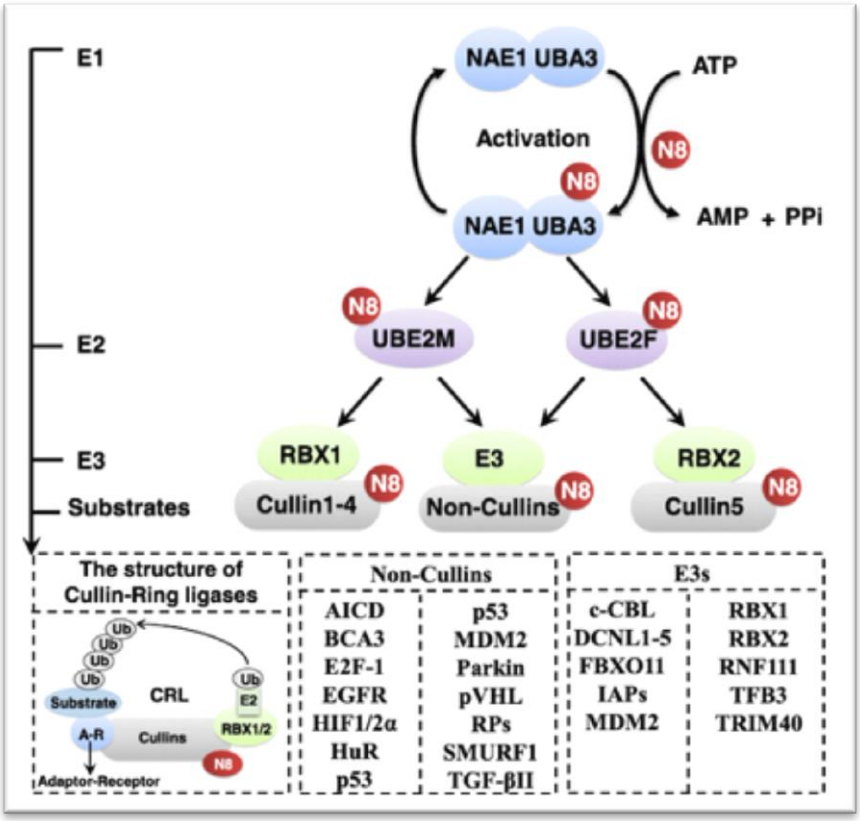

Figure 7: Cullin Neddylation enzymatic cascade. **[67]**

2.2.6. NEDD8 protein structure:

Neural precursor cell expressed developmentally down-regulated protein 8(NEDD8) is a Ubiquitin-like protein which plays an important role in cell cycle control and embryogenesis via its conjugation to a limited number of cellular proteins. **[68]** The NEDD8 is translated as 81 amino acid protein, which is almost 60% identical and 80% homologous to the ubiquitin molecule with 9 kDa molecular mass **[69],** it was first isolated from the mouse brain and then further research was carried out. Research suggests that the protein stability may be improved in certain cases by covalent modification using the NEDD8 enzyme **[70].**

The NEDD8 pathway relevance in cancer has been reported in several studies as described in the above section. The use of crystallography to study the NAE in complex with its substrates has provided crucial insights into critical protein–protein interactions as well as the catalytic mechanism of the E1 enzyme, which is responsible for the initial neddylation process, amongst other discoveries. **[71]**

Inhibition of the NEDD8-activating enzyme (NAE), the key E1 enzyme in the neddylation cascade, has been considered an attractive anticancer strategy with the discovery of the first-in-class NAE inhibitor, MLN 4924. **[72]**

2.2.7. NEDD8-activating enzyme E1 (NAE1)

NAE consists of catalytic subunit UBA3 (also known as NAEβ) and the regulatory subunit amyloid-beta precursor protein-binding protein 1 (APPBP1, also known as NAE1). **[73]** NAE activates NEDD8 to initiate neddylation process by recognizing the alanine 72 in NEDD8, **[74-75]** and continues the NEDD8 transfer cascade by activating the C-terminus of NEDD8 with diGly.(see figure 8) **[76]**

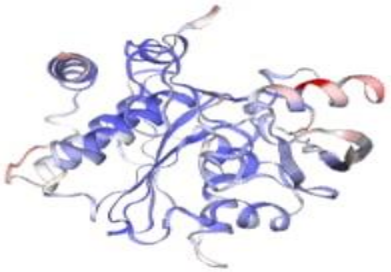

Figure 8: NEDD 8 –activating enzyme E1 structure

2.2.8. Neddylation in health and disease

The neddylation pathway is tightly regulated in order to maintain protein homeostasis and proper operation of various cellular processes. Dysregulation of neddylation or de- neddylation pathways is associated with several human diseases, including metabolic disorders,[**77]** liver dysfunction**,[78]** neurodegenerative disorders**,[79]**cardiac diseases, immune-related diseases**[80]** (see Fig 9), and most importantly, cancer (see Fig 10) **[81]** Targeting neddylation is, therefore, considered as a potential therapeutic approach for the treatment of these diseases.

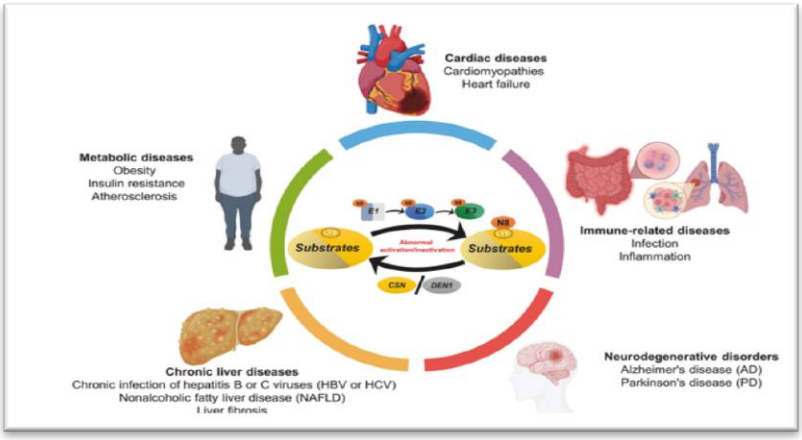

Figure 9: Abnormal neddylation in human diseases. **[82]**

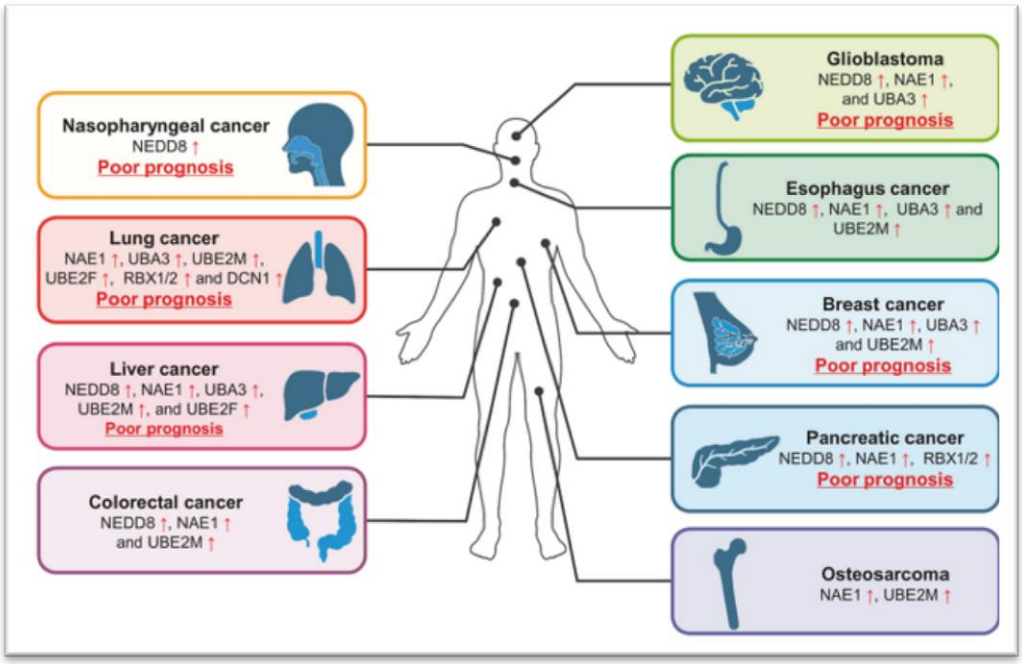

Figure 10: Abnormal neddylation in cancers. **[83]**

Neddylation pathway is hyper-activated in many types of human cancers, and overexpression of some neddylation components is associated with advanced stages of diseases and poor survival of cancer patients. **[83]**

2.2.9. Esophageal cancer (EC)

Esophageal cancer (EC) is the 8th most common cancer worldwide and is ranked 6th for cancer-related mortality **[84].**

Esophageal cancer is a disease in which malignant (cancer) cells form in the tissues of the esophagus. The esophagus is the hollow, muscular tube that moves food and liquid from the throat to the stomach. The wall of the esophagus is made up of several layers of tissue, including mucous membrane, muscle, and connective tissue. Esophageal cancer starts on the inside lining of the esophagus and spreads outward through the other layers as it grows **[85].** The two most common forms of esophageal cancer are named for the type of cells that become cancerous:

- **Squamous cell carcinoma (ESCC):** Cancer that forms in the thin, flat cells lining the inside of the esophagus. This cancer is most often found in the upper and middle part of the esophagus, but can occur anywhere along the esophagus. This is also called epidermoid carcinoma **.[85]**

- **Adenocarcinoma:** Cancer that begins in glandular cells. Glandular cells in the lining of the esophagus produce and release fluids such as mucus. Adenocarcinomas usually form in the lower part of the esophagus, near the stomach. **[85]**

Smoking, heavy alcohol use can increase the risk of esophageal cancer. Signs and symptoms of esophageal cancer are weight loss and painful or difficult swallowing **[85]**

2.2.10. Cullin Neddylation and EC

Esophageal squamous cell carcinoma (ESCC) is the major histologic subtype of esophageal cancer with high incidence and mortality. However, few achievements have been made in the development of targeted drugs**.[86]**Currently, the inhibition of cullin neddylation by targeting overactivated neddylation pathway has emerged as an attractive approach for anticancer therapy**[87-88]** Our previous study reported that MLN4924, a specific inhibitor of NAE, significantly inhibited the tumor growth of ESCC by blocking cullin neddylation and inactivating CRLs activity.**[89]**

3. Plants

Using drugs made from plants to cure and prevent disease is known as phytotherapy. Since phytotherapy is a science-based medical practice, it differs from other, more conventional methods like medical herbalism, which is frequently connected to traditional knowledge and depends on an empirical perception of medicinal herbs. An herbalist's method has typically not been tested in rigorous biological studies or controlled clinical trials, although there are many pharmacological investigations and trials of certain phytotherapeutic formulations. There are differences in how these data are interpreted and accepted for use in phytotherapeutic procedures. While some nations perceive phytotherapy as a kind of traditional medicine, others think it is sufficient to license phytotherapeutic products as medicines **[90]**.

3.1. Fenugreek (*Trigonella foenum-graecum L)*

Trigonella foenum-graecum L., often known as *fenugreek* (see fig 11, 12), and in Arabic" الحلبة" is a native of central Asia and one of the oldest members of the Fabaceae family of medicinal plants. It has a remarkable therapeutic and nutritional profile **[91].** *Trigonella*, more precisely *Trigonella foenum-graecum L.*, or *fenugreek*, is an important traditional medicinal and culinary plant in Algeria. Algeria's coastal regions, high plateaus, and even the Hoggar region are all home to its cultivation. Because of its abundance in carotenoids, polyphenols, vital amino acids, iron, and other nutrients, this plant is prized for its medicinal qualities. In Algeria, where

fenugreek is used as a spice and a medicinal herb, researchers have expressed interest in learning more about the health advantages of this plant **[92].**

Figure 11: *Trigonelline* leaves**. [93]**

Figure 12: *Trigonelline* seeds. **[93]**

3.1.1 Scientific Classification [94]

Kingdom: Plantae

Clade: Tracheophytes

Clade: Angiosperms

Clade: Eudicots

Clade: Rosids

Order: Fabales

Family: Fabaceae

Subfamily: Faboideae

Genus: Trigonella

Species: T. foenum-graecum

Binomial name: *Trigonella foenum-graecum.*

Arabic name : الحلبة

3.1.2. Pharmaceutical uses

A variety of qualities may be found in f*enugreek* seeds, but in particular, they have a fragrant scent, a bitter flavor, carminative qualities, and antibacterial and antioxidant activities **[95].** Fenugreek has also been linked to pharmacological properties like antitumor, antiviral, antibacterial, anti-inflammatory, hypotensive, and antioxidant **[96].** Fenugreek seeds contain phenolic acids, including vanillic acid, coumaric acid, ferulic acid, and gallic acid. These acids have a higher potential for antioxidants **[97, 98].**

The analysis of the literature shows that fenugreek can be utilized as a therapeutic agent to regulate illness conditions and that it considerably reduces the pathological symptoms of neurodegenerative disease, particularly AD **[99].**

Fenugreek is a promising natural agent for cancer prevention and treatment because of its bioactive components, which have demonstrated substantial promise in suppressing the growth of several types of cancer cells by triggering apoptosis and cell cycle arrest**.[100]**

3.1.3. Traditional uses

Fenugreek is one of the earliest medicinal plants, used in Roam and Egypt to facilitate childbirth and enhance milk flow, according to records from ancient civilizations. Egyptian ladies continue to utilize this plant to make Hilba tea, which helps with sedative stomach issues and menstruation discomfort **[100].**

This plant is also used in Chinese traditional medicine to strengthen the body, alleviate gout, and improve physique. In the East, this herb was taken by people with extremely thin bodies to have strong, well-developed bodies. This plant has been used as a tonic, spice, and inducer of breast milk in Indian traditional medicine. In non-medical contexts, Egyptians have used this plant to mummify bodies and to burn and fumed it with incense during religious rites **[101].**

3.1.4. Chemical compounds

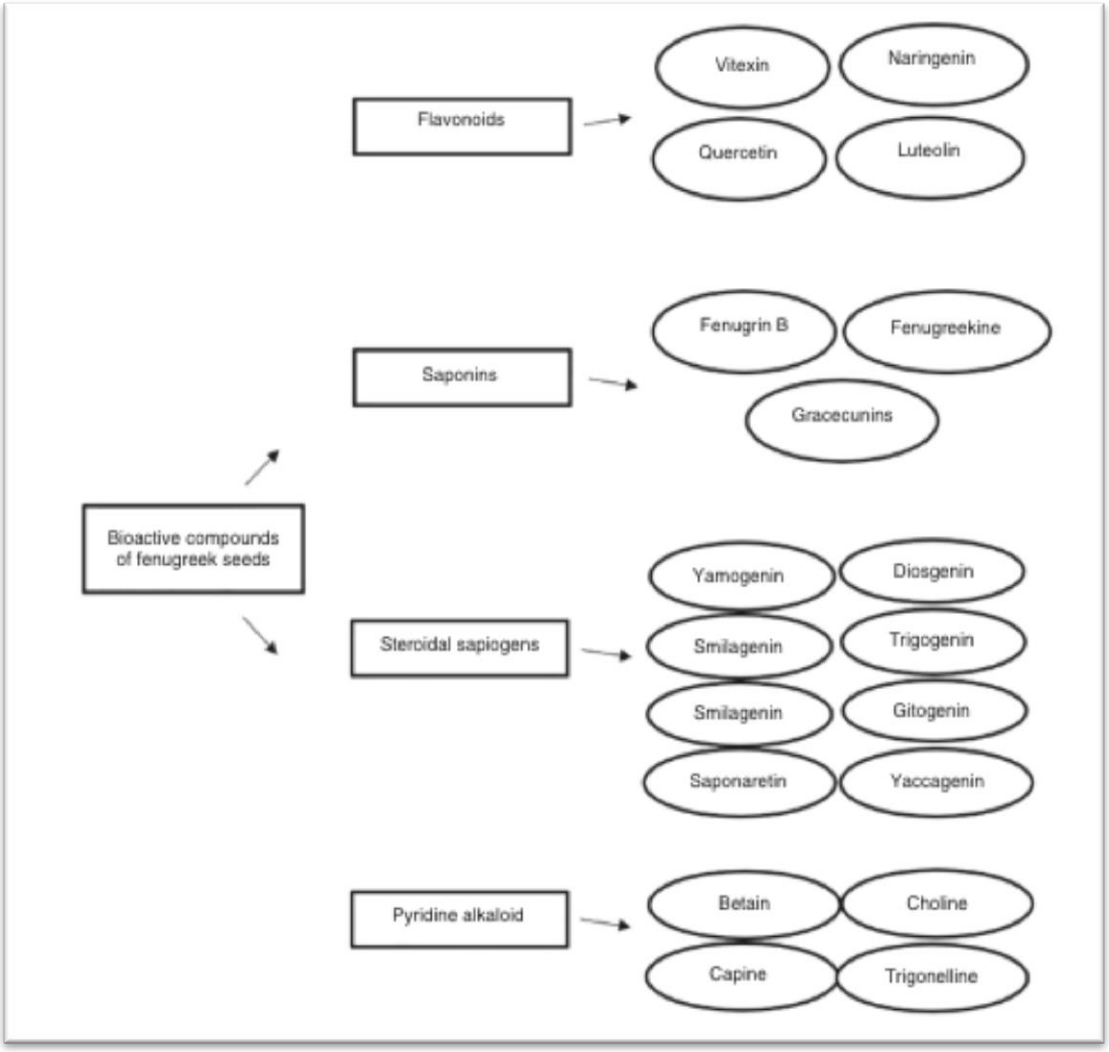

Figure 13: The bioactive compounds of *fenugreek* seeds **[102].**

3.2. *Sage* (*Salvia officinalis L)*

Salvia, also known as *Salvia officinalis L* (see fig 14), and in Arabic] "المريمية, سواك النبي"[**103]**, is a perennial aromatic herb that is grown all over the world for its flavor, culinary, and medicinal uses. It is a member of the Lamiaceae family of plants. Sage is a widely used culinary and medicinal herb that is valued as a commodity in the spice and pharmacy industries due to its widespread popularity. Herbal stores frequently sell sage and other aromatic herbs that have been shade-dried at room temperature to preserve their aromatic qualities. The herb is widely available, and it is a crucial component of the tea blends made in the Mediterranean region as well as utilized in food preparation**. [103].**

Figure 14: Arial parts of *Salvia officinalis* **[104]**

3.2.1. Scientific Classification [105]

Kingdom: Plantae.

Subkingdom: Tracheobionta.

Division: Magnoliophyta.

Class: Magnoliopsid.

Subclass: Asteridae.

Order: Lamiales.

Family: Lamiaceae.

Genus: Salvia.

Binomial name: *Salvia Officinalis L*

Arabic name : المريمية

3.2.2. Uses of *sage*

Sage is used in folk medicine and traditional medicine all across the world. The Latin name for the plant, *Salvia*, means "curative," indicating its value and health-promoting qualities **[106].** In some Asian and Northern American countries, the plant's aerial portions are used to treat diabetes, rheumatism, gout, and diarrhea **[107].** In addition, sage is used to treat inflammations, sore throats, and upper respiratory ailments, including dyspepsia and ulcers **[103].** It is also used to cure heartburn. Additionally, *sage* has been shown to be effective in age-related cognitive problems **[108].** It is well known to calm down Alzheimer's sufferers and enhance their memory **[109].** The taste, antioxidant, and antibacterial qualities of the plant leaves make them widely

employed in the culinary sector **[110].** Additionally, the plant is used as a part of the perfumery and cosmetic industries **[106].**

Salvia officinalis extract's effectiveness and safety were tested over a 4-month period in individuals with mild to moderate Alzheimer's disease at a fixed dose of 60 drops per day. The study's findings show that S. *officinalis* extract is effective in treating mild to moderate Alzheimer's disease. Furthermore, *S. officinalis* may help patients feel less agitated, although this has to be verified**.[111]**

3.2.3. Chemical compound

The major compounds of sage *(S. officinalis)* are shown in this table 1 below:

Table 1: chemical composition of *salvia officinalis.L* dried aerial parts **[112]**

Compound	Content %
Trans-Salvene	2.681
Pulengone	1.004
Tricyclene	0.554
Alpha-Pinene	6.600
Beta-Pinene	2.469
Myrcene	1.492
1.8-cineol	13.035
Gamma-Terpinene	3.256
Alpha-Terpinene	1.125
Thujone	13.250
Beta-Thujone	0.858
3-Cyclopentene-1-acetaldehyde, 3-trimethyl	0.863
Camphor	17.750
Borneol	3.724
Terpinene-4-ol	1.146
Alpha-Terpineol	0.622
Borneolacetate	3.557
Myrtemyl acetate	0.905
Carvacrol	1.512
Triazole-3-carboxylic acid	1.273
2,4-Cycloheptadien-1-one imethyl	0.448
Terpinolene	0.385
Beta-caryophyllene	5.071
Eremophilene	1.666
Alpha-Humulene	5.481
Aromadendrene	0.640
ALpha-Guaiene	0.407
(+)-Leden-alpha4(1H)-Azulenone,octahydro-1-methy	1.480
Viridiflorol	0.355
Alpha-Selinene	0.416

3.3. *Date palm (Phoenix Dactylifera.l)*

The *date palm* is a common name for *Phoenix dactylifera* **[113]** is a flowering-plant species in the palm family, Arecaceae , cultivated for its edible sweet fruit called dates. The species is widely cultivated across northern Africa, the Middle East, Horn of Africa, Australia, South Asia, and California. **[114**].It is naturalized in many tropical and subtropical regions worldwide **[114,115,116]**. *P. dactylifera* is the type species of genus *Phoenix*, which contains 12–19 species of wild date palms **[117]**.

3.3.1. *Date palm* fruit

Date fruits (*Phoenix dactylifera*) are fruits known for their high nutritional value, and also for their pleasant taste. They have been cultivated in the Middle East and the Indus Valley for thousands of years. There are different types of date fruits, and their classification is performed based on external characteristics such as color, size, diameter and shape. Traditionally, the classification of these fruits used to be done manually. **[118]**

3.3.2. Scientific Classification [119]

Kingdom: Plantae

Division: Magnoliophyta

Class: Liliopsida

Order: Arecales

Family: Arecaceae

Genus: Phoenix

Species: *P. dactylifera*

Arabic name: التمر

3.3.3. *Date Seeds*

Date seeds, also known in Arabic (النواة, البذرة)**,** a by-product of date fruit production, are usually treated as waste, utilized as animal feed or just disposed of **[120].** However, *date seeds* comprise 10–15% of date fruit fresh weight, and are rich in phenolic compounds **[121].** There have been extensive studies carried out on the effects of *date seeds* in terms of pharmacological activities, such as antioxidant, anti-inflammation, antidiabetic, antibacterial, and antiviral properties **[122-123].** Owing to its health benefits, date seeds possess high potential as a nutritional therapeutic agent for several chronic diseases **[124].**

Date seeds can effectively inhibit cancerous growths, making them a viable candidate for use as an anticancer treatment. DSEs have the ability to decrease cancer cell line viability at high doses over extended exposure times. **[125]**

3.3.4. Chemical compounds

The average weight of *date seeds* is 5.6–14.2% of the fruit. They are a good source of phytochemicals such as phenols, sterols, carotenoids, anthocyanins, procyanidins, and flavonoids **[125-126]** (see figure 15).

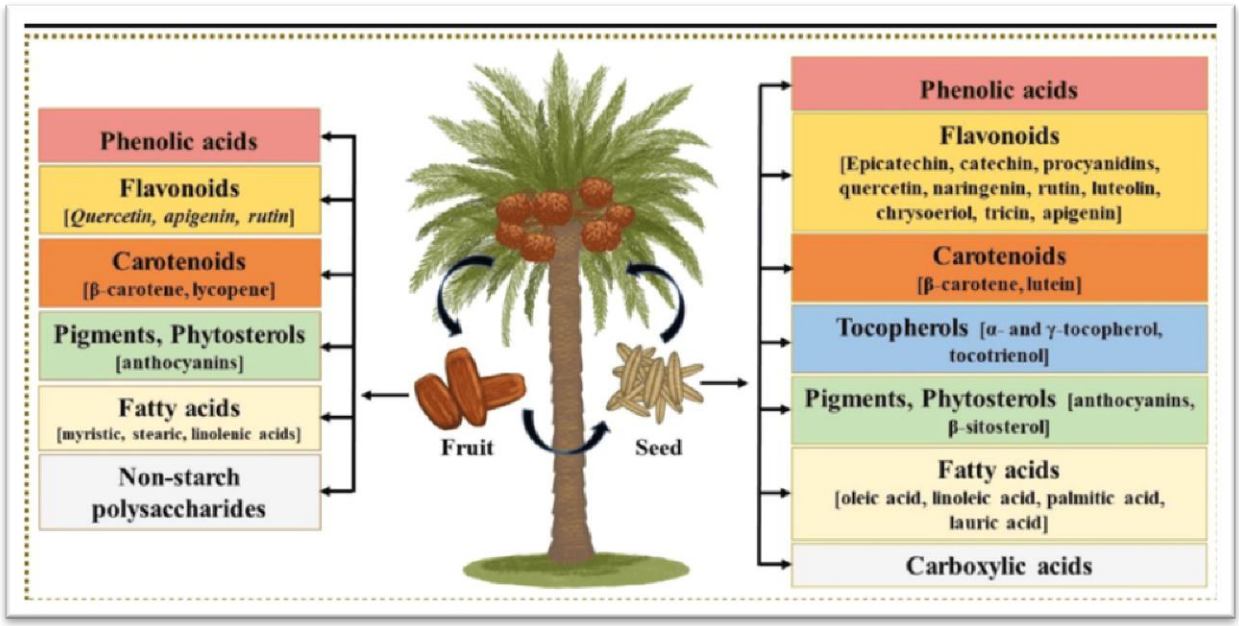

Figure 15: Bioactive constituents from *date fruit* and seed**. [133]**

3.3. 5. Pharmaceutical uses of *date seeds*

Date fruits and seeds are considered to have significant nutritive and pharmacological properties. Moreover, they can be used in various cosmetic and beauty products (see fig16). A lot of cosmetic products contain high amounts of chemical compounds, which are mostly derived synthetics such as hydroquinone **[134].** Hamman reported that activated carbon derived from date stones worked as a catalyst in the reactivity of hydroquinone **[134].** In addition, date stones are used in the production of cosmetics. Thus, nanotechnology-based cosmetic products have been attracting consumers; this approach may be used in the design of a new range of cosmetics **[135].** The development of nano-based cosmetic delivery vehicles, activated carbon, single-walled nanotubes, and nano-sized vitamin E has been successfully employed in cosmetics **[136].**

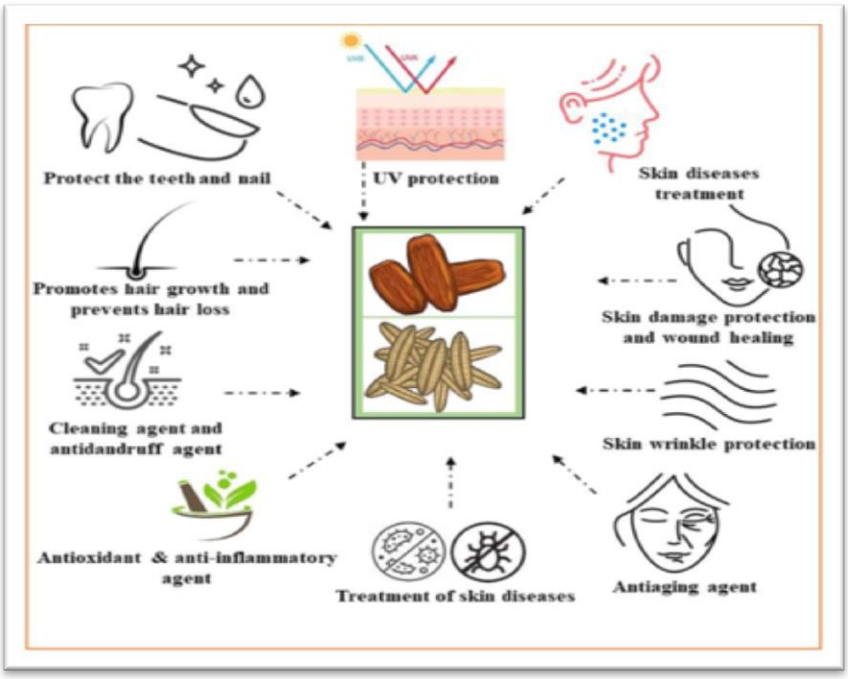

Figure 16: Illustration of the cosmetic applications of *date fruits* and seeds. **[137].**

The therapeutic effects of *P. dactylifera* and its constituents have been alleged since antiquity. It has been abundantly used as an antitussive, restorer, laxative, demulcent, and diuretic in Ayurveda (the traditional system of medicine in India) **[138].** Moreover, it was also used to treat disorders of the reproductive and endocrine systems **[138].**

Other tree parts of *P. dactylifera*, such as pollens, fruits, leaves, pits, and their derivatives, have been passed down in numerous folk and traditional systems of medicines to cure different health disorders and diseases **[138].** Historically, this practice of using dates for treating disease has been intensely adopted by specific cultures, including Iraq, Algeria, Iran,

Egypt, Morocco, and India. In South-Eastern Morocco, dates are mainly used to treat diabetes and hypertension **[138].**

P. dactylifera it possesses strong anti-inflammatory properties against gastrointestinal disturbances, arthritis, chronic pulmonary diseases, and asthma **[139].** Not only is this, but ajwa date is also used for sharpening this memory. In Turkey, a unique herbal coffee called "Hurma" is made from the date's seeds and consumed to improve memory **[139].** Moreover, the antioxidant activity of ajwa date and its constituents could also help in preventing or savaging the production of free radicals linked with the onset of AD. Low glycemic index (GI) diets such as dates with a low GI are effective in managing diabetes mellitus. **[140]**

Conclusion

Esophageal cancer and Alzheimer disease are considered as one of the diseases of the age, as they are considered as fast spreading diseases in the body, from their current treatment with drugs and radiotherapy the disease is controlled, but with more complications in side effects on the other hand. On this basis, the detailed study of the diseases was carried out using medicinal herbs to minimize the side effects and inhibit the disease.

This next side of the study summarizes recent findings of critical role played by molecular docking in the process of drug discovery and development. The application of docking approach will assist to design a dosage form in the most cost effective and time saving manner.

Experimental study

I. Molecular docking

I.1.Introduction

Molecular docking is a computer technique that is widely used in drug development and bioinformatics to simulate the binding process of molecules to anticipate their interaction, namely protein-ligand docking **[141] [142].**

This method, which provides insights into ligand-protein interactions, binding conformers, and affinity estimates, is essential for comprehending biological events prior to experimental validation **[143].** Dynamic ligand-protein interactions may now be simulated thanks to recent developments, which have made the transition from inflexible models to more complex approaches that take into account the dynamic character of molecular interactions over time **[144].** High-resolution representations of intermolecular interactions are made possible by molecular docking, which can provide important new information about biochemical and biophysical interactions not possible with conventional experimental techniques **[145].** It is also a vital tool in computer-aided drug design, helping to clarify structure-activity correlations, find promising medicinal compounds, and support structure-based drug design.

I.2.Principle of molecular docking

The process of inserting a molecule (ligand) into a target protein's active site in three dimensions (3D) space is known as docking.

Predicting the affinity of the [ligand-protein] combination and the precise location of the ligand within the protein's active site are two crucial factors.

The many ligands in the collection have an impact on affinity prediction; some are more appropriate than others. Although in distinct orientations, the site is predicted to be associated to the same ligand molecule. **[146]**

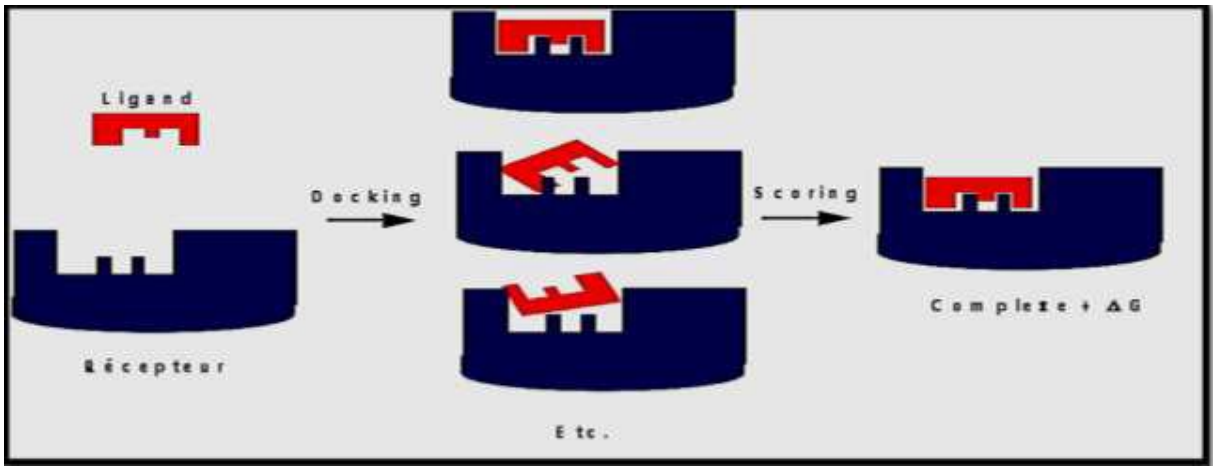

Figure 1: Docking stimulation and scoring **[147]**

I.3. Molecular docking tools

Because the majority of active substances are tiny molecules (ligands) that interact with a biological target of therapeutic interest (protein), docking software is a necessary tool for every useful instrument in biology, pharmacy, and medicine. **[148]**.

A macromolecular protein receptor known as the "target," a small molecule known as the "ligand," and a Docking program that predicts the most advantageous conformation of the ligand within the selected receptor are the only necessary components for practicing molecular docking. **[149]**

I.3.1.Ligand

Any atom, ion, or molecule with chemical properties that enable it to attach to one or more central atoms or ions is referred to be a ligand. Most frequently, the terms "ligand" are used in the fields of coordination and organometallic chemistry, which are subfields of organic chemistry. **[149]**

A ligand in biology is a molecule that binds reversibly to a target macromolecule, protein, or nucleic acid; the term "ligand" comes from the Latin "ligandum," which means "binder." Ligands typically have functional roles in biology, such as structural stabilization, catalysis, regulating enzyme activity, or signal transmission. **[149]**

This word, which is frequently used in the study of proteins, refers to the molecules that specifically and non-covalently interact with the protein to support its functions. **[149]**

A receptor protein's conformation, or three-dimensional (3D) structure, is frequently altered when a ligand binds to it. **[149]**

Induced adjustment is the name for the conformational change that is aided by the energy derived from the interactions between the protein and its ligand. **[149]**

Thus, this structural alteration may be able to alter its activity and functional status. **[149]**

There are two ways to obtain the ligands' structure:

-The first method involves using ligands from the literature or the pdb that may be created, optimized, and saved in various formats (mol, pdb, mol2, etc.) using molecular building tools like Titan. **[150]**

-The second method involves using virtual and commercial collections of molecules known as "chemical libraries," which are databases of chemical structures sometimes referred to as "chemical libraries" or "the most used chemicals paces," according to PubChem. **[150]**

I.3.2. Receptor

Receptor Since proteins are the most common type of macromolecule, we may obtain the receptors by using the 3D structures of these molecules, which are freely available in the PDB database. It is a sizable repository of biological macromolecule structural data, including proteins and nucleic acids (DNA, RNA). **[150]**

The structural data is gathered using NMR spectroscopy and X-ray crystallography, and it is freely available on the internet through websites designated by its member organizations, such as PDBe, PDBj, RCSB PDB, and so on. **[150]**

In May 2018, there were around 141616 bio-macromolecule structures in the PDB.The many three-dimensional conformations, which contain various details about the protein in question and are readable by docking software, can be downloaded under the PDB extension. **[150]**

As an illustration, consider the receiver's name, the group that deciphered the structure, the experimental setup, etc. **[150]**

Additionally, it includes details on the heteroatoms, secondary structure, primary structure, and the atomic coordinates (X, Y, and Z) that specify each atom's precise location within a conformation. **[150]**

Modeling by homology steps in to build the target's three-dimensional structure if it hasn't been deposited in the library yet and it has a protein with similar sequences in it. **[150]**

I.3.3 AutoDock tools

An automatic docking tool set is called AutoDock. Its purpose is to forecast the way that tiny molecules, such medication candidates or substrates, would attach to a known three-dimensional receptor. **[151]**

It has been enhanced and changed throughout time to provide new features, and several engines have been created. AutoDock is currently available in two software generations: AutoDock Vina and AutoDock 4. We have created an accelerated version of AutoDock4 that is hundreds of times faster than the original single-CPU docking code, called AutoDock-GPU, more recently. The atomic affinity grids are not only useful for docking but also for visualizing. For instance, this can direct the invention of improved binders by organic synthesis chemists. Additionally, we have created a graphical user interface known as AutoDock Tools, or ADT for short, which assists in docking analysis and selecting which bonds in the ligand, will be treated as rotatable.(see figure 2) **[151]**

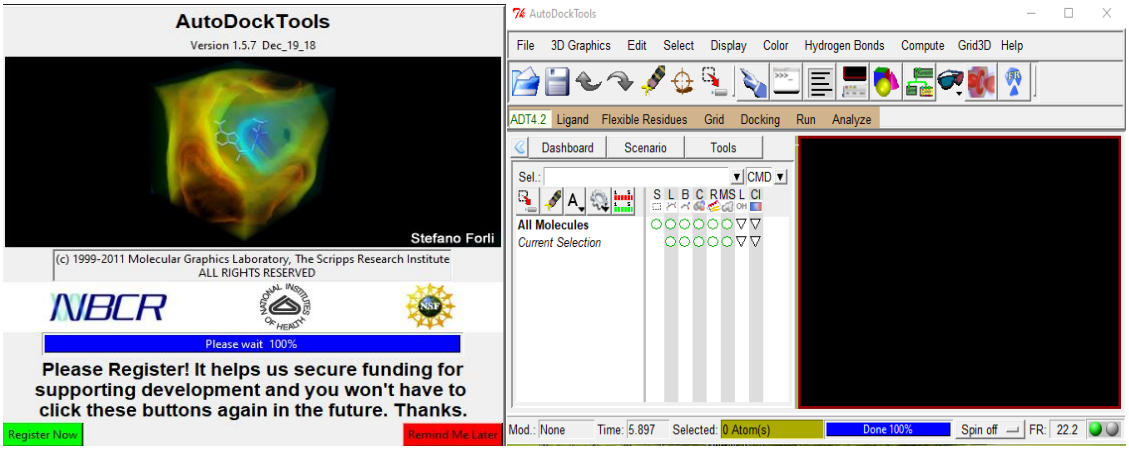

Figure 2: AutoDock tools

I.3.4 AutoDockVina

The newest addition to the AutoDock family, AutoDockVina, was unveiled in 2010. Dr. Oleg Trott created it at The Scripps Research Institute's Molecular Graphics Lab. Its user-friendliness is one of the numerous ways that it is different from earlier iterations. All that is needed is a box description of a search space and three-dimensional molecular structures (with polar hydrogens only, since AutoDockVina still utilizes the United Atom model). The simulation does not require partial charges, solvation parameters, or previously determined interaction energy grids. It uses

the Iterated Local search global optimizer, as opposed to previous versions, which gave the user an option of search algorithms. This algorithm accepts steps based on the Metropolis criterion, with each step consisting of mutation followed by local optimization. The original paper contains information on this approach as well as the scoring formula that AutoDockVina uses. **[152]**

I.3.5 BIOVIA Discovery Studio

BIOVIA Discovery Studio brings together over 30 years of peer-reviewed research and world-class in silico techniques such as molecular mechanics, free energy calculations, bio therapeutics develop ability and more into a common environment.

It provides researchers with a complete toolset to explore the nuances of protein chemistry and catalyze discovery of small and large molecule therapeutics from Target ID to Lead Optimization(see figure 3)**. [153].**

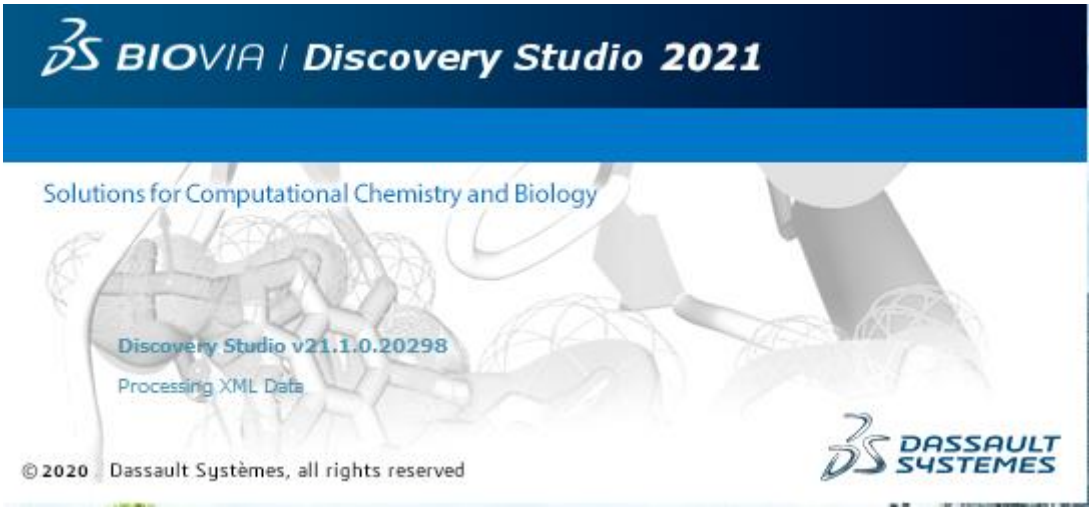

Figure 3: BIOVIA Discovery Studio

1.4. Gaussian

A popular software program for computational chemistry, Gaussian is used to calculate molecules' electrical structures. It is well-known for its ability to forecast different molecular attributes including energy, geometries, and vibrations, as well as to simulate and optimize molecular structures. Gaussian models molecular systems effectively and precisely by applying techniques such as Gaussian process regression and Density Functional Theory (DFT). **[154]**

Figure 4: Gaussian 09 **[155]**

1.4. 1.The role of molecular optimization

When it comes to maximizing the energy and shape of molecules, Gaussian is essential. The main points are below:

- ✓ Gaussian employs methods like Density Functional Theory (DFT) and Gaussian process regression to model molecular systems accurately and efficiently, enabling successful optimization of molecular geometries. **[156] [157]**
- ✓ In Gaussian optimization, forces and energy gradients are used to iteratively modify atomic coordinates with the goal of convergently obtaining the lowest energy state and most stable molecular structure**. [158]**

Gaussian allows researchers to study the behavior of molecules at the quantum level, aiding in the understanding of chemical reactions, molecular interactions, and material properties by providing optimized molecular structures. **[159]**

I.5.Databases

I.5.1.PDB (Protein Data Bank)

Is an international database of biological macromolecules' three-dimensional structures, mainly proteins and nucleic acids. In essence, NMR spectroscopy or X-ray crystallography is used to determine their structures (see figure 5). **[160]**

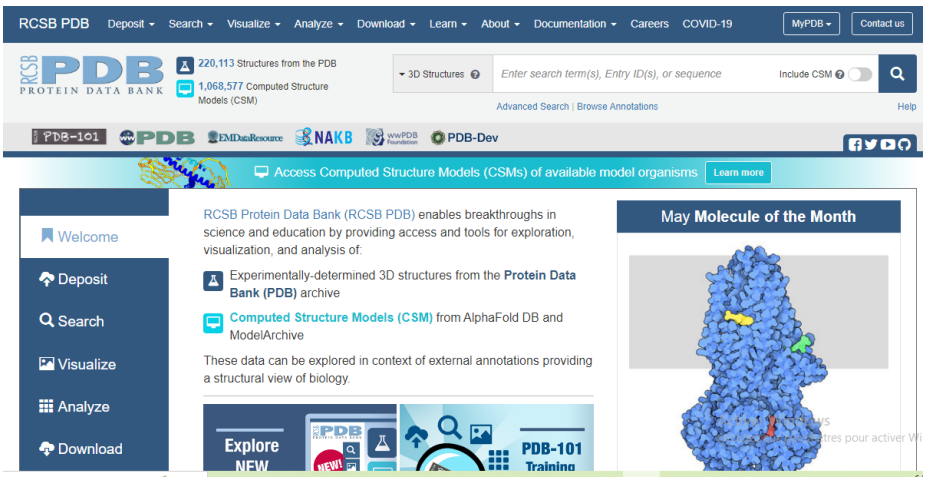

Figure 5: Screenshot of interface of Protein Data Bank

1.5.2. Uniprot

UniProt release 2020_04 contains over 189 million sequence records, with >292 000 proteomes, the complete set of proteins believed to be expressed by an organism, originating from completely sequenced viral, bacterial, archaeal and eukaryotic genomes available through the UniProtKB Proteomes portal(see figure 6) (https://www.uniprot.org/proteomes/) .**[161]**

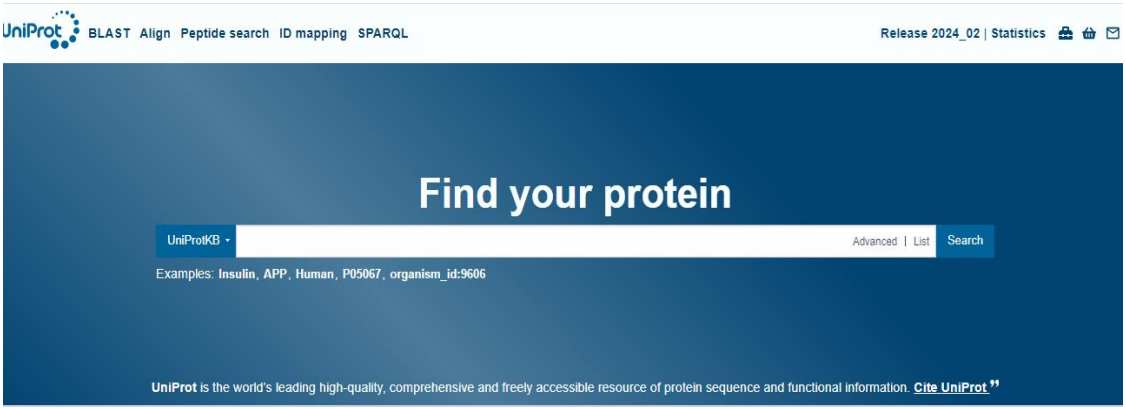

Figure 6: Screenshot of interface of Uniprot

I.5.3 Pubchem

It is an NCBI (National Center for Biotechnology Information) database of chemical compounds maintained in the United States. There are currently millions of compounds within it, all of whose physico-chemical properties and structure are publicly available. (see figure7)**[162]**

We utilized this collection to highlight the structural similarities between our ligand

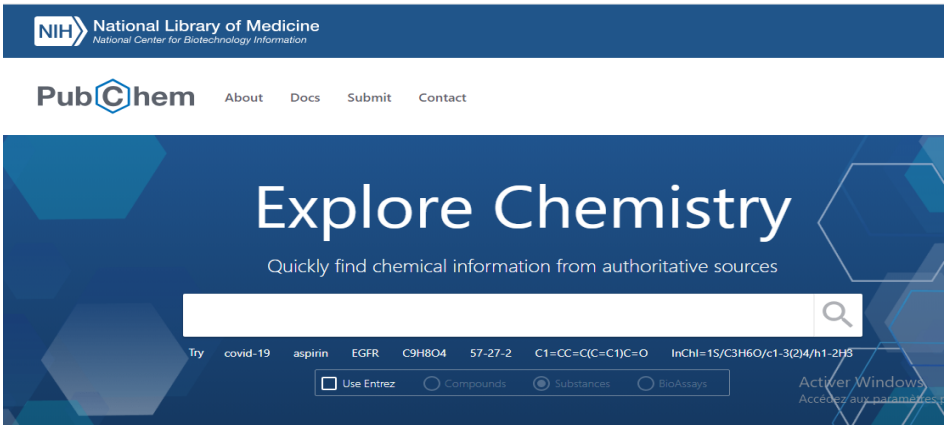

Figure 7: Screenshot of interface of PubChem

I.5.4. SwissADME

SwissADME is a web-based tool that predicts various pharmacokinetic properties and drug-likeness rules for small molecules. It is developed and maintained by the Swiss Institute of Bioinformatics (SIB) and provides valuable insights into the absorption, distribution, metabolism, and excretion (ADME) properties of chemical compounds.(see figure 8)

SwissADME offers a range of features, including the prediction of physicochemical properties such as lipophilicity, solubility, and molecular weight. It also provides estimations of pharmacokinetic properties like blood-brain barrier penetration, human intestinal absorption, and cytochrome P450 inhibition. The tool can be used to assess the drug-likeness of compounds based on various criteria and rule-of-thumb guidelines.

Researchers and scientists in the field of drug discovery and development often utilize SwissADME to evaluate the ADME properties of potential drug candidates, aiding in the early stages of the drug design process. It is a freely accessible tool that can be accessed online through the SwissADME website. **[163]**

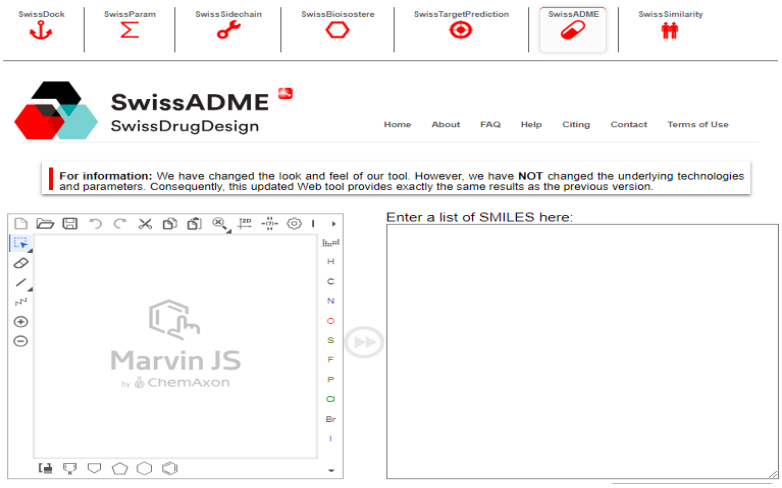

Figure 8: Screenshot of Interface of SwissADME

I.5.5.ProTox 3.0 - Prediction Of Toxicity Of Chemicals

ProTox 3.0 is a free and open-access webserver for predicting the toxicity of chemicals using molecular similarity and machine learning models.(see figure 9) **[164]** It can predict 61 different toxicity endpoints, including:

- ✓ Acute toxicity
- ✓ Organ toxicity (hepatotoxicity, neurotoxicity, respiratory toxicity, cardiotoxicity, nephrotoxicity)
- ✓ Clinical toxicity
- ✓ Molecular-initiating events (MIEs)
- ✓ Adverse outcomes (Tox21) pathways
- ✓ Mutagenicity, carcinogenicity, cytotoxicity, immunotoxicity, BBB-permeability, ecotoxicity, nutritional toxicity **[164]**

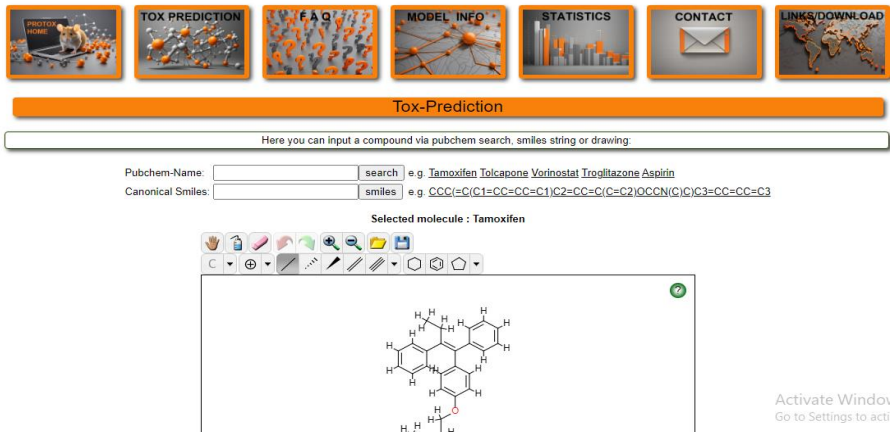

Figure 9: Screenshot of Interface of Protox 3.0

I.5.6. STRING:Protein-Protein Interaction

The STRING (Search Tool for the Retrieval of Interacting Genes/Proteins) database is a comprehensive biological database and web resource that systematically collects and integrates protein-protein interactions, both physical and functional. It is a key tool for understanding cellular processes and provides a platform for annotating structural, functional, and evolutionary properties of proteins.(see figure 10)[**165] [166]**

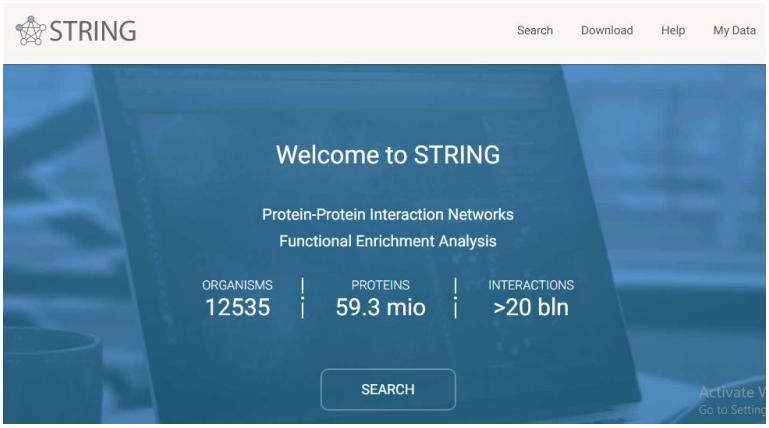

Figure 10: Screenshot of Interface of STRING. Protein-Protein Interaction

I.5.7. Protein-Ligand Interaction Profiler

The Protein-Ligand Interaction Profiler (PLIP) is a web-based tool designed to detect and visualize non-covalent protein-ligand interactions in 3D structures. It is a fully automated service that does not require any structure preparation and can handle a wide range of interaction types, including hydrogen bonds, hydrophobic contacts, pi-stacking, pi-cation interactions, salt bridges, water bridges, and halogen bonds.(see figure 11)**[167]**

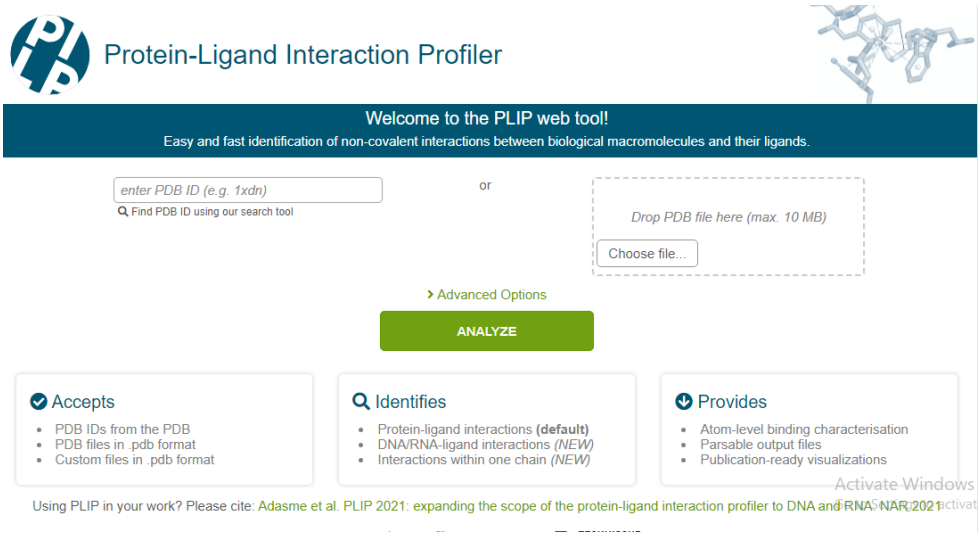

Figure 11: Screenshot of Interface of PLIP

I.6.8.CB-Dock

For protein-ligand blind docking, CB-Dock is a flexible and effective tool that helps with high-accuracy ligand poses and binding site research **[168] [169]** (see figure 12). With a success rate of over 70% for the highest-ranking poses with the lowest RMSD values, it provides a productive and intuitive platform for predicting the binding sites of proteins without any prior

information **[170].** Furthermore, CB-Dock2, an upgraded version, outperforms many previous blind docking tools with an amazing success rate of about 85% for binding pose prediction by integrating CB-Dock with a template-based docking engine **[171].**

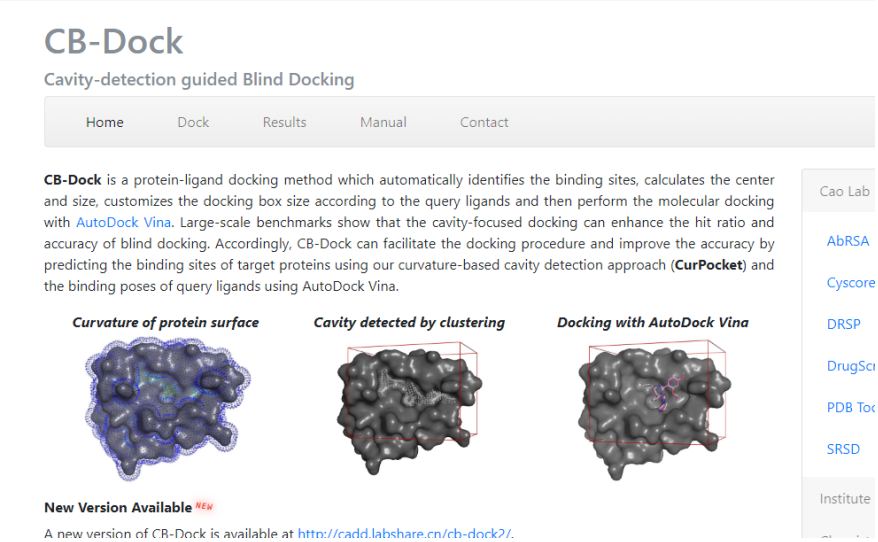

Figure 12: Screenshot of Interface of CB-Dock

I.4.9. Drug Likeness Tool (DruLiTo 1)

One open-source virtual screening tool for predicting a compound's drug-likeness is called the Drug Likeness Tool (DruLiTo 1)(see figure 13). It assesses the structural characteristics of molecules to ascertain their propensity to be drugs using a variety of drug-likeness criteria, including Lipinski's rule, MDDR-like rule, Veber rule, Ghose filter, BBB rule, CMC-50 like rule, and Quantitative Estimate of Drug-likeness (QED)**.[172]**

Figure 13: Screenshot of Interface of Drug Likeness Tool (DruLiTo 1)

II. Material and method

II.1.In vitro study

II.1.1.Inroduction

This side provides an overview of the physical and chemical properties of *Trigonella foenum-graecum* , *Phoenix dactylifera L* and *Salvia officinalis* sinensis and its extracts, as well as the development of antibacterial activity against pathogenic bacteria.

This work is carried out jointly with

- Laboratory of the process engineering department of HASSIBA BEN BOUALI CHLEF University.
- Laboratory of physic-chemical - SAIDAL- Algiers.,Dar El baida.
- Laboratory of Microbiology-EHP SOEUTS BADJ- Chlef
- Laboratory scientific police, Algiers
- Laboratory of chemical vegetal-water- energy HASSIBA BEN BOUALI Chlef , Wlad Fares
- Internship took place from February to May 2024.

II.1.2. Material

II.1.2.1. Biological material

The antibacterial activity of *Trigonella foenum-graecum* , *Phoenix dactylifera L* and *Salvia officinalis* extracts was evaluated conducted against three reference strains. These are gram negative and positive bacteria . The latter are available at the level of Microbiology -EHP SOEUTS BADJ- Chlef

- Gram-negative bacterial strains*: Escherichia coli* and *Streptococcus spp*

- Gram-positive bacterial strains: *Staphylococcus aureus.*

II.1.2.2. Equipment used

II.1.2.2.a. Equipment

- Pressurized rotary evaporator (Heidolph).

- Refractometer (Abbe de WAY).

- Hot plate stirrer (VELP SCIENTIFICA)

- Oven (BINDER, MEMMERT).

- Glassworks (PYREX, ISOLAB).

- Precision balance (OHAUS).

- UV-visible spectrophotometry

- Grinder (10g TRISTAR).

- Muffle furnace (CONTROLS).

- pH meter

-Fridge (IEBHERR).

II.1.2.2.b. Glassware:

- Round-bottomed flask

- Vials

- Funnels

- Beakers

- Test tubes

- Graduated pipettes

- Erlenmeyer flask

- Separating funnel

- Watch glass

- Magnetic rung

- Micropipette

- Volumetric flasks

- Filter funnel

II.1.2.3 Chemical reagents

Table 1: Chemical reagents

Products	Properties
Ethanol (C2 H6 O)	M= 46 g/mol
Distilled water (H2O)	M = 18 g/mol
DPPH	M = 394.3g/mol
Ascorbic acid ($C_6H_8O_6$)	M = 176.12 g/mol

II.3. Plant materials:

II.3.1. plant preparation

II.3.1.1. Harvest

Plants selected for this study: *sage* (*salvia officinalis*), *Fenugreek* (Phoenix dactylifera L), *palm date* (*Phoenix dactylifera L*).

Sample 1: *salvia officinalis* leaves was procured from the local market of Chlef, Algeria during March 2024.

Sample 2: *Trigonella foenum-graecum L*, were collected from the local market of Wad Smar region, Algiers, Algeria

Sample 3: *Phoenix dactylifera L* seed was collected in March 2024, from the region of Chlef , Algeria. The part considered for this study is the seeds.

II.3.1.2. Drying

- We dried each one of the three plants in the oven at 40 degrees for 24 hours.
- The weight each two hours is measured until stabilizes (see figure 16)

(1) **(2)** **(3)**

Figure 14: Shows plants used: **(1)** salvia officenalis **(2)** *Trigonella foenum-graecum L*

(3) *Phoenix dactylifera L*

II.3.1.3. Grinding and conservation

The dried peel is reduced to a fine powder using an electric grinder. This operation breaks the cell membranes and the extracellular matrix and release the organelles and molecules contained in the cell, which increases their contacted surface with the different solvents used and consequently improve the extraction yield. The resulting powder (figure 15) is stored away from air, humidity and light in hermetically sealed glass Bottles

Figure 15: the three plants in powder form

II.3.2.Extraction process

II.3.2.1.Method of extraction by maceration

II.3.2.1.a. Solvent extraction

The extraction was made by a maceration of 50 g of plant in 500 ml of solvent (ethanol) for 72 hours in a closed container and at room temperature under agitation. the steps are illustrated in **(Figure 16)**

(1)

(2)

(3)

(4)

(1)

(2)

(3)

(4)

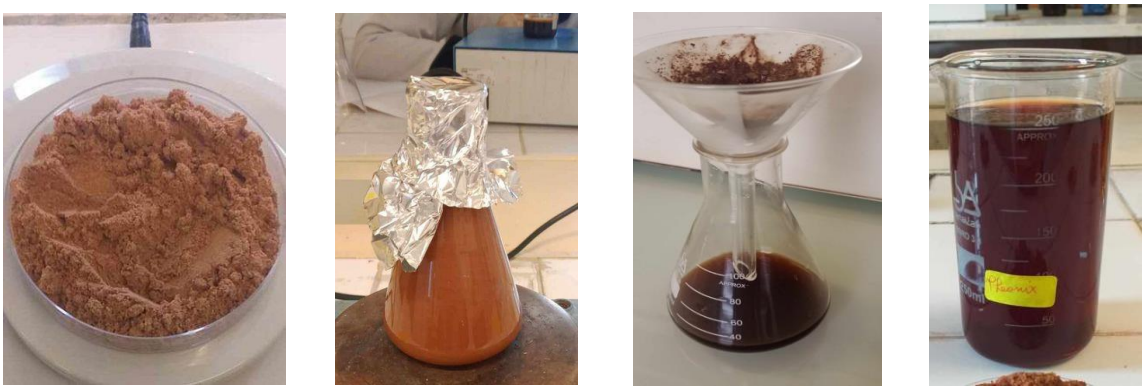

(1) (2) (3) (4)

Figure 16: Extraction steps (1) weight gain, (2) maceration, (3) filtration, (4) filtrate

II.3.2.1.b.Rotary evaporator

After 72 h, the solution is filtered by a 150mm diameter filter. Then the separation of the solvent from the extract is done using a device called Rota vapor «rotary evaporator». In this apparatus, vacuum evaporation (Figure 17) is carried out using a vacuum pump with a control valve. During evaporation the flask is rotated and immersed in a heated liquid bath. The device is equipped with a refrigerant with a condensate recovery tank. The rotation of the balloon creates a larger exchange surface allowing rapid evaporation. Lowering the pressure allows the solvent to evaporate at a reduced temperature of 55°C and the extract is recovered avoiding thermal degradation

Figure 17: Rotary Evaporator "Rotavaporation"

The extract is then kept for the ensuing analyses at 4°C in the dark.

II.3.2.1.c. Extract yield

The plant is exhausted, and the filtrate is dried at 40°C before being weighed and the extraction yield (R) is determined using the formula below

R (%) = ((P0 − P1) / P0) * 100 …….. (1)

R: Yield.

***P*0**: original weight.

***P*1**: Weight after extraction and drying.

II.4.Physicochemical study of the extracts

II.4.1.pH meter Analysis

- **Preparation of the device:** We make sure that the pH meter is clean and calibrated

For precise measurements, we use buffer solutions (pH 4, PH 7 and PH 10). (Figure 18)

- **Preparation of the sample:** Pour *salvia officinalis* into a clean container and immerse the pH meter electrode in the solution to allow the result to be read.

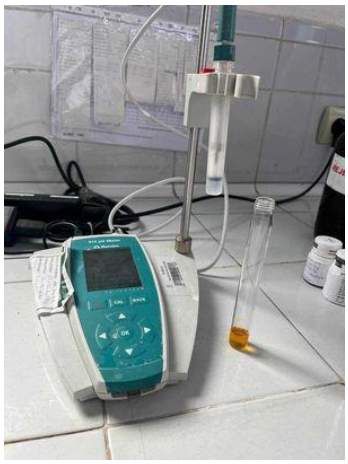

Figure 18: pH meter

II.4.2.Density

The density of a substance is denoted d and corresponds to the ratio of the density of this substance by the density of pure water to define the density of our extracts; we assumed a method that depends on the measurement of the density of the extract and the density of the water

$$d=\frac{\rho extract}{\rho water} \ldots\ldots\ldots (2)$$

$\rho\ extract$**:** the density of the extract

$\rho\ water$**:** the density of water =1

Figure 19: Densimeter

II.4.3.Visible UV

- **Principle of visible UV**

UV-visible electronic transitions are the most critical chemical energies in a molecule (Approximately from 13000 to 50000 $Cm-1$ or 160 to 665 kJ $mol-1$). The energies involved are on the same order of magnitude as the molecules' binding energies, and this radiation can occasionally trigger bond breakage. They generate electronic transitions between different levels of energy in molecules in general (Figure 20) **[173].**

Figure 20: Spectrophotometer visibe UV **.**

II.4.4.Determination of antioxidant potential

II.4.4.1.Determination of antioxidant activity by the DPPH test

- **Principle of the DPPH test**

The antiradical activity of the extracts was tested by using the radical DPPH (Blois method (1958) with some modifications).

DPPH, 2.2'-Diphenyl-1 picrylhydrazyl (Sigma, C18H12N5O6: PM-394.33), is a stable free radical soluble in methanol (or ethanol) with an intense violet color, it exhibits a maximum absorbance at 517 nm. When an antioxidant molecule reduces the DPPH radical.

The purple color quickly disappears to a pale yellow color, according to the following reaction **(figure 21) [174].**

DPPH*+ (AH) n ⟶ DPPH-H+ (A*) n

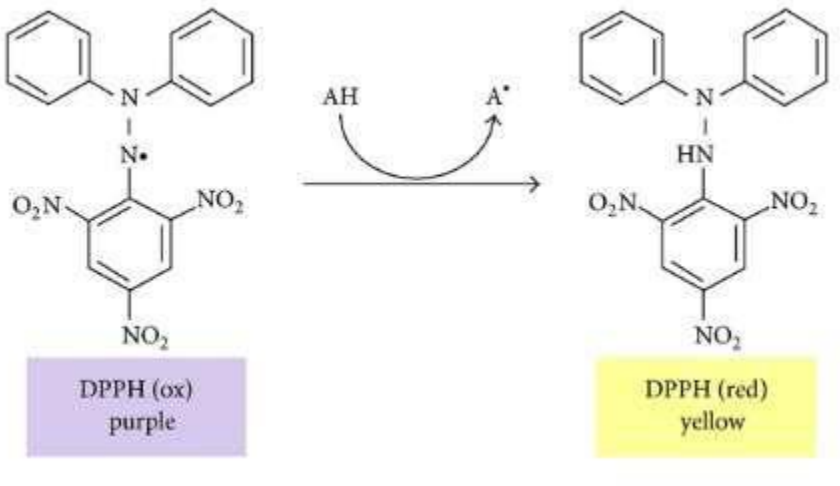

Figure 21:.Principle of DPPH radical scavenging capacity assay **[174].**

II.4.4.2.Operating mode

- **Preparation of the oxidizing solution of the DPPH**

The preparation of the DPPH solution is 0.004% (m/v), obtained by dissolving 0.004g of DPPH in 100ml of ethanol **(Figure 22)**

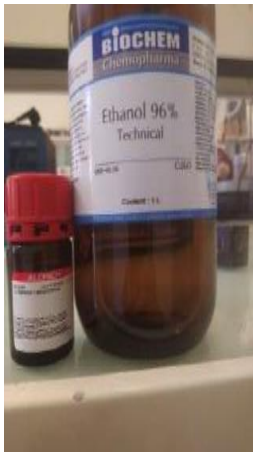

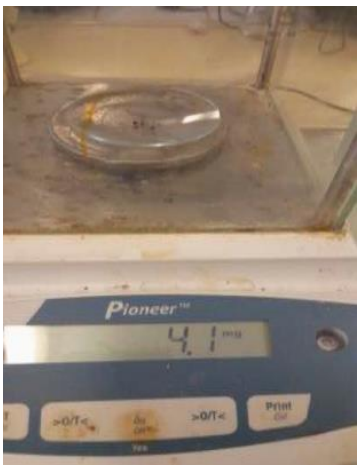

Figure 22: Preparation of DPPH solution **.**

- **Preparation of extract concentrations**

Take 2 ml of the extracts and fill in with ethanol until 4 ml

C0= 0.1 g/l ⟶ V0=2 ml

C1=? ⟶ V1= 4ml

C0 V0 = C1 V1 ⟶ C1= 0.05 g/L

C1 V1 = C2 V2 ⟶ C2 =0.025g/L

C2 V2 = C3 V3 ⟶ C3 = 0.0125g/L

C3 V3 = C4 V4 ⟶ C4 = 0.00625 g/L

C4 V4 = C5 V5 ⟶ C5 = 0.003125g/L

Figure 23: Preparation of extract concentrations.

After the 30min incubation, the reading is done by visible UV at 517 nm, the blank is Ethanol.

II.4.4.3. Determination of inhibition

The evaluation of antioxidant activity using the DPPH method is expressed as percentage according to the following formula:

$$\% \text{ Inhibition} = \frac{\text{Abs Controle} - \text{Abs Extrait}}{\text{Abs Controle}} \cdot 100 \quad \ldots\ldots\ldots\ldots \text{(3)}$$

II.4.4.4. IC50 determination

The percentage of inhibition is expressed by the value of the IC50, knowing that the IC50 is the concentration of extract necessary to obtain 50% of the reduced form of the radical DPPH. **[175].**

II.4.5.Chromatographic and spectroscopic method of separation and identification

II.4.5.1. GC MS Analysis

The analysis and identification of the chemical composition of the extracts of the three studied species were carried out by chromatographic techniques. Gas chromatography coupled with mass spectrometry (GC-MS) allowed us, using spectral databases, to determine the compounds.

This analysis is a quality control to determine the most pharmacologically active compounds. In order to extract the three species: *Sage* (*Salvia officinalis*), *funegreek* (*Trigonella foenum-graecum L*), *date seeds* (*Phoenix dactylifera L*) dried, ethanol was used as an extraction solvent. The analysis was conducted at the Algiers Forensic Laboratory. Apparatus: GC MS model CLARUS 500 brand Perkin-Elmer

II.4.5.2. GC-MS Method

The experimental conditions of the GC-MS system were: standard non-polar capillary column TR 5-MS, dimension: 30 Mts, ID: 0.25 mm, film thickness: 0.25 µm. The flow rate of the mobile phase (carrier gas: He) was adjusted to 1 ml min-1.

In gas chromatography, the temperature program (furnace temperature) was increased from 40°C to 220°C to 4°C min-1 and the injection volume was 1 µl. The samples were fully analyzed at a range of 20 and 550 m/z and the results were compared using the Wiley and Nist spectral library research program.

II.4.6. Microbiological study

II.4.6.1.Antimicrobial activity of extracts

- **Strains used**

In our study, we tasted the sensitivity of three reference bacterial strains (American Type Culture Collection 'ATCC')from the microbiology laboratory at the EHP SOEURS BADJ CHLEF two (2) Gram negative and one (1) Gram positive: *staphylococcus aureus ATCC 6538, Streptococcus spp ATCC 12228, Escherichia coli ATCC 8739.*

All these micro-organisms are pathogenic, have different potentials depending on the type of infection they cause, cause hospital infactions and resistant to antibiotics, which is why they have to make choices. The strains, culture media, grams and incubation temperatures are listed in the table below (Table 2):

Table 2: Microbial strains used for antimicrobial test.

Number	Microorganisms	Gram	Culture medium	Incubation temperature
1	*Staphylococcus aurous ATCC6538*	Positive	Chapman	37
2	*Escherichia coli ATCC14028*	Negative	Hektoen 'slp' mackook	37
3	*Streptococcus spp ATCC 12228*	Negative	Chocolat gelose or cold gelly	37

- **Operating mode**

- Aseptically pour the agar culture medium (soya agar) and (Muller Hinton) in super fusion into Petri dishes at a rate of 10 to 15mL per dish.

The growth medium is left to cool and solidify on the bench (under the hood).

- A bacterial suspension corresponding to the standards of 0.5 Mc Ferland was prepared from a pure and young culture (24 hours old).**(** figure 24**)**

Figure 24: Preparation of the bacterial suspension

These standards equivalent to an optical density of 0.08-0.1 at 625 nm, this inoculum is used to inoculate MH or SA agars poured into Petri dishes by a swab soaked in the suspension by tight streaks.

-Using sterile forceps, place sterile Schleicher & Schuell discs Ø 9 mm in diameter as needed on the surface of the Petri dish containing inoculated agar then impregnated with 15 µl of each extract. The inoculated dishes containing the discs of the extracts were put at 4° C. for 2 hours to facilitate the diffusion of the extracts. The Petri dishes were closed and left to diffuse at room temperature for 1 hour. They were subsequently incubated at 37° C. for 24 hours. **[1].**

After incubation, the absence of bacterial growth expressing an antimicrobial activity results in a translucent halo around the disk, of the same color than sterile agar and whose diameter is measured using a calliper (expressed in mm). **[175].**

Reading is done by measuring the diameter of the inhibition zone around each disc using a calliper or a ruler in (mm). The results are expressed by diameter of the inhibition zone and can be symbolized by signs according to the sensitivity of the strains versus extracts. **[176].**

- D≥30mm: Very strongly inhibitory.
- 21mm≤D≤29mm: Strongly inhibitory.
- 16mm≤D≤20mm: Moderately inhibitory.
- 11mm≤D≤16mm: Slightly inhibitory.
- D<10mm: Non-inhibitory**.**

Figure 25:.Reference bacterial strains (American Type Culture Collection (“ATCC”) microbiology laboratory at the EHP SOEUTS BADJ CHLEF **.**

II.2.In silico study

Ii.2.1.RECEPTORS (THE PROTEINS):

The therapeutic targets that we have studied in our work are the P2X7 and the NAE1

we used PDB to download the NAE1 we used the Uniprot database to download the P2X7

Neddylation activating enzyme NAE1: 3GZN

P2X Purinoceptor 7 P2X7: Q99572

- Write the ID of NAE1 in the search to obtain the 3D structure

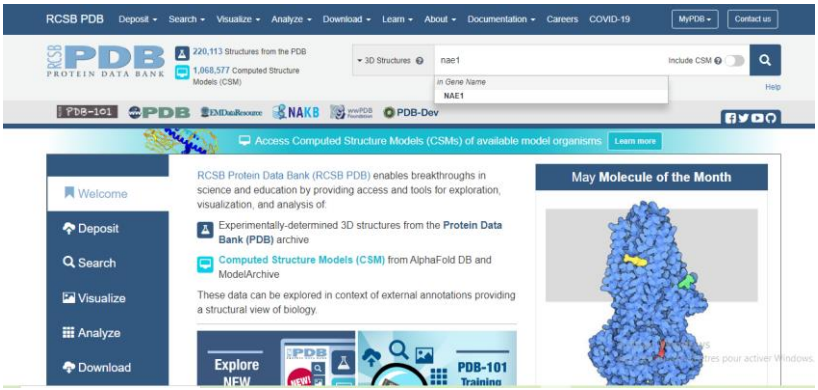

Figure 26: Interface Copy of research about NAE1 in PDB

Figure 27: Interface Copy of download NAE1 structure from PDB

- In the Uniprot databases search about P2X7 (Figure 28)

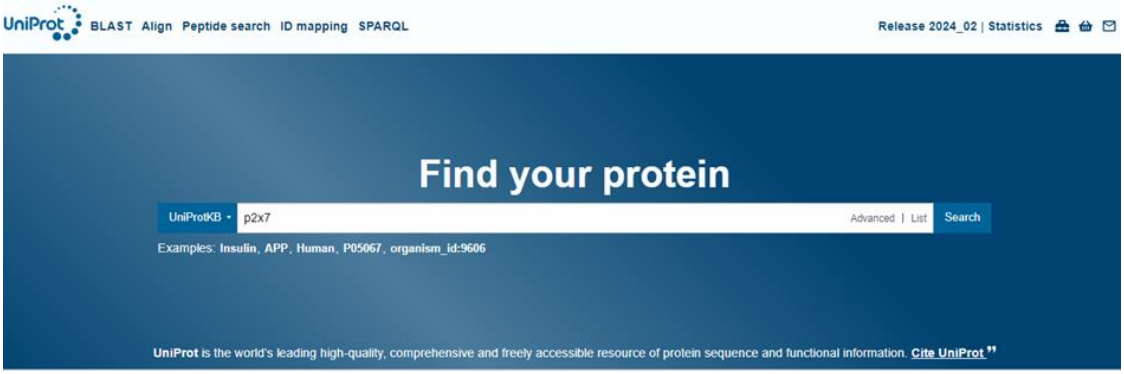

Figure 28: Interface Copy of research p2x7r in Uniprot database

- From the results we should choose the protein homo sapiens (Figure 29)

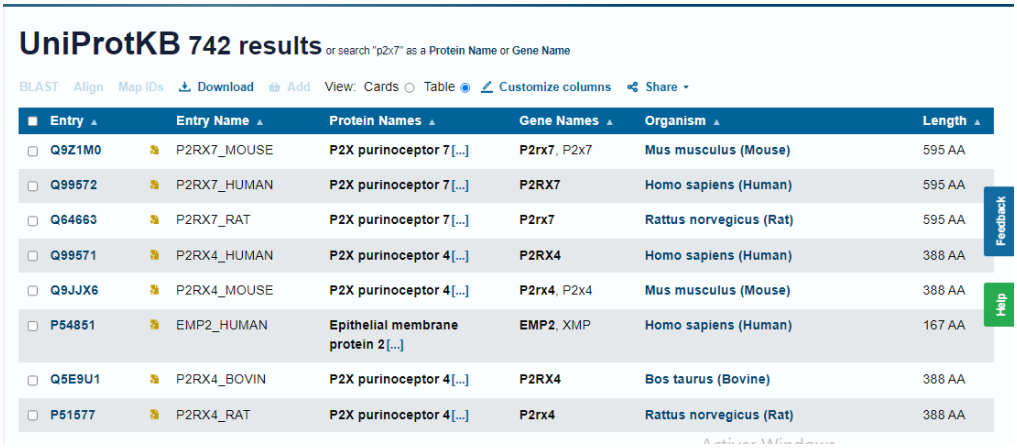

Figure 29: Interface Copy of Uniprot results about p2x7 research

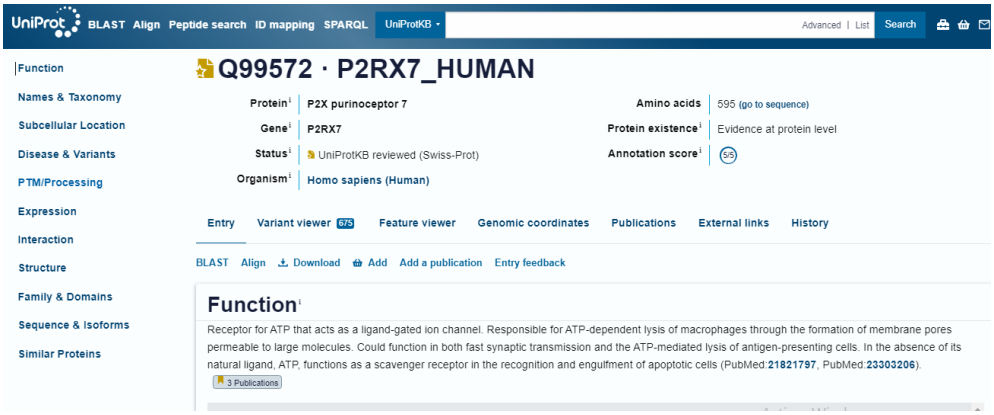

Figure30: Interface Copy of some information about the P2X7 receptor

- Go to structure (Figure 31).

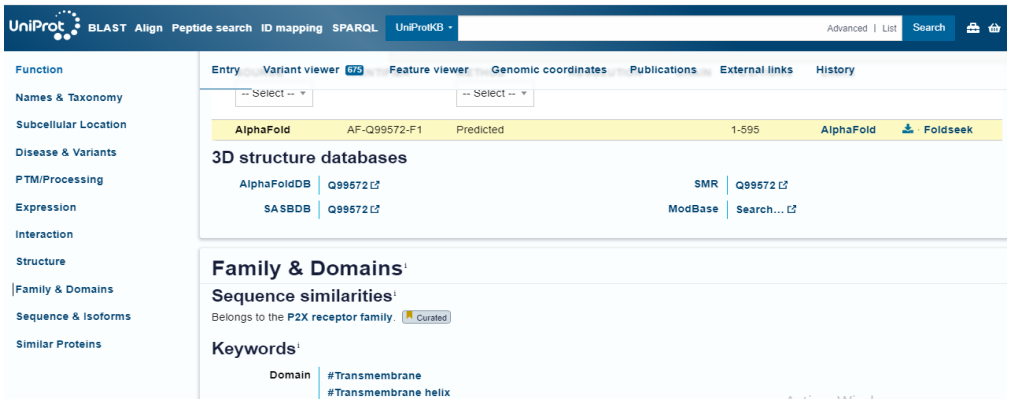

Figure 31: Interface Copy of structure of P2X7 can download

- Choose the Alpha FoldAD structure than download the PDB file (Figure 32).

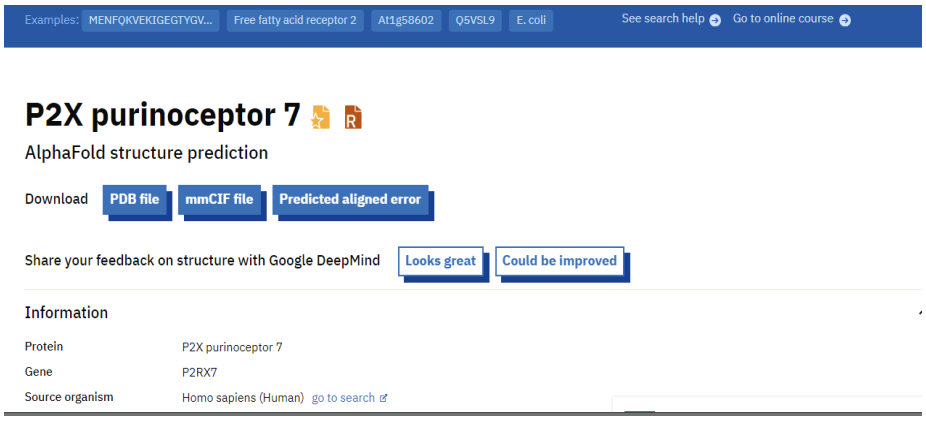

Figure 32: Interface Copy of downloading the PDB file of P2X7R

II.2.1.1.Protein preparation After obtaining the 3D structure of each target (**P2X7, NAE1),** Converting the protein from the PDB format to the PDBQT format using the Autodock

- The first step is to open a file (Figure 33) to save the 3D protein obtained from the PDB database

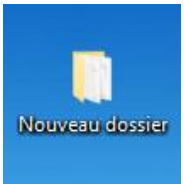

Figure 33; Example of opening a new document ['computer acer intel HD 500 GB HDD file].

- The second step is to open the program "AutoDock Tools"

[Edit, Delete, Delete All Molecule, CONTINUE]. Now we bring a protein from a file to a program and prepare it with the following operations (Figure 34)

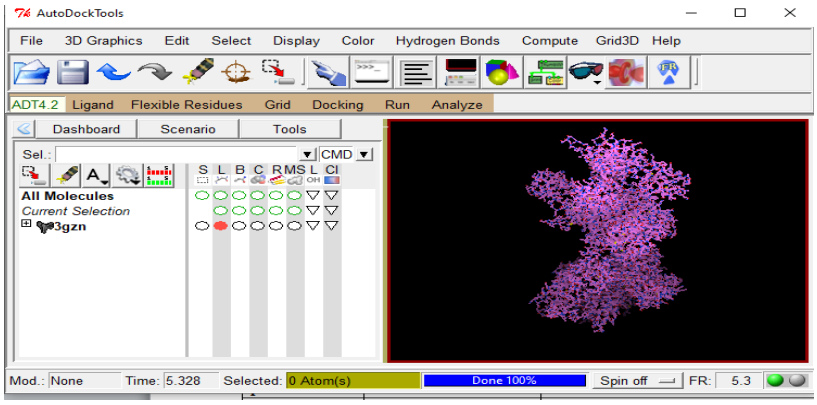

Figure 34: Interface Copy of NAE 1 in the autodock

- Edit Add Delete water if present in the molecule **[Edit->Delete Water] (Figure 35)**.

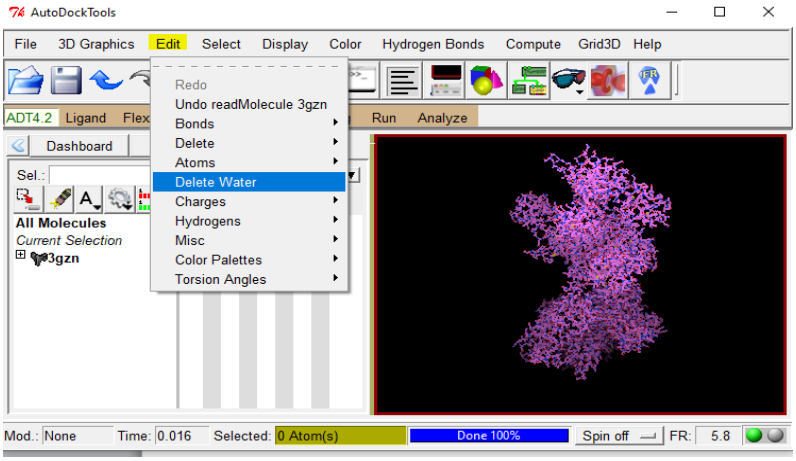

Figure 35: Interface Copy of delete water from NAE1

- Add charges **[Add Kollman Charges, ok]** (Figure 36).

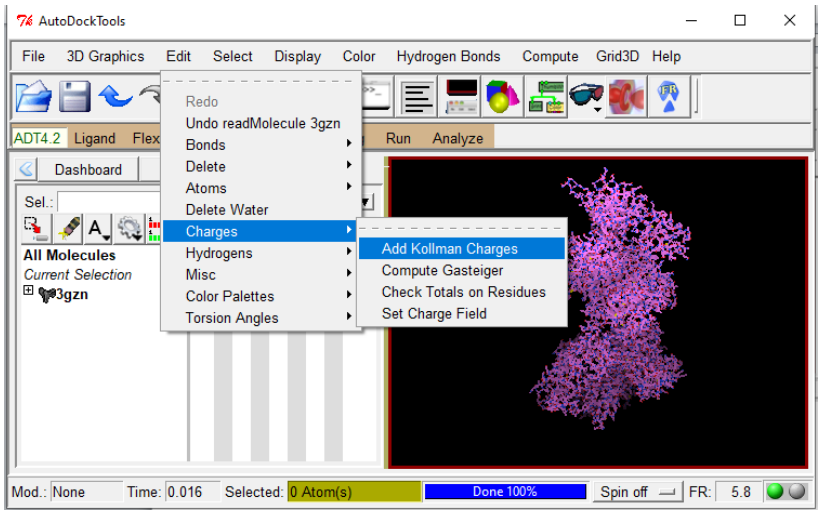

Figure 36: Interface Copy of adding charges

- Add Hydrogen to protein **[Edit , hydrogens , Add , polar Only , ok]** (Figure37).

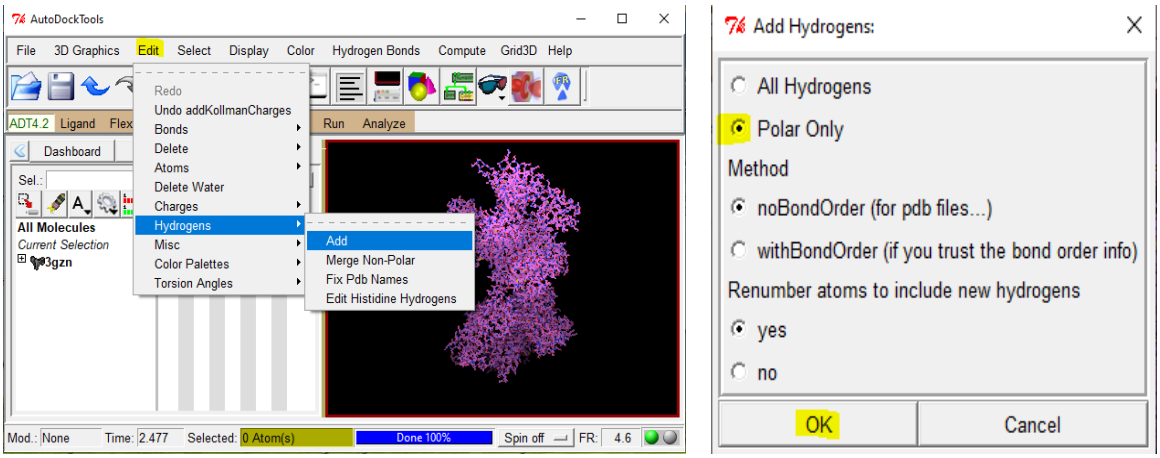

Figure 37: Interface Copy of adding hydrogen atoms

- Then save the changes made **[grid, macromolecule, choose]** and a window appears in (Figure 39) we save the changes in the previous file with the name protein PDBQT.

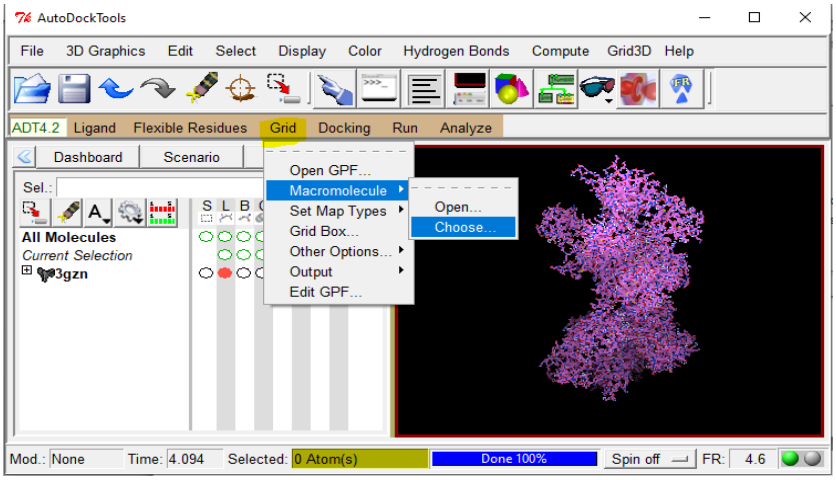

Figure 38: Interface Copy of saving the change made

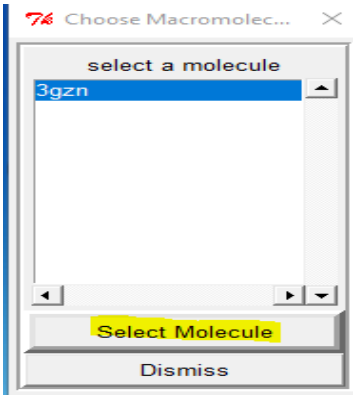

Figure 39: Interface Copy of the window to choose the protein to save

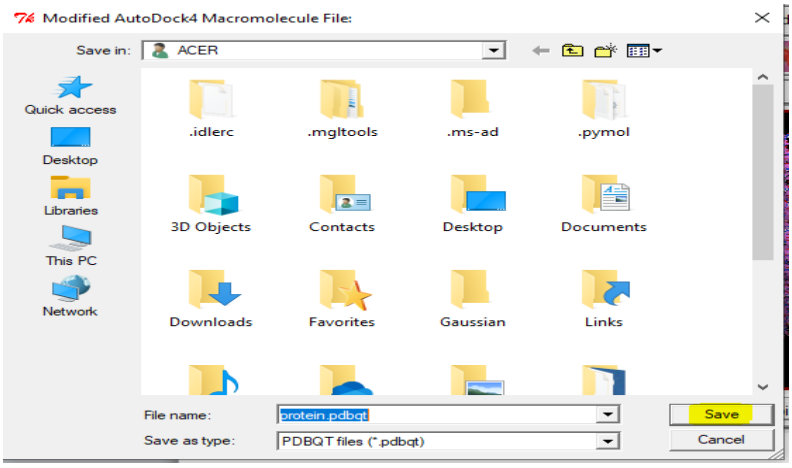

Figure 40: Interface Copy of saving the file with the name protein PDBQT.

II.2.2.Inhibitors (ligand)

The data on chemical constituents in sage, fenugreek and date seeds was obtained from Pubchem database, about **75** compounds.

41 compounds remained after double-listed compounds were eliminated. The SwissADME database predicted these compounds' drugability. Where we set Lipinski violation = 0, and gastro-intestinal=high. We used the ProTox-III webserver, to predict the toxicity of these compounds, and from the results of molecular docking of each molecule where the best interaction between molecule and receptor is high. With these criteria ultimately led to the selection of **6** biologically active compounds

The first step is to download the molecules from the database Pubchem we download them in 3D in the previous file.

Table 3: Molecules choosed to target our proteins

Plants	Molecules	Structure 3D
Trigonella	**Tricin**	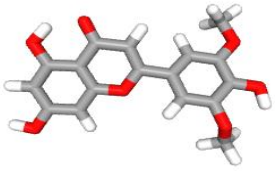
	Olmelin	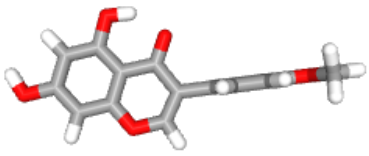
	7,4'-dihydroxyflavone	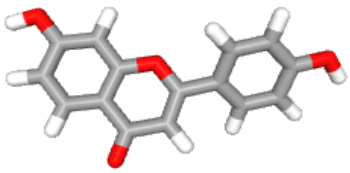

Phoenix D	**Tricin**	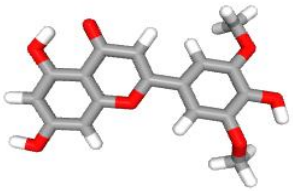
	Apigenin	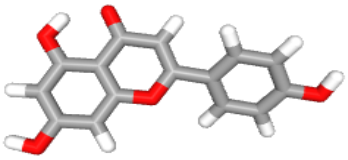
Salvia Officinalis	**Linalool**	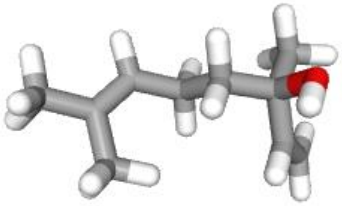
	Carnosol	

II.2.2.1.Preparation of ligand

II.2.2.1.a.Optimization of molecules

The collected structures of the phytochemicals were further optimized by semi-empirical PM6 method coded in the computational program Gaussian 09 W

- First, we should open the ligand file with GaussView app (Figure 41)

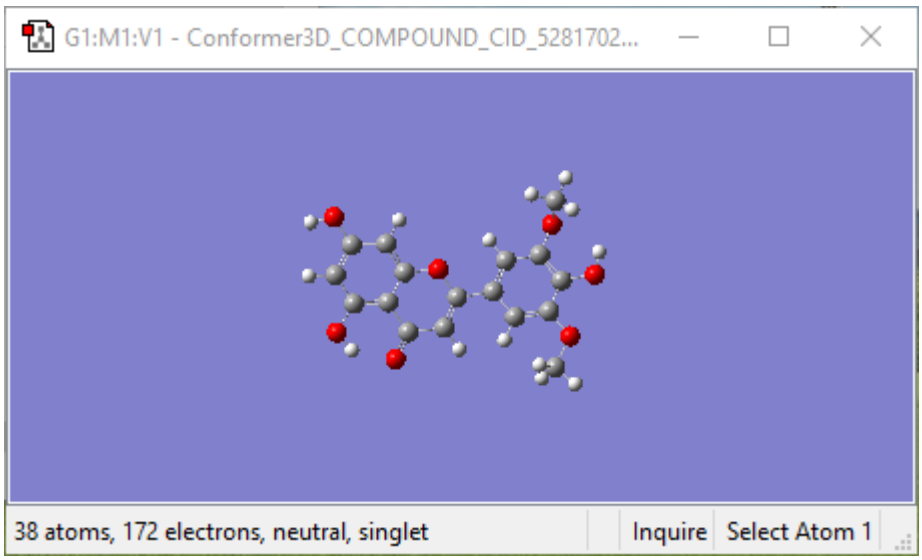

Figure 41: Interface Copy molecule of Tricin in GaussView

Click on **[calculate, Gaussian calculation setup]**(Figure 42)

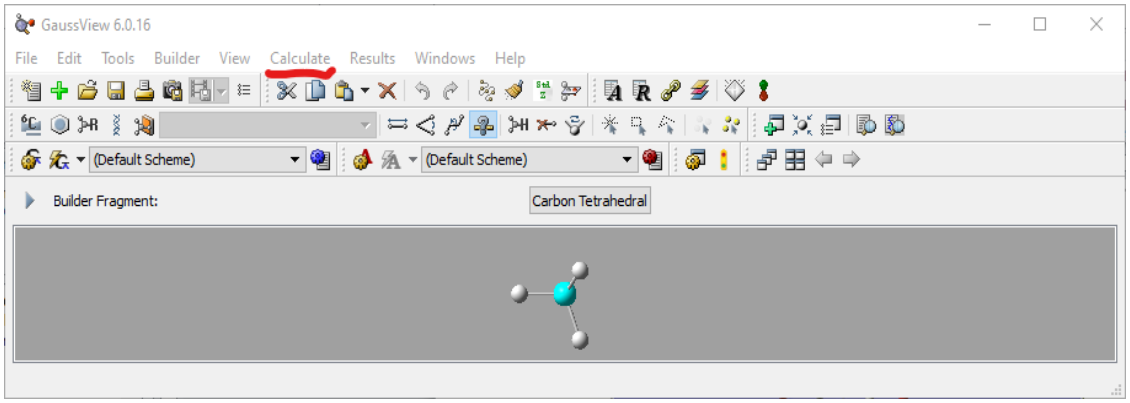

Figure 42: Interface Copy of choosing calculate

Change the type of job **[job type, energy , optimization]**(Figure 43)

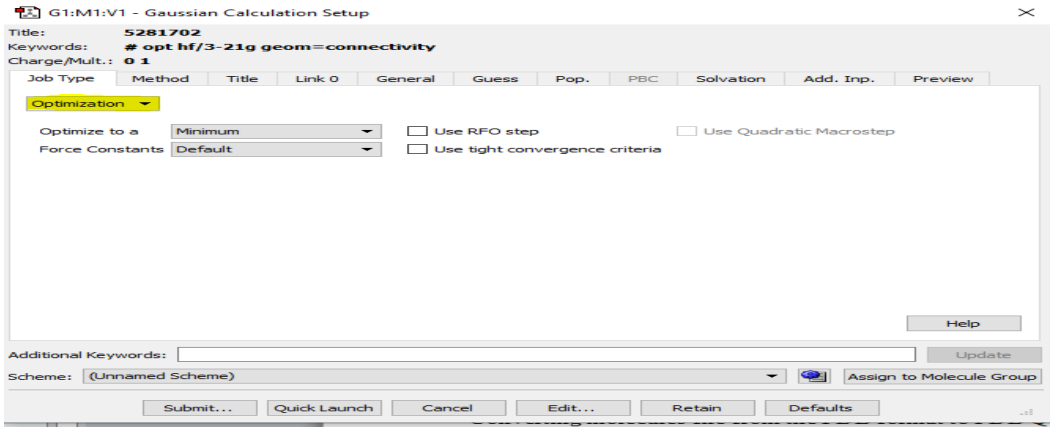

Figure 43: Interface Copy of selecting the job type optimization

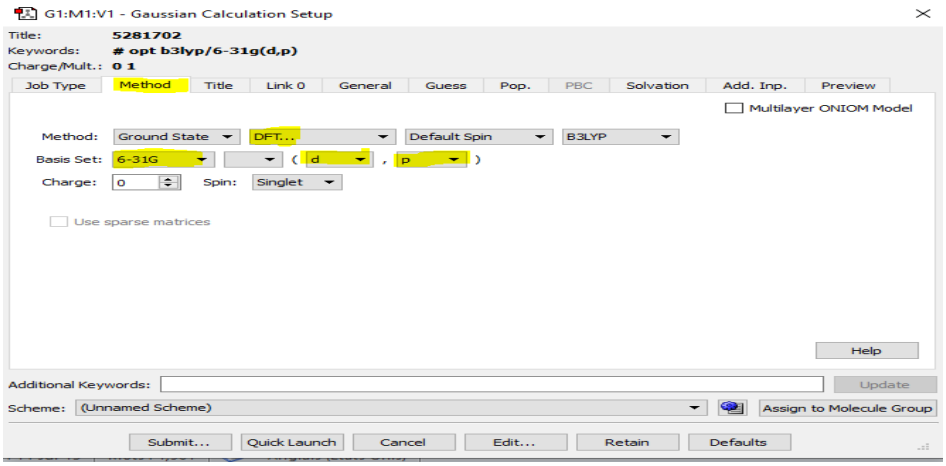

Figure 44: Interface Copy of DFT condition

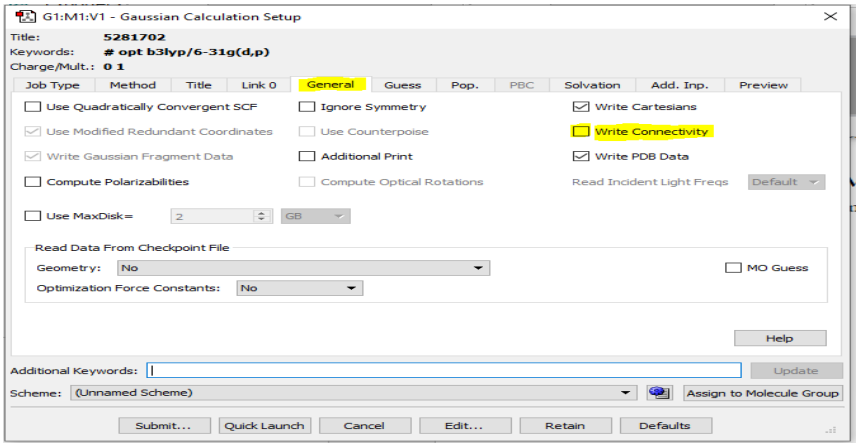

Figure 45: Interface Copy of general condition

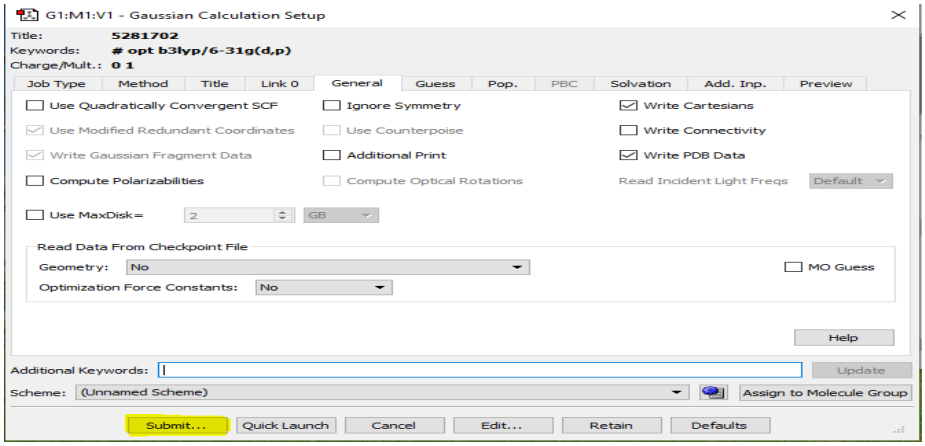

Figure 46: Interface Copy of submitting the job

- The optimized structures were converted to the PDB format by using the program GaussView 5.0.(Figure 47)

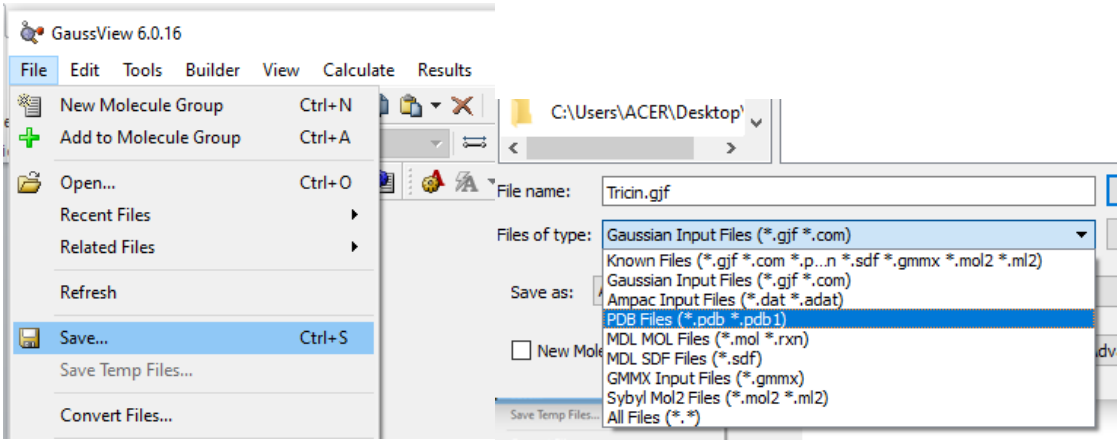

Figure 47: converting the file from GJF format to PDB format

- Converting molecules file from the PDB format to PDB QT using the AutoDock tools

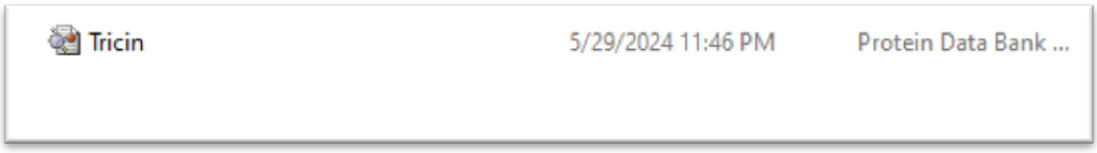

Figure 48: Interface Copy of molecule of Tricin optimized

- So we copy the molecule in the form of PDB in a program AutoDock Tools and it is after that we return to the program **[Edit , Delete ,Delete All Molecule , CONTINUE].**(Figure 49)

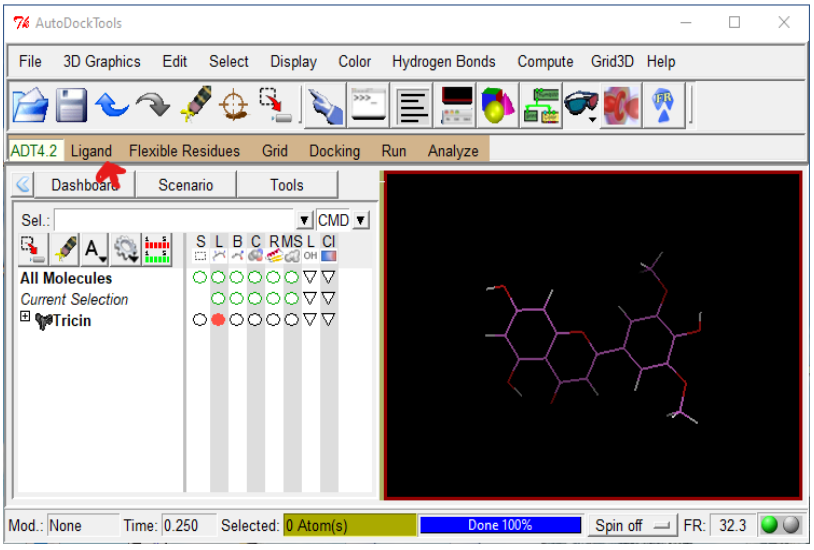

Figure 49: Interface Copy of the molecule Tricin optimized in Autodock tools

- Then we click on **[ligand, input, choose, select Molecule for Auto Dock, ok]** (Figure 50).

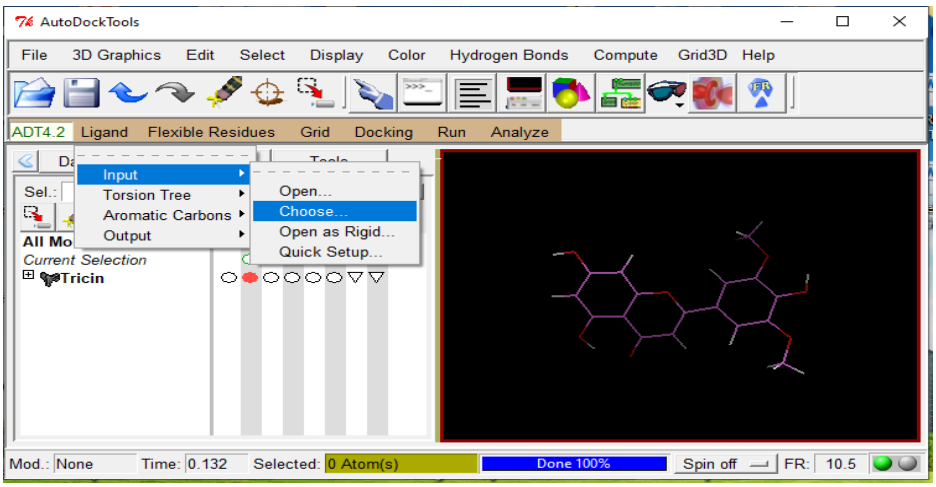

Figure 50: Interface Copy of input ligand

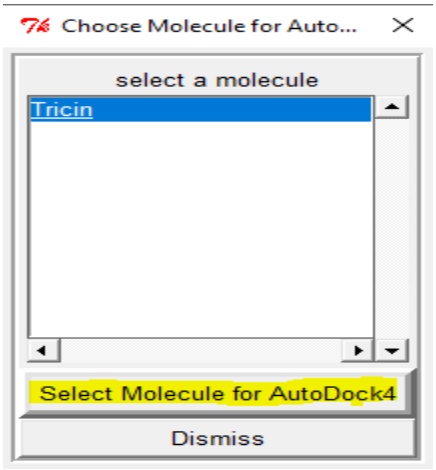

Figure 51: Interface Copy of the window to choose the protein to save

The next step is to save the changes by clicking **[ligand, Output, Save As PDBQT…]** we Call ligand.PDBQT and click save to Previous File (figure 51)

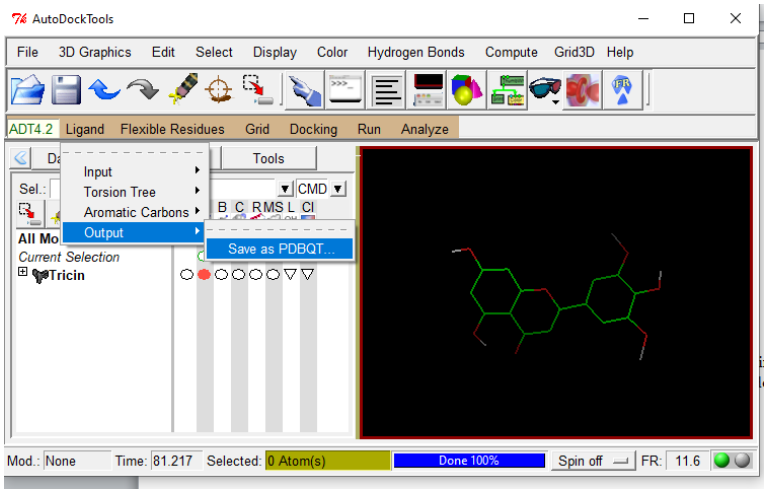

Figure 52: Interface Copy of steps for change the target to PDBQT

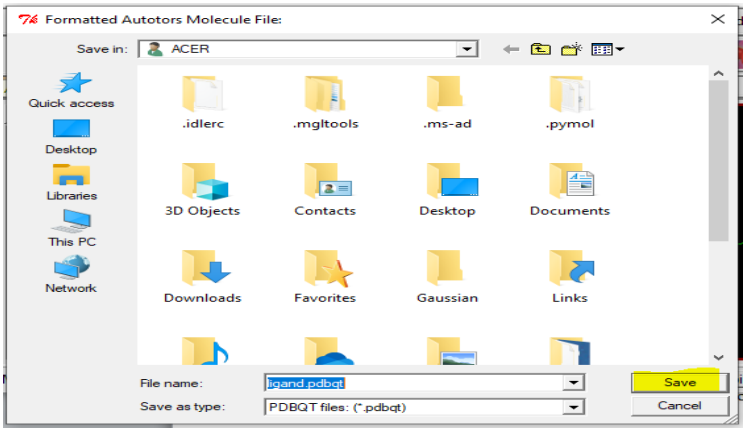

Figure 53: Interface Copy save ligand PDBQT to file

Now, both the ligand and the protein are prepared.

I.5.3. Protein-ligand docking

- The first step is to go back autodoock tools to A0
- The second step is to copy the protein. PDBQT into a program autodoock tools and we add the ligand.PDBQT (Figure 54).

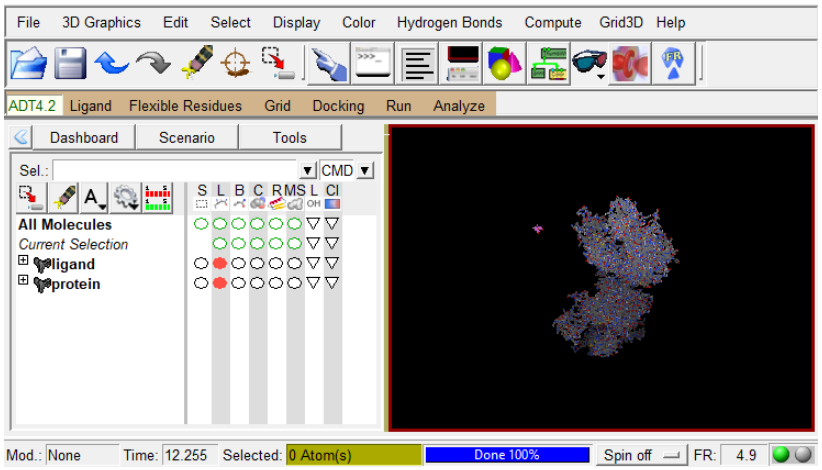

Figure 54: Interface for protein transcription. PDBQT in the Autodock Tools program and add ligand.PDBQT

- Now we click on **[Grid, Macromolecule, choose, ok]** copy a protein and click on Select Molecule (figure 55) and we click on **No.**

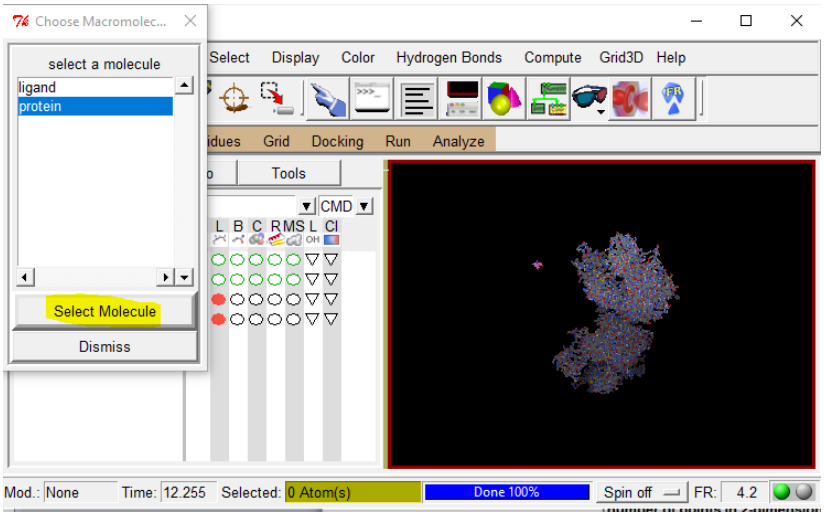

Figure 55: Identification interface of the selected protein molecule in the Autodock Tools.

- we click **[Grid , Grid Box]** (Figure 56)

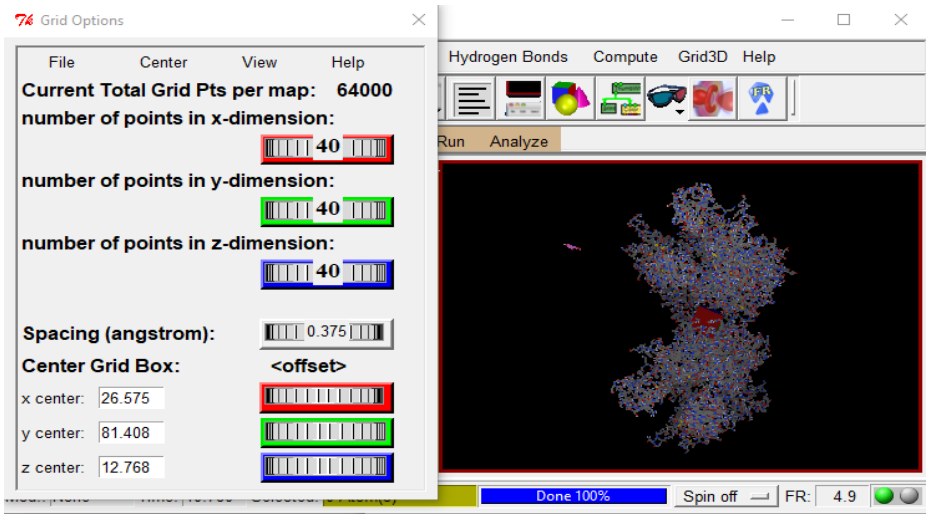

Figure 56: Interface of center Grid Box

- We click on **[File, Output grid dimensions file]** and save it as grid.txt in the previous file.
- We open the previous file and we find the changes we made, the information in file grid.txt (figure 57).

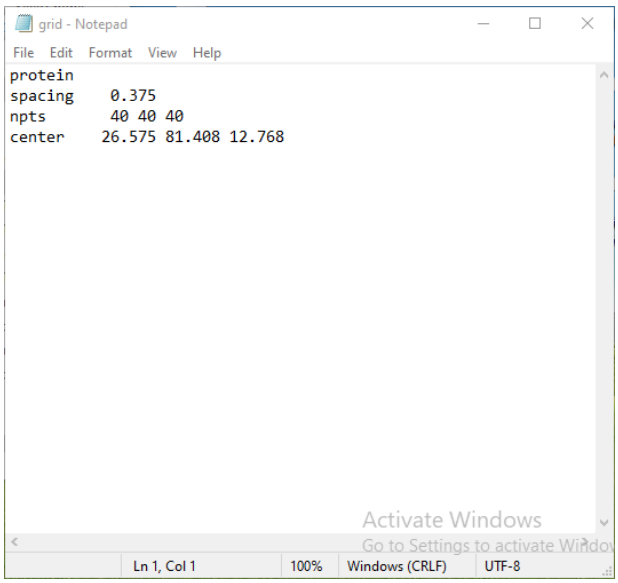

Figure 57: Interface of grid.txt

• We open the file txt and call it “conf” and put the information and dimensions which we will work with amarrage (figure 58).

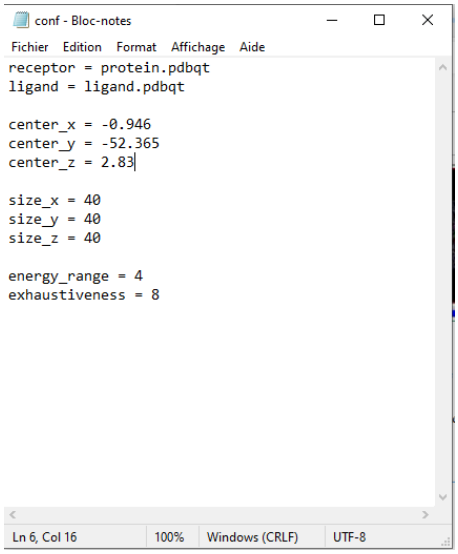

Figure 58: Interface of conf.txt

- In the previous file, we add 3 files from vina as follows **[vina , vina-licence , vina-split]** , After collecting in one file the PDBQT protein, ligand. PDBQT, grid and conf and 3

files from vina, we are now looking for Command Prompt (**cmd**) on the computer and open it (figure 59).

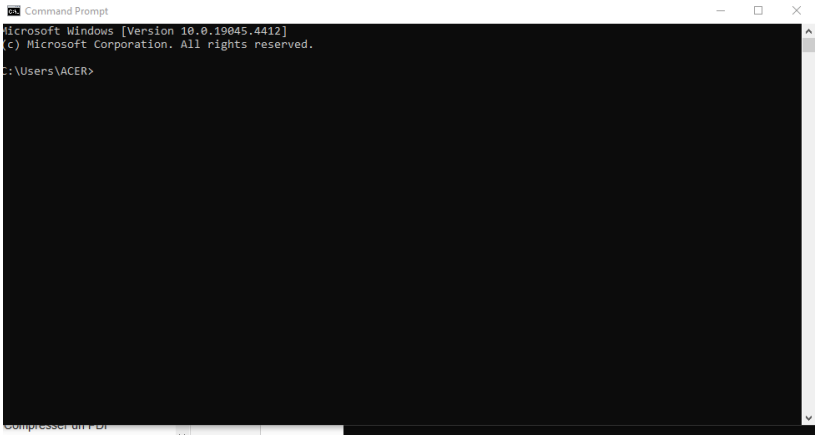

Figure 59: Interface of Command Prompt (cmd).

• We write cd and then copy the link in the previous file containing the information we changed earlier, then paste it in cmd and press Enter and type **[vina.exe - - config config .txt - - log log.txt]** and press the enter button and wait for it to appear In the file two files log.txt (figure 60) and ligand-out. PDBQT

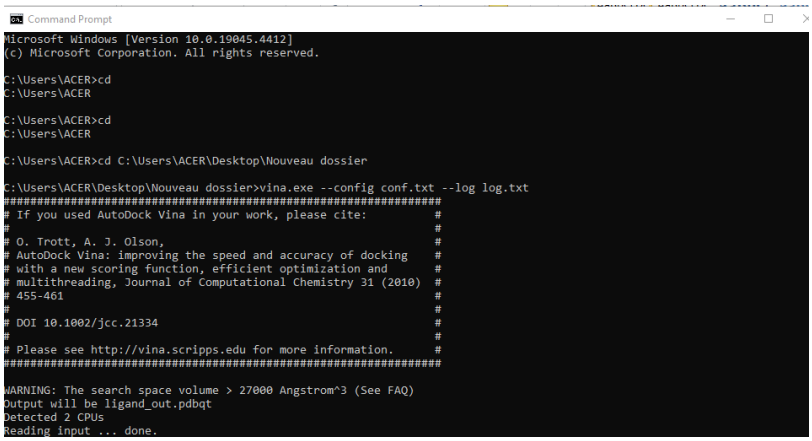

Figure 60: Interface of cmd execution

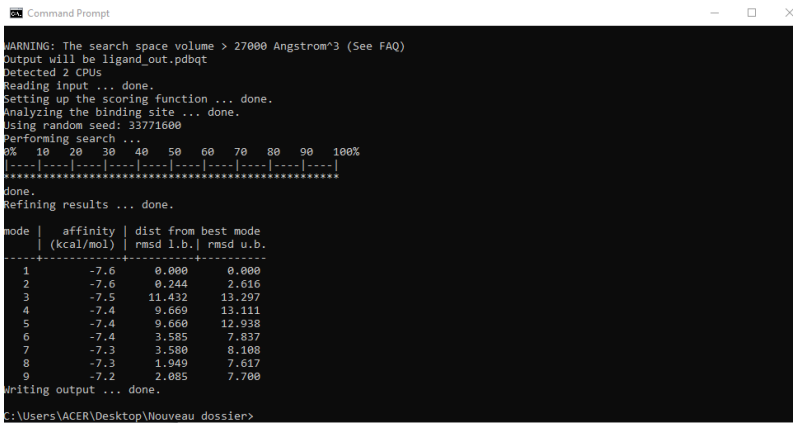

Figure 61: Interface of table in the form of energy

When I search, two files appear when the search is finished from cmd in the previous file as follows log and ligand-out. PDBQT in which the search results are

- At the last stage, we open a program BIOVIA Discovery Studio, We click on a file and then open it and then display the open dialog box and choose the previous file to open it and click on all files and then choose ligand-out. PDBQT and click on open and it appears on BIOVIA Discovery Studio and then click on the first box ligand-out-model-0, we repeat the same process and get protein. PDBQT, then we remove the ligand groups by copying it and clicking on Delete we copyligand-out-model-0and paste it at protein. PDBQT, and click on ligand Interaction and convert it to show 2D Diagram (figure 62).

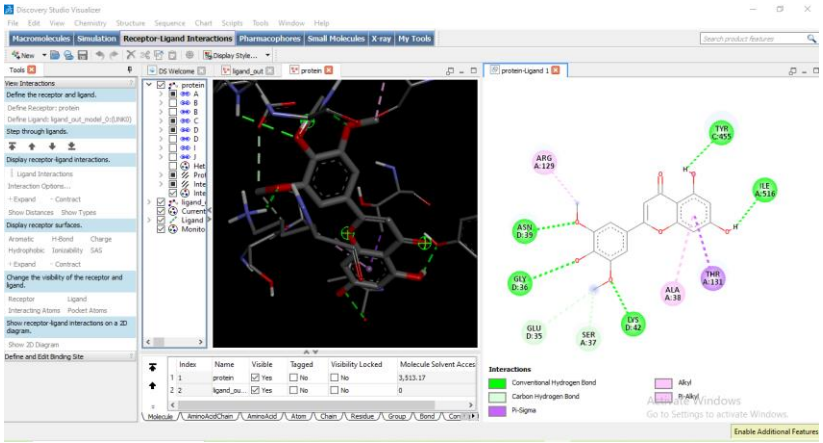

Figure 62: interfaces for ligand-out. PDBQT in program BIOVIA Discovery Studio and add protein. PDBQT show 2D Diagram and Interaction and charge.

- We do The same applies to the rest of the proteins and ligands

Conclusion

This review outlines new research on the crucial role that molecular docking plays in the drug discovery and development process. Using the docking strategy will help create a dosage form in the fastest and most efficient way possible

II.3.Emulsuspension formulation

II.3.1.suspension

Suspension formulation involves the creation of a stable mixture of a drug in a liquid vehicle, often water. The goal is to ensure that the drug particles remain suspended uniformly throughout the liquid, maintaining their intended therapeutic activity and preventing settling or sedimentation**.[177]**

II.3.2.Emulsuspension

Emulsuspension formulation strategies involve combining the principles of emulsions and suspensions to create stable and effective drug delivery systems.**[178]** Emulsuspensions are complex formulations where solid particles are suspended in an emulsion system. These particles can be located in the oil phase, the aqueous phase, or at the oil-water interface, providing enhanced stability and versatility**.[179]**

II.3.2.Equipment used

II.3.2.1.Equipment

- Thermometer
- pH meter
- Oven
- vacuum pump

II.3.2.2.Glassware

- Vials
- Beakers
- Filter funnel
- Magnetic rung

II.3.3.Scanning

We made two sweeps the first was for the suspension (Table 4) to know the quantity of clay we should use, the second was for the emulsuspension formulation (Table 5).

- Our suspension contain (water+ clay)

Table 4: Scanning of the quantity of clay for the best suspension

Water(ml)	**80**	**80**	**80**	**80**	**80**	**80**
Clay (g)	**2**	**2.5**	**3**	**3.5**	**4**	**4.5**

Table 5: Scanning of the formulation

	1	2	3	4	5	6	Role
Material Name	g/ml	g/ml	g/ml	g/ml	g/ml	g/ml	
Salvia officinalis	6.25	6.25	6.25	6.25	6.25	6.25	PA
Trigonella	6.25	6.25	6.25	6.25	6.25	6.25	PA
Phoenix	6.25	6.25	6.25	6.25	6.25	6.25	PA
purified Water	80	80	80	80	80	80	Solvent
Clay	2	2.5	2.5	3	3.5	2.5	Polymer
Olive oil	6.25	6.25	6.25	6.25	6.25	6.25	Conservative
Soap	2	3	4	4	5	3.5	emulsifying agent

II.3.4.Manufacture directions

1- Add 80ml water purified to a stainless steel manufacturing vessel and heat to 60 °C TO 70°C.
2- Add 2.5 g of clay powder and mix well
3- Put all the lipids (olive oil; bio extract fenugreek, palm date and sage) and mix the ingredients
4- Add 3.5 g of soap and mix the all from 5 to 10min.

All the steps of the formulation are shown in the following images:

Step 1:

Figure 63: Put the water over the oven until it reaches 70 degrees

Step 2:

Figure 64: adding clay

Step 3:

Figure 65: Adding the bio extracts of the three plants

Finally step 4: Add 3.5g of soap and mix well.

II.3.5. Sterility test of formulation

To test the sterility of final formulation, place the product on absorbent paper and apply to a nutrient Agar and incubate in the oven for 24 h at 37 ^{0}C to determine the viral load.

II.3.6. Stability test of formulation

We put the finished product in a test tube and center it every 5 min and 10min and at speed 2000 tour/ min and 4000tour/min

Figure 66: Centrifuge material

Conclusion

This part approves the antioxidant activity and antimicrobial activity of the three plants.

The molecules that inhibit the P2X7 receptor was 7,4'-dihydroxyflavone from *Fenugreek*, Linaool, and carnosol from sage. We can make inhibition of NEDD8 by targeting the activating enzyme of neddylation NAE1 using Tricin, Olmelin and 7,4'-dihydroxyflavone from the *Fenugreek* and by Tricin and Apigenin from *palm date* extract.

We made a new type of pharmaceutical formulation which is emulsuspension.

III. Results and discussions

III.1. Introduction

This side presents the results collected from the in vitro and in silico studies that we have done in the previous study and their interpretations.

III.2.In vitro

III.2.1.Extraction yield

(1) **(2)** **(3)**

Figure 67: Filtration of extract **(1)** *Sage* **(2)** *Fenugreek* **(3)** *Date seeds*

$$R\ (\%) = ((P0 - P1) / P0) * 100$$

R: Yield.

P_o: initial weight.

P1: Weight after extraction and drying.

- **Yield calculation** : calculating yield extraction for *salvia officinalis*

$$R\ \% = \left(\frac{20-12.06}{20}\right) \times 100 \quad \Longrightarrow \quad R\%=39.7\%$$

The average yields of the prepared extracts were calculated according to the plant matter

Table 6: shows the yields obtained

Plant	Solvent	Initial weight	Final weight	Yield%
Salvia officinalis	Ethanol+ water (80%+20%)	20g	12.06g	39.7
Trigonella foenum-graecum	Ethanol+water (70%+30%)	20g	13.97g	30.15
Phoenix dactylifera L seed	Ethanol+ water (80%+20%)	20g	14.88g	25.6

The yield of the extraction of ethanolic extracts obtained by maceration from sage, date seeds and fenugreek is 39.7%, 25.6% and 30.15% respectively. This yield is obtained after a period of 72 hours.

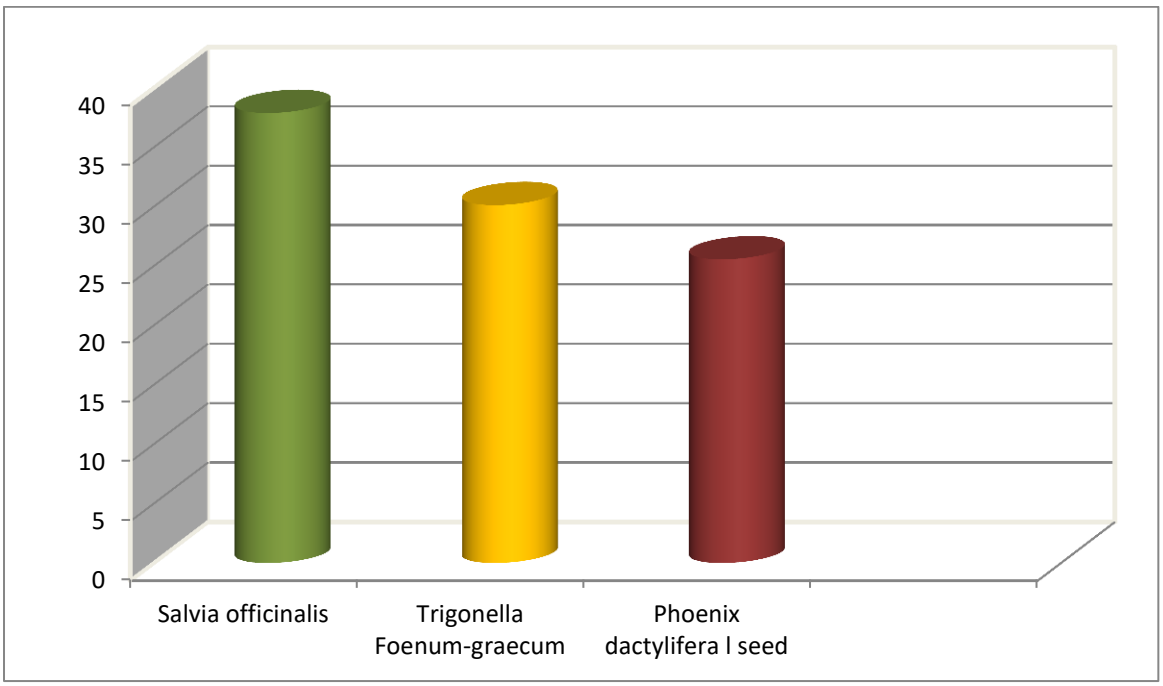

Figure 68: Histogram of the yield of ethanolic extracts

Table 7: shows the appearance of the plants extract

Plant / Appearance	Sage	Fenugreek	Date seeds
color	Green	yellow	Reddish-brown
Characteristic smell	Yes	Yes	Yes

III.2.2. Physicochemical study of extracts

III.2.2.1. Physicochemical analysis

Table 8: shows the pH, Density, and Conductivity results analyses

Plant	*Sage*	*Fenugreek*	*Date seeds*
pH extract	5.239	6.252	5.344
Density(g/cm^3)	0.4836	0.9807	0.4322

III.2.2.2.visible UV

To determine the Wavelength λmax of our extracts in fact a scan in the interval [$400nm - 800nm$] we find different wavelengths for each extract:

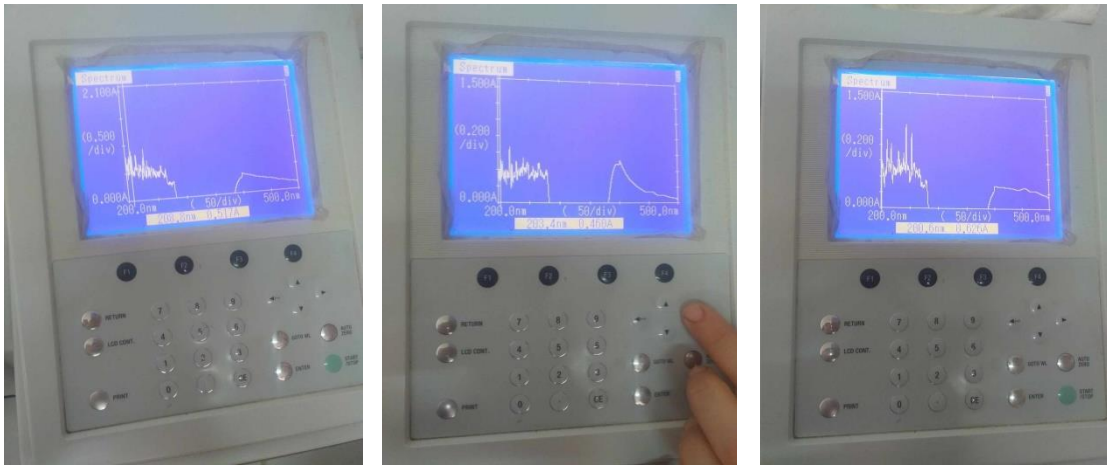

(1): *Sage* **(2): *Fenugreek*** **(3): *Date seeds***

Figure 69: Represent the UV scan of the three plants**. (1): *Sage,* (2): *fenugreek*, (3): *date seeds***

Table 9: The different wavelengths of each plant

Sage		*Fenugreek*		*Date seeds*	
$\lambda_{max}(nm)$	Abs	$\lambda_{max}(nm)$	Abs	$\lambda_{max}(nm)$	Abs
401.2	0.357	401.0	0.523	455.2	0.273

The maximal wavelengths are shown in the table

III.2.2.3. Chemical composition analysis (GCMS)

Chemical analysis of ethanolic extracts of *Sage* (*Salvia officinalis), Fenugreek* (*Trigonella foenum-graecum*), by phase chromatography gas coupled to mass spectrometry (GC - MS) have allowed to obtain the results summaries below.

GC-MS gas chromatography mass spectra reveal that our extract contains different molecules, with a retention time and a molecular weight characteristic of each molecule.

- ***Salvia officinalis:*** Chromatogram of ethanolic *salvia officinalis* obtain with maceration ,see figure below

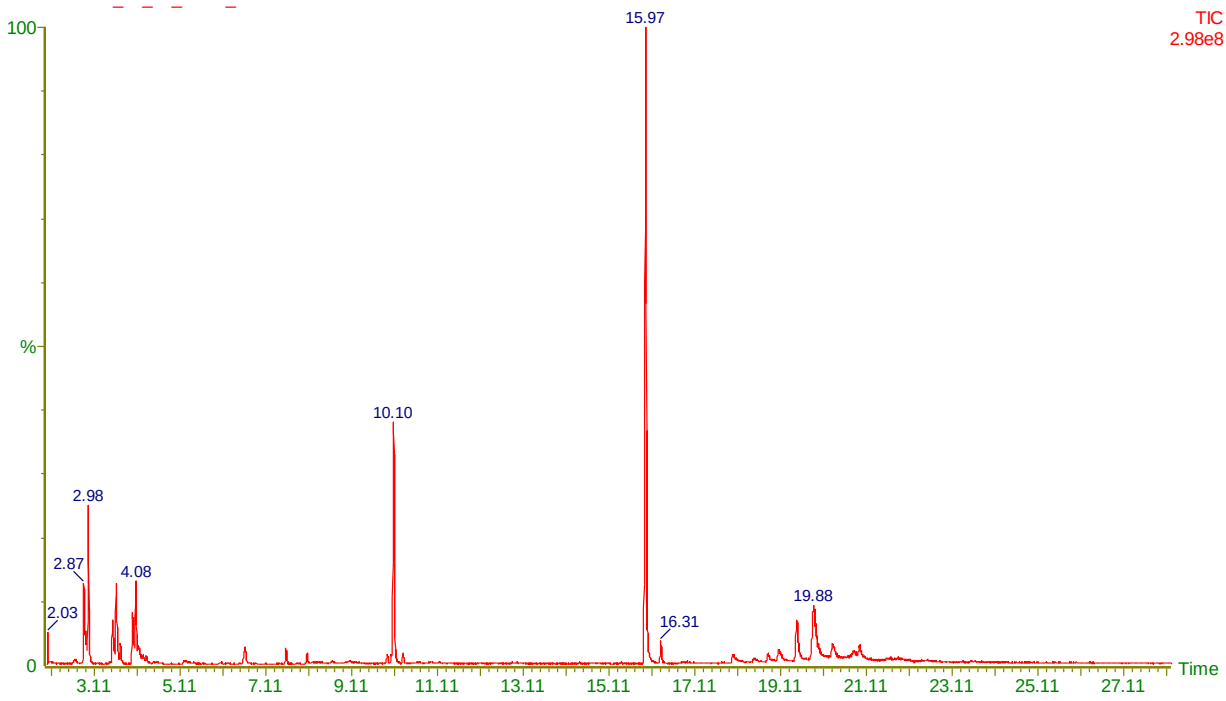

Figure 70: Chromatogram of ethanolic *sage*

Mass spectrum:

a) 3,7-dimethylocta-1,6-dien-3-ol t=2.98 min

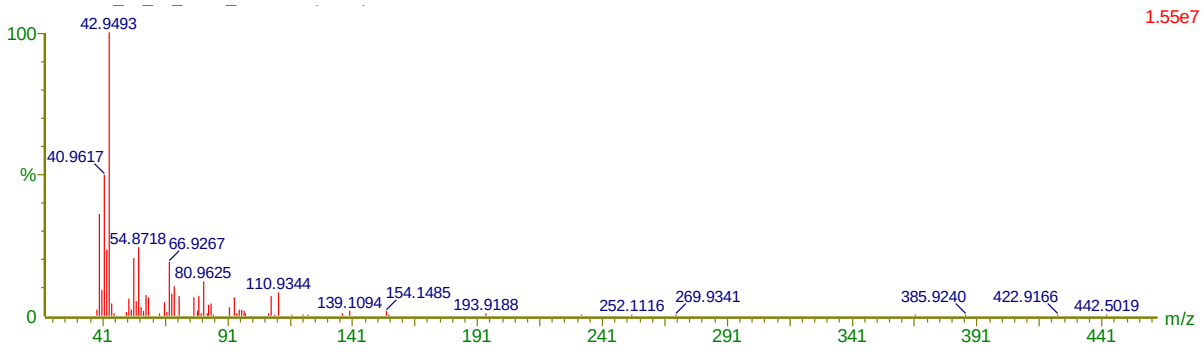

Figure 71: Mass spectrum of 3,7-dimethylocta-1,6-dien-3-ol with a retention time of 2.98 min.

b) 2, 5-Octadiene t=3.63 min

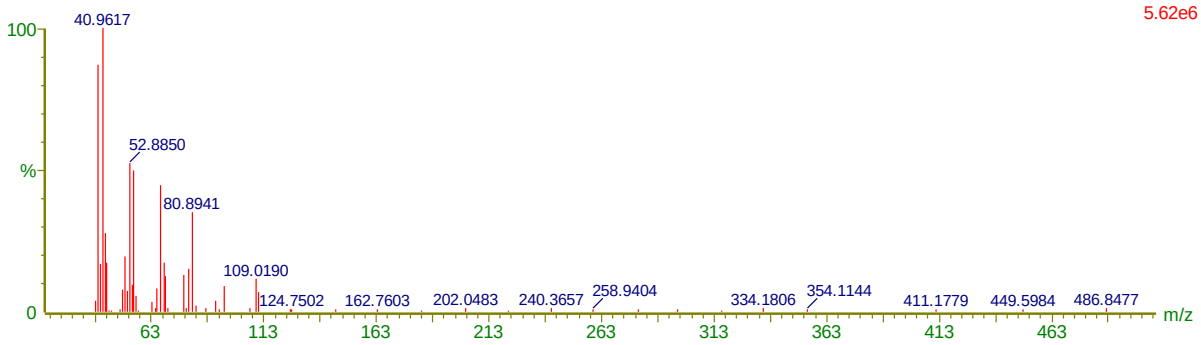

Figure 72: Mass spectrum of 2, 5-Octadiene with a retention time of 3.63 min.

c) 4-Mythyl-1, 4-heptadiene t=4.08 min

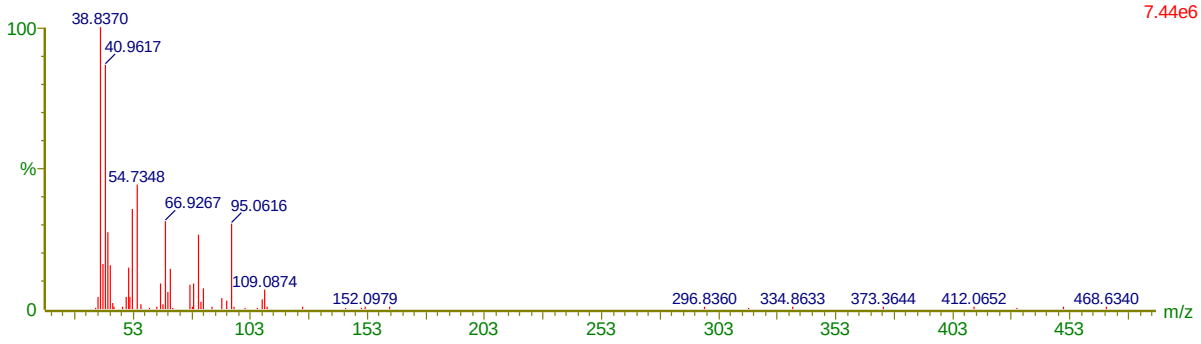

Figure 73: Mass spectrum of 4-Mythyl-1, 4-heptadiene with a retention time of 4.08min.

d) Caryophyllene diepoxide t=10.10min

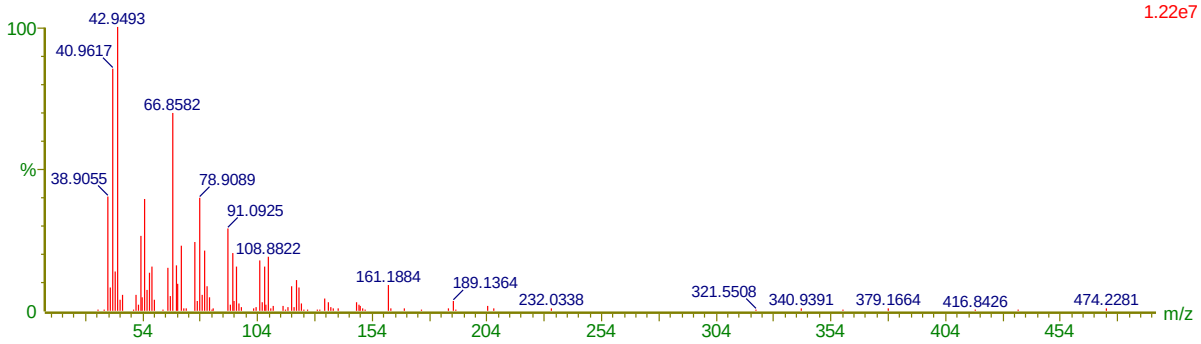

Figure 74: Mass spectrum of Caryophyllene diepoxide with a retention time of 10.10min.

e) 1, 3-Dioxane, 5, 5-dimethyl-2-(1-methylthenyl) t=19.49 min

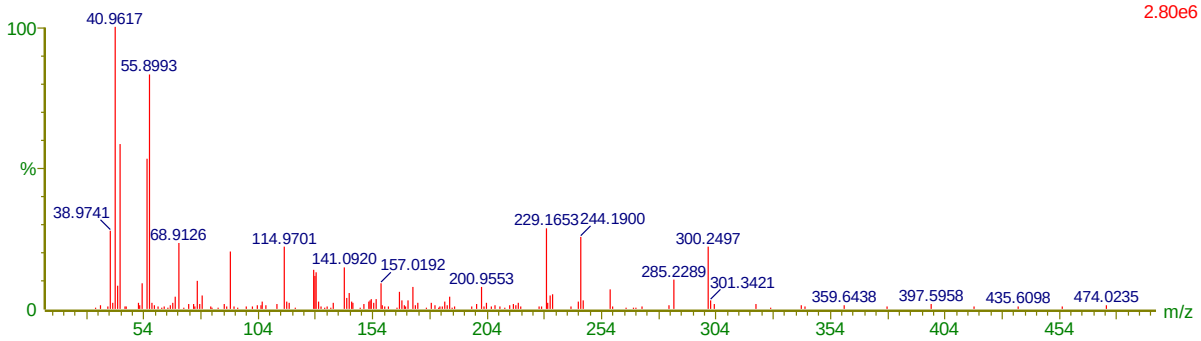

Figure 75: Mass spectrum of 1, 3-Dioxane, 5, 5-dimethyl-2-(1-methylthenyl) with a retention time of 19.49min

f) 1,3-Dioxane ,2-isopropenyl-5,5-dimethyl t=19.88

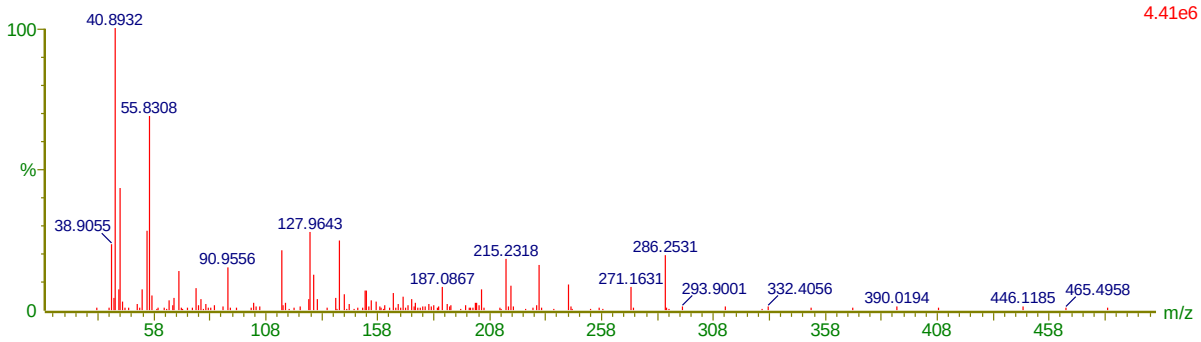

Figure 76: Mass spectrum of 1, 3-Dioxane, 2-isopropenyl-5, 5-dimethyl with a retention time of 19.88 min

Table 10: Molecule compounds of extract sage obtained by CG-MS analysis

Molecule	Retention time (min)	Molecular weight(g/mol)
3,7-dimethylocta-1,6-dien-3-ol	2.98	154.25
2, 5-Octadiene	3.63	110
4-Mythyl-1, 4-heptadiene	4.08	110
Caryophyllene diepoxide	10.10	236
1, 3-Dioxane, 5, 5-dimethyl-2-(1-methylthenyl)	19.49	156
1,3-Dioxane ,2-isopropenyl-5,5-dimethyl	19.88	170

- ***Trigonella foenum-graecum**:* Chromatogram of ethanolic *fenugreek* obtain with maceration ,see figure below

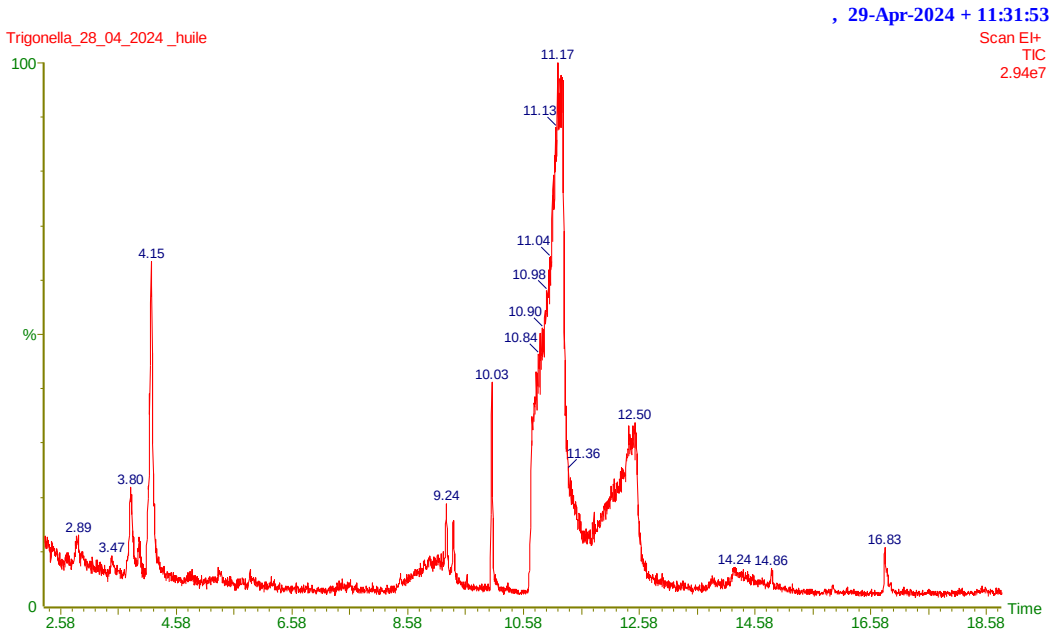

Figure 77: Chromatogram of ethanolic *fenugreek*

Mass spectrum:

a) N-heptane skellysole t=2.8

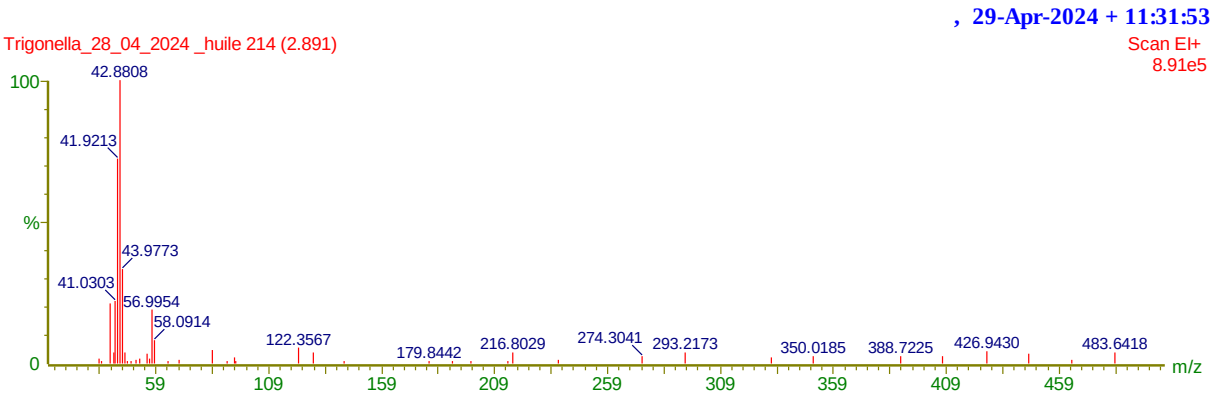

Figure 78: Mass spectrum of N-heptane skellysole with a retention time of 2.8 min

b) 1-Butanol, 3-methyl t=3.80 min

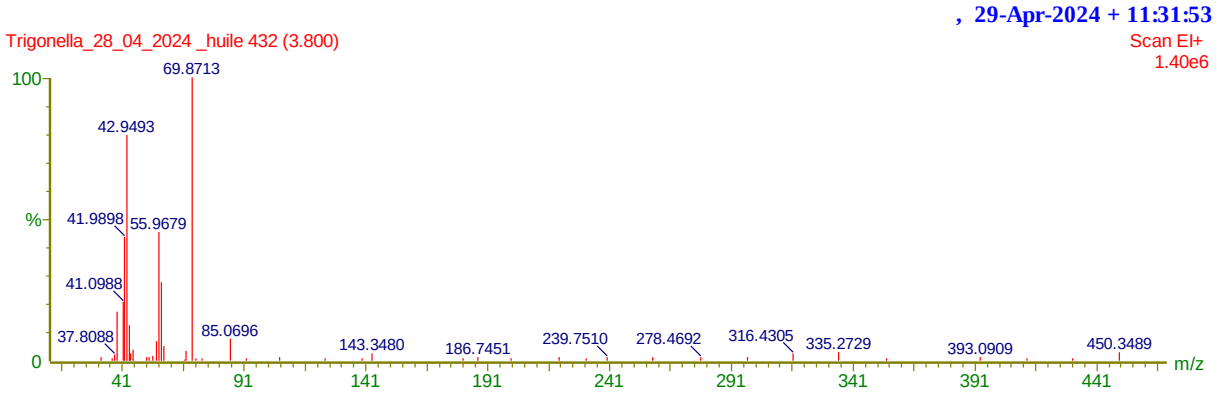

Figure 79: Mass spectrum of 1-Butanol, 3-methyl with a retention time of 3.80min

c) Heptane,3,4-dimethyl t=4.15 min

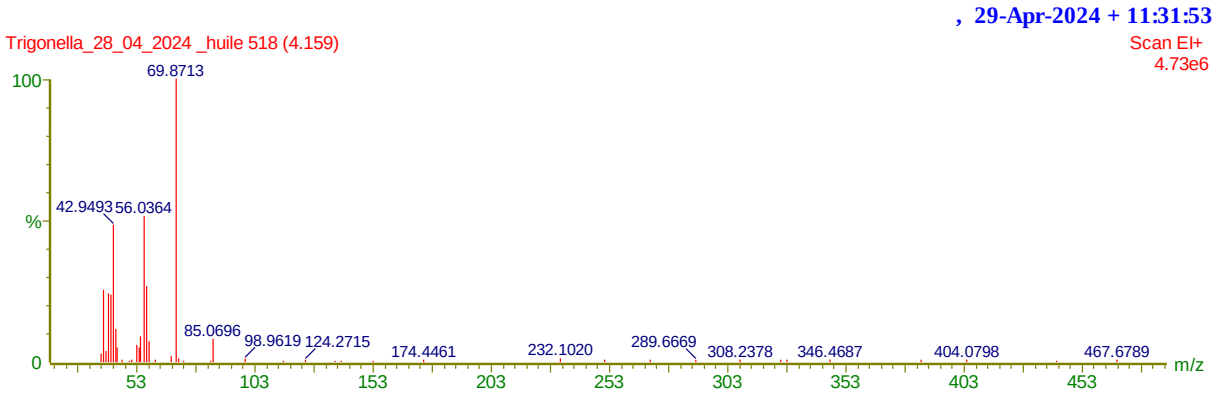

Figure 80: Mass spectrum of Heptane, 3, 4-dimethyl with a retention time of 4.15min

d) Hexanoic acid t=11.17 min

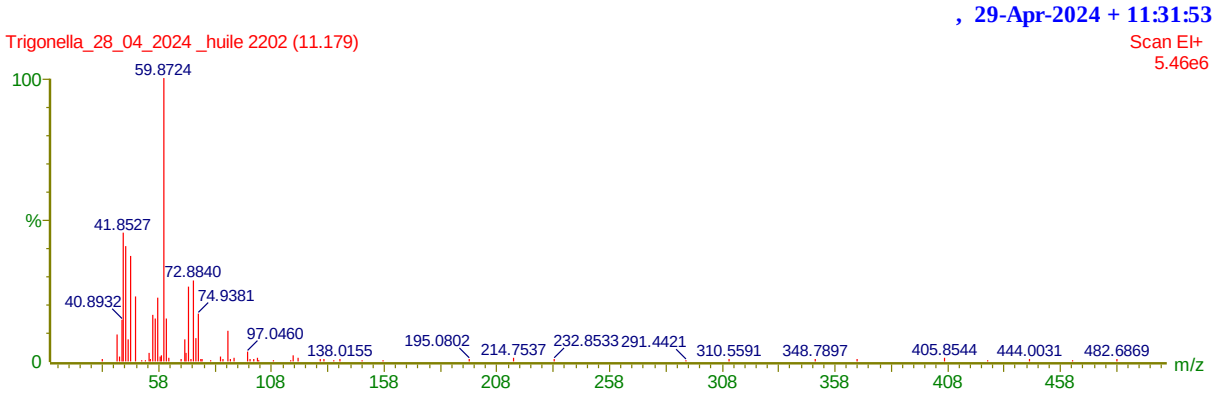

Figure 81: Mass spectrum of Hexanoic acid with a retention time of 11.17min

e) 5-Acetyl-longipinandiolone t=16.83 min

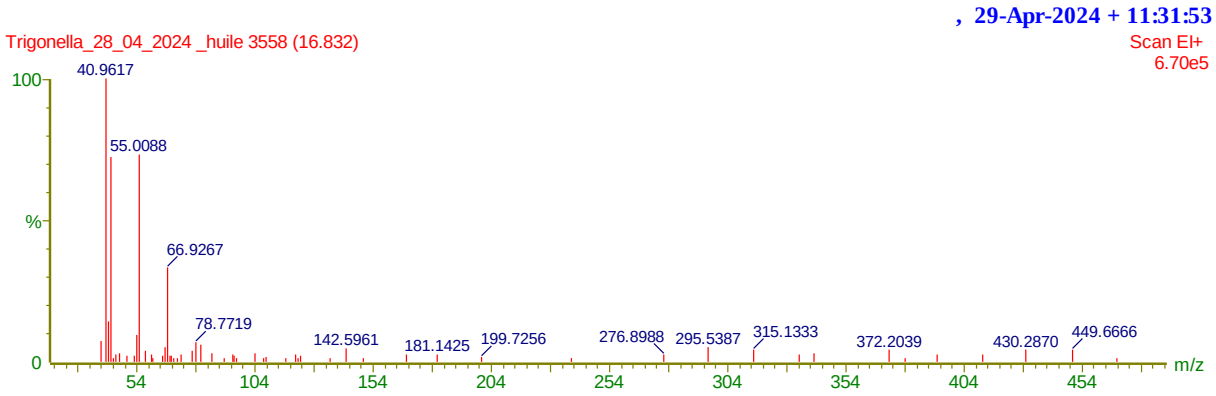

Figure 82: Mass spectrum of 5-Acetyl-longipinandiolone with a retention time of 16.83min

Table 11: molecule compounds of extract fenugreek obtained by CG-MS analysis

Molecule	Retention time (min)	Molecular weight(g/mol)
N-heptane skellysole	2.89	72
1-Butanol, 3-methyl	3.80	88
Heptane, 3,4-dimethyl	4.15	128
Hexanoic acid	11.17	116
5-Acetyl-longipinandiolone	16.83	294

Optimal conditions used for this study:

- Equipment: GCMS model CLARUS 500 from Perkin-Elmer

GC method:

- Injected volume: 1ul
- Injector temperature: 250 deg
- Column: Elite series 5-MS, 30 m, 0.25 mmID, 0.25 um stationary phase thickness

Temperature programming:

- Initial temperature: 70 deg for 4 min
- Ramp: 4deg/min to 220 deg for 15 min
- Analysis time 56.5 min

MS method:

- Ionisation mode: Electron impact
- Energy: 70 ev
- Temperature: source: 250 deg
- Transfer line temperature: 250 deg
- Solvent delay: 5.9 min
- Software: TURBOMASS

Component identification by searching spectral libraries: NIST, PFLEGER, NBS,WILEY

III.2.1.4. Antioxidant activity

The antioxidant activity of sage, fenugreek and date seeds extract was determined by reducing the free radical DPPH.

III.2.2.4. a. Determination of antioxidant activity

To evaluate the antioxidant effect of *sage*, *fenugreek* and *date seeds* extracts by 2,2'-diphenyl-1-picrylhdazyl (DPPH) radical technique was used.

Indeed, it is the one that is used all over the world **[174]** and the most widely used to screen the anti-radical activity of a single compound or a mixture of compounds **[174].**

The DPPH radical is one of the most commonly used substrates for the rapid and direct assessment of antioxidant activity due to its stability in radical form and its simplicity of analysis **[175].**This spectrophotometric method uses the violet-colored DPPH (2,2'-diphenyl 1picrylhydrazyl) radical as a reagent, which turns yellow in the presence of RLS sensors, and is reduced to 2,2'-diphenyl-1-icrydrazine **[175].**

After 30 min of incubation of the DPPH-extract solution (at different concentrations), the violet color turns to yellow.

This color change is due to the reduction of DPPH, which shows that the sample has a DPPH

The values obtained allowed to draw exponential curves with the presence of a stationary phase which signifies the almost total reduction of DPPH in its non-radical form.

From these curves, it is possible to determine the percentage of inhibition obtained as a function of the concentrations used as well as the value of IC50 of each extract.

We tested the extract of sage, fenugreek and date seeds, the values obtained allowed to draw curves, the results represented in showed us that the reduction in capacity is proportional to the increase in the concentration of our samples.

The results of DPPH are summarized in table and figure, which indicates the uptake of DPPH as a function of extract concentration, with increasing uptake.

Figure 83: DPPH incubation of sage, fenugreek and date seeds extracts at different concentrations.

The antioxidant activity of the extracts can be visualized by the change from the purple color DPPH+ to the yellow color DPPHH for different concentrations of extract in a solution of DPPH. This test is determined by the decrease in absorbance of an alcoholic solution of DPPH at λ= 517nm.

Figure 84: result of the antioxidant analysis for the three extracts

The values presented according to the figures and the tables show the reducing capacity of each plant extract at different concentrations.

The antioxidant activity of extracts can be visualized by switching from violet color DPPH+ to yellow color DPPHH for different extract concentrations in a DPPH solution

Control: (ethanol + DPPH) = 0.6075 Abs

The evaluation of antioxidant activity using the DPPH method is expressed in the figures (see figures 9, 10, 11) below according to the following formula:

$$\%\mathbf{inhibition} = \left(\frac{\mathbf{Abs\ controle - Abs\ extract}}{\mathbf{Abs\ controle}}\right) * \mathbf{100}$$

- AA % of *Sage* extract

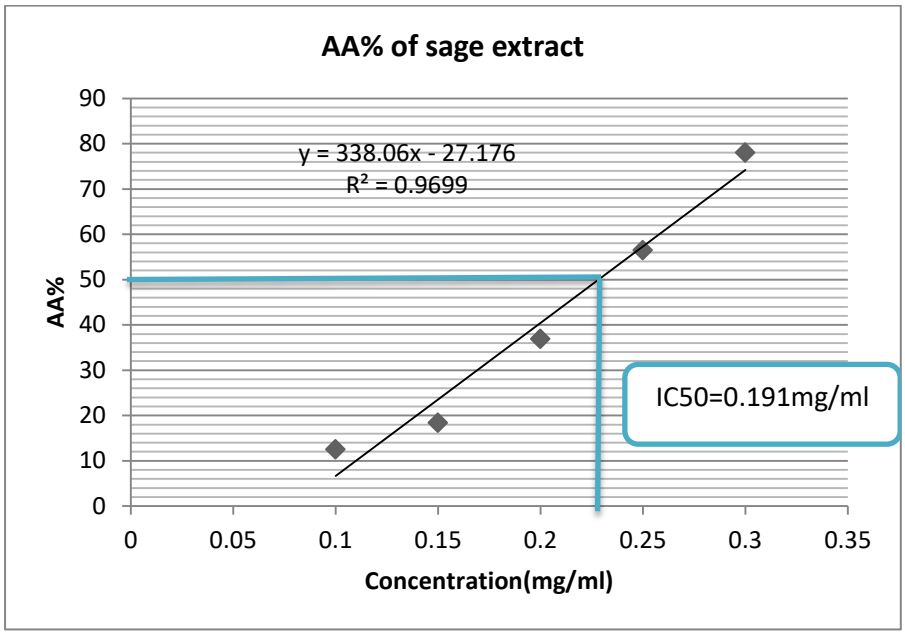

Figure 85: Antiradical activity of *sage* extract

- AA % of Fenugreek extract

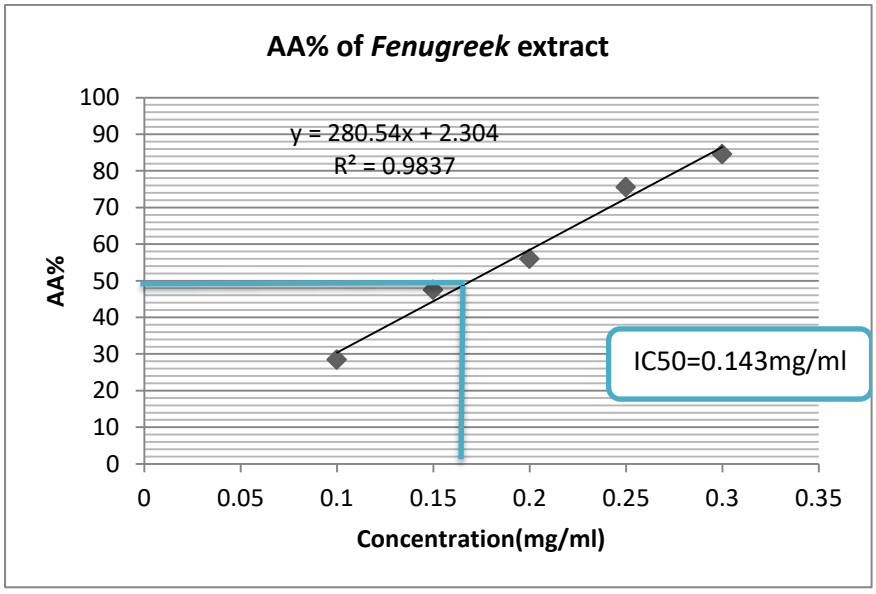

Figure 86: Antiradical activity of *Fenugreek* extract

➢ AA % of *Date seeds* extract

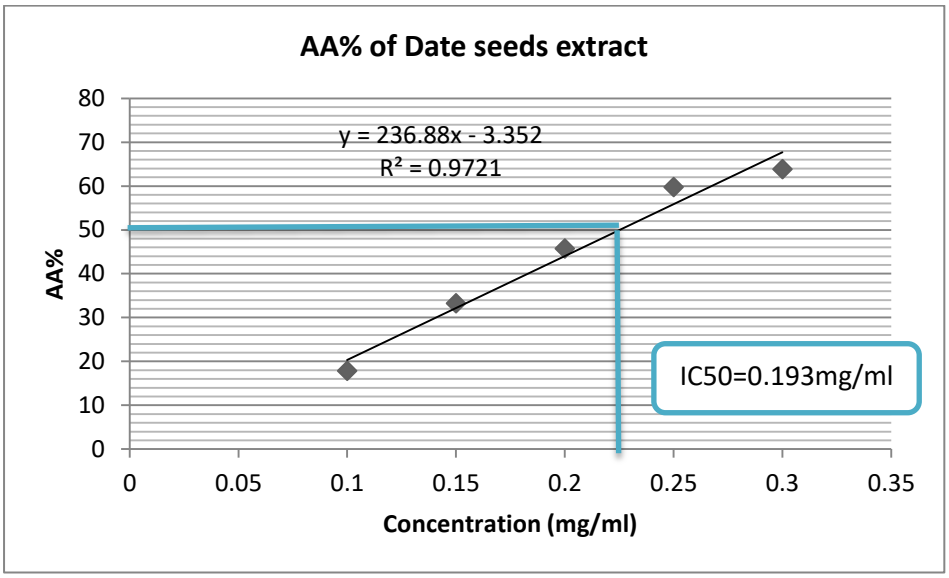

Figure 87: Antiradical activity of *Date seeds* extract

The three figures show an increase in the percentage inhibition (PI) of the absorbance of the DPPH of the extracts tested. Solution as a function of the concentrations of the extracts tested. At the lowest concentration (0.05 mg/ml), PI=15.63% for *Sage*, PI=11.98% for *Fenugreek* and PI=15.29% for *Date seeds*, while at the highest concentration (0.3 mg/ml), PI=85.36% is highest for Fenugreek.

• This shows that the *Trigonella foenum-graecum* species has a high antioxidant potential.

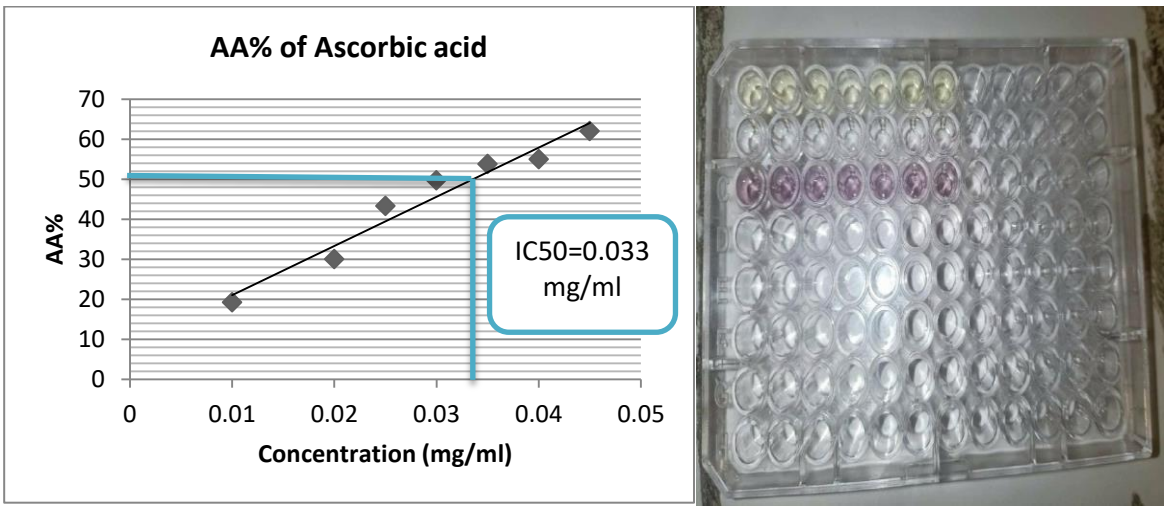

Figure 88: Antioxidant activity of ascorbic acid

- The results showed that the increase in extract concentration (OD at 517nm) was proportional to the increase in ascorbic acid concentration.

- All our extracts showed inhibitory concentration 50 that were significantly higher than those of the reference (ascorbic acid), with the latter showing an almost total reduction from a concentration of 0.0337 mg/ml. It should be noted that our extract shows acceptable antioxidant activity.

- The antioxidant activity assessed for the different extracts that the standard used is expressed in IC50 (inhibitory concentration 50); this is the concentration of extract that neutralizes (reduces) 50% of the free radical (DPPH), the lower the IC50, the more powerful the antioxidant potential of the extract. All the antioxidant activity results expressed as in IC50 is shown in the table below

Table 12: shows the IC50 for each plant

Plant	*Sage*	*Fenugreek*	*Date seeds*	Ascorbic acid
IC50(mg/ml)	0.191	0.143	0.193	0.0337

III.2.2.5Antibacterial activity study of selected plants extract

The antimicrobial effect of sage ,fenugreek and date seeds extracts was studied in vitro, using the method of diffusion of discs on solid agar medium (Mueller-Hinton) for bacteria. The antimicrobial activity of the extracts was estimated in terms of the diameter of the inhibition zone around the discs containing the extracts to be tested against pathogenic germs including (Gram + and Gram – bacteria).

The observations made showing the effect of the three plants extracts on growth bacterial strains tested: *Escherichia coli* (ATCC 1428), *Streptococcus spp* (ATCC12228) and *Staphylococcus aureus* (ATCC 6538).

The results are represented in the figures below

(1) (2) (3)

Figure 89: Representation of The antibacterial effect of *sage*, *fenugreek* and *date seeds* (1) *Escherichia coli* (ATCC 1428), (2) *Staphylococci aureus* (ATCC 6538), and *Streptococcus spp* (ATCC12228)

This table shows the diameters of the inhibition zone for each extract of the three plants selected that we tested the sensitivity of three reference bacterial strains (American Type Culture Collection 'ATCC')

Table 13: Representation of the diameters of the inhibition zone for each extract

	Inhibition zone(mm)		
Plant / MICROORGANISME	**Sage**	**Fenugreek**	**Date seeds**
Escherichia coli ATCC1402 (Gram negative)			
StaphylococcusaurousATCC6538 (Gram positive)	19		12
Streptococcus spp ATCC 12228 (Gram negative)	7		

- **Evaluation of the antibacterial activity of the three extracts**

✓ The *sage* ethanolic extract shows a moderate antibacterial activity against *Staphylococcus aurous* (ATCC6538) and non-existent against *Streptococcus spp* (ATCC 12228) with diameters of 19mm and 7mm respectively.

- ✓ The antibacterial activity of *Fenugreek* is non-extent with the ethanolic extract against the entire microorganism tested.
- ✓ The date seeds extract show a non-inhibitory effect against all the three bacteria.

III.2.3.Emulsuspension Formulation

III.2.3.1.Result of scanning of clay

The purpose of this scanning is to obtain the small quantity of clay and most stable suspension.

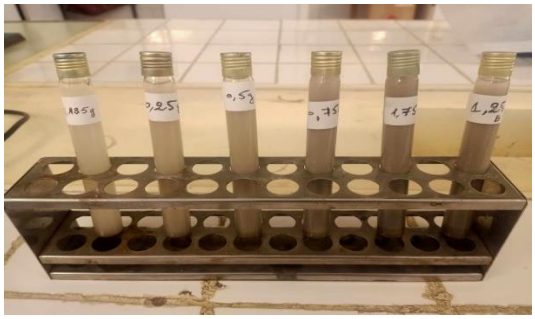

Figure 90: The result of sweeping

III.2.3.2.Results of the scanning

The result of formulation after 1 day

Figure 91: The different formulations after 24h

- ➢ The result of formulation after 2 days

Figure 92: The different formulations after 48h

Depending on the condition of the five (5) formulations after 48h we have selected the 3rd and the 4th formulations as the best.

To achieve a good formula, we make another scanning between this two formulation (3 and 4) based on a solution more stable with a minimum amount of clay**.**

III.2.3.3.The final formulation (Figure 93)

- Water: 80mL
- Clay:2.5 g
- Soap: 3.5 g
- Sage oil: 6.25 Ml
- Dale palm oil: 6.25mL
- Fenugreek oil: 6.25 ml

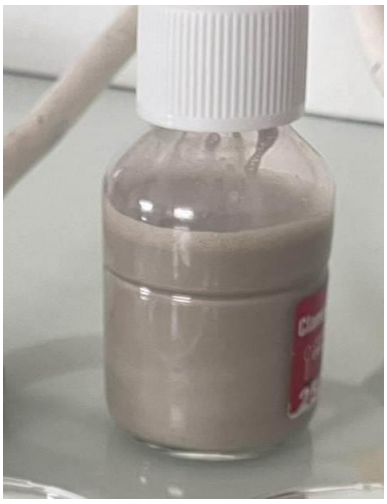

Figure 93: Final formulation

Table 14: Result organoleptic and physicochemical control of final emulsuspension

Parameters	1	2	3	4	5
Color	Gray	Gray	Gray	Gray	Gray
Smell	Acceptable	Acceptable	Acceptable	Acceptable	Acceptable
Taste	Acceptable	Acceptable	Acceptable	Acceptable	Acceptable
Phase separation	Yes	yes	no	No	Yes

II.2.3.4.Test of sterility

The result shows that our product have few charge (<6 cell) of benefit bacteria present in final product (see figure 94)

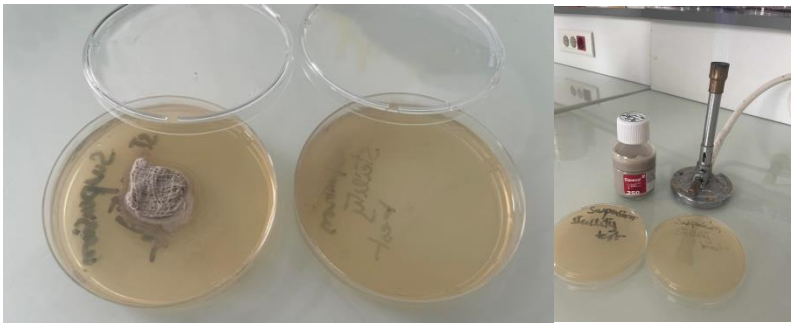

Figure 94: Result of sterility test

II.2.3.5.Test of stability

The result of centrifuge shows that the emulsuspension can be separate after long time of centrifugation as 5 min in 2000 tour

Table 15: results of stability test

Time (min)	**5**	**10**	**5**	**10**
Tour (round/min)	**2000**	**2000**	**4000**	**4000**
Result		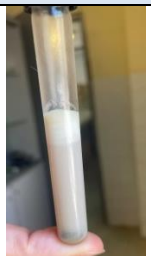	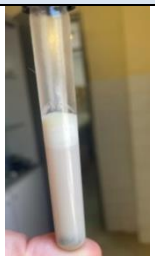	

As we can see in table 15 as much we apply more speed with time the separation is taken. The stability of our product is taking in medium rate.

III.3.In silico results

III.3.1.Preparation of targets

We used the PDB database to upload the NAE1 (the neddylation activating enzyme) and the UNIPROT data bank to upload the P2X7 receptor. The table below represents the PDB format and the PDBQT format for each protein.

Table 16: The PDB and PDBQT format of the targets

Target	PDB format	PDBQT format
P2X7	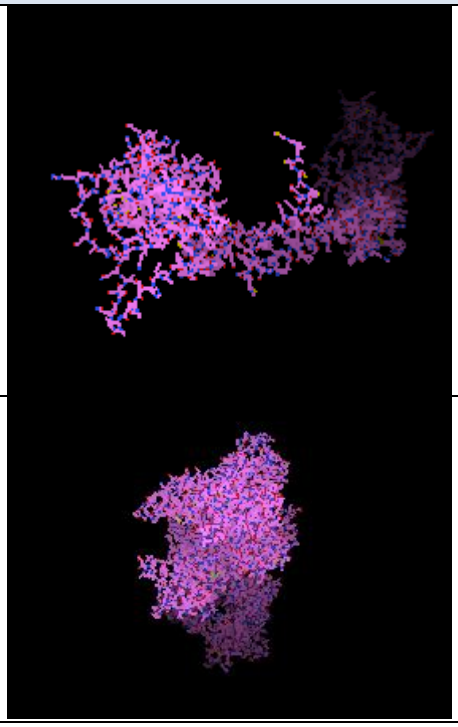	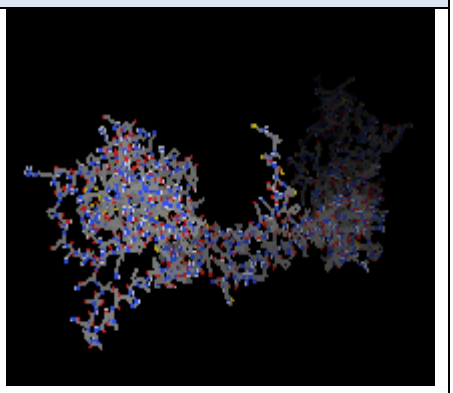
NAE1		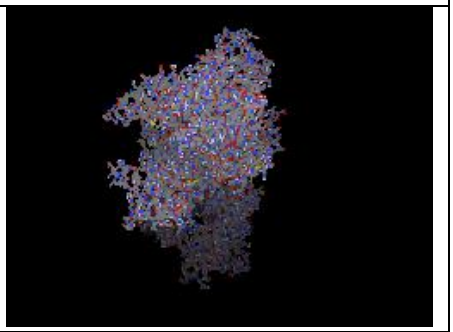

This part represents the result of molecular docking

III.3.2. Preparation of ligands

Optimizing of the molecules by changing molecule form SDF to GJF , we convert the 6 compounds from GJF to PDB then to PDBQT format using Guaussian / Gaussview and Autodock tools. The result are representing in the table 17 :

Table 17: PDBQT and Gaussian output format of ligands prepared

Ligands	GJF format	PDBQT format
Tricin	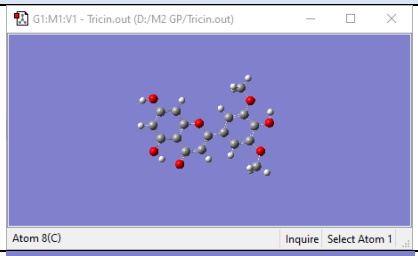	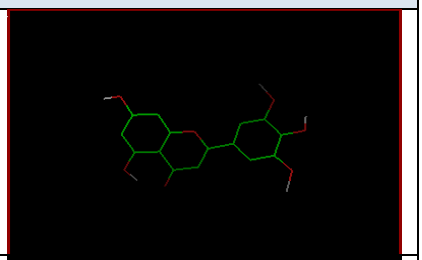
Olmelin	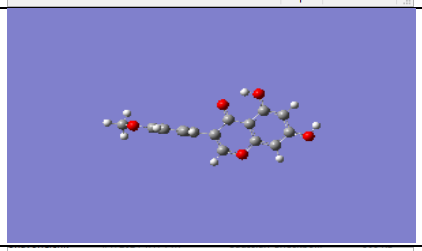	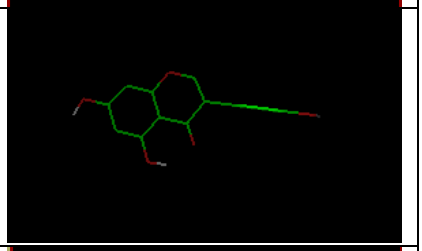
7,4’-dihydroxyflavone	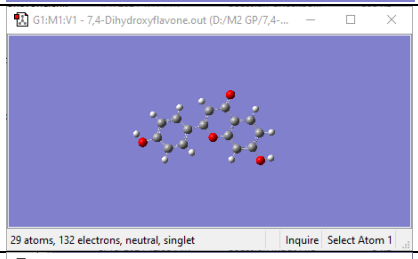	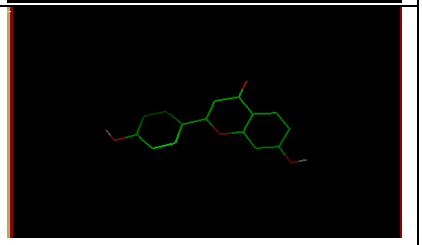
Apigenin	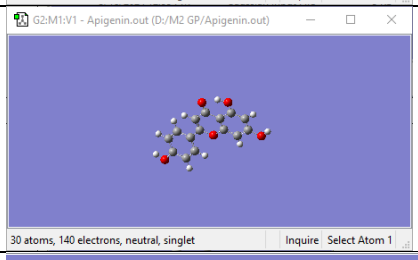	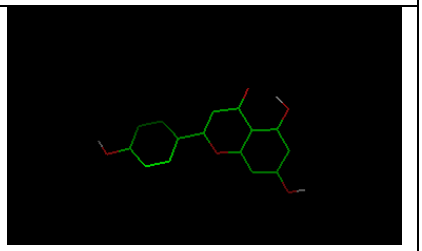
Linalool	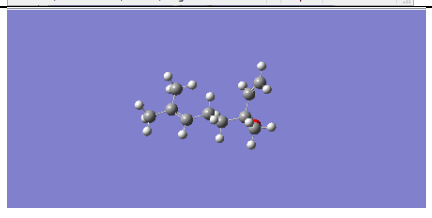	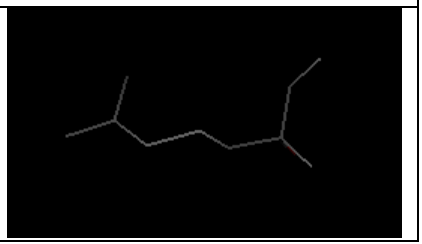

Carnosol	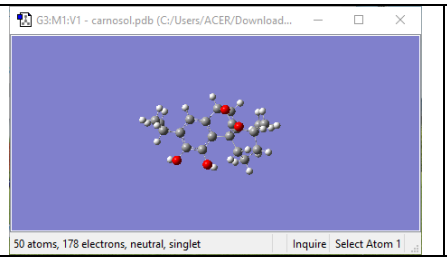	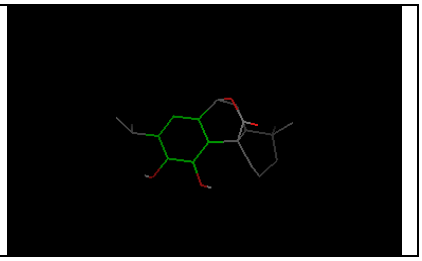

II.3.2.a) Applying Lipinski's rule

Lipinski was necessary to complete our study of the 7 compounds. We used the DruLiTO app to achieve the application of the rule and we collect the results in the table

Table 18: results of molecules proprieties

Molecules	MW (g/mol)	LogP	HA	HD	GI abs
Tricin	330.18	5.108	4	2	High
Olmelin	284.07	1.364	5	2	High
7,4'-dihydroxyflavone	254.06	1.219	4	2	High
Apigenin	270.05	1.138	5	3	High
Linalool	154.17	2.468	1	1	High
Carmosol	330.18	5.108	4	2	High

MW: Molecular weight

LogP: water/octanol partition coefficient ($-2 \leq \log P \leq 5$).

HA: Hydrogen acceptor (nO,N)(≤ 10).

HD: Hydrogen Donor (nOH,NH)(≤ 5).

GI abs: Gastro-intestinal absorption

Interpretation

- LogP (Partition Coefficient): The Log P interval between **1.138 ≤log p≤5.108**. The value is indicator of lipophilicity. As we see Lipinski's rule suggests that compounds with a logP value between -0.4 and 5.6 are more likely to have good oral bioavailability.
- Hydrogen Donors: we can class it on interval of (01-03). Lipinski's rule does not specify a maximum limit for hydrogen donors, but a higher number of hydrogen donors might indicate the potential for forming hydrogen bonds .for example Apigenin.
- Hydrogen Acceptors: we can class them in interval of (01-03). Similarly, Lipinski's rule does not have a specific limit for hydrogen acceptors, but a higher number may indicate the potential for forming hydrogen bonds like Olmelin and Apigenin**.[176]**

III.3.2. b) Boiled egg

We can use swissADME also as reference to class our molecules in terms of their nature lipophilic or hydrophilic; molecule using boiled egg diagram as we can (figure 95)

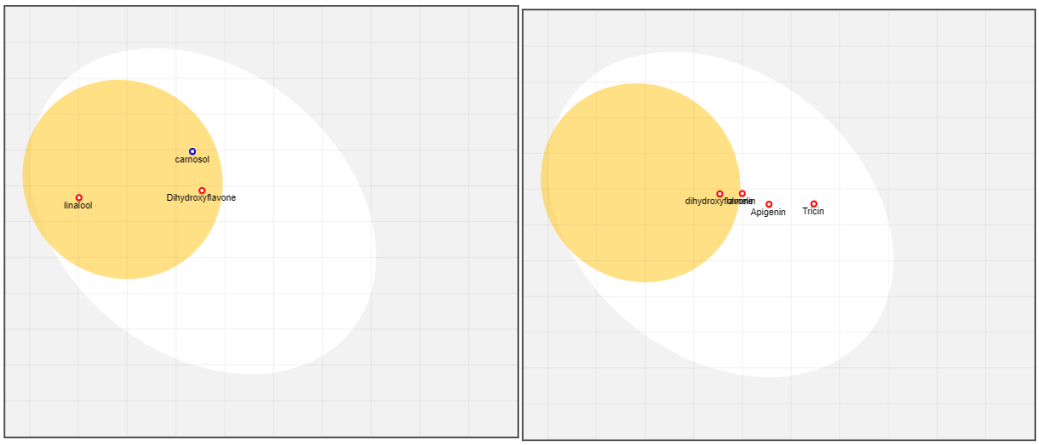

(1) **(2)**

Figure 95: The BOILED-egg model of compounds obtained through SwissADME for **(1):**P2X7 receptor, (**2):** NAE1 receptor

From this diagram can classified molecules: molecules setting in the yellow part are predictive to be passed through blood brain barrier but molecule classified in white part are predictive to be absorbed in gastrointestinal tract so we classified molecule as Tricin ;Olmelin ; Apigenin as hydrophilic molecules also 7,4'-dihydroxyflavone ; Linalool ; and Carnosol are lipophilic molecules.

There is another class that could be added swissADME show in the boiled egg: a bleu point present the molecule that can be affected to nervous system with P-glycoprotein also the red point present the molecule that cannot be affected to nervous system with P- glycoprotein. All molecules are affected to nervous system except carnosol.

III.3.3. Interaction results

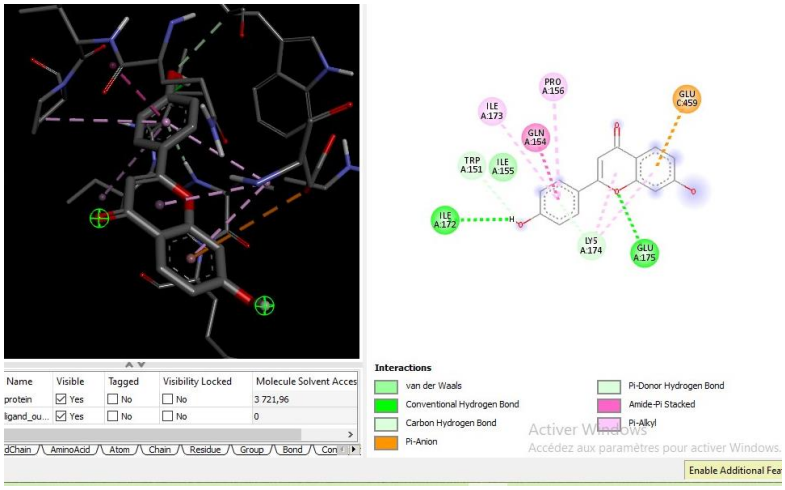

Figure 96: Interaction between the NAE1 enzyme and the ligand 7,4'-dihydroxyflavone

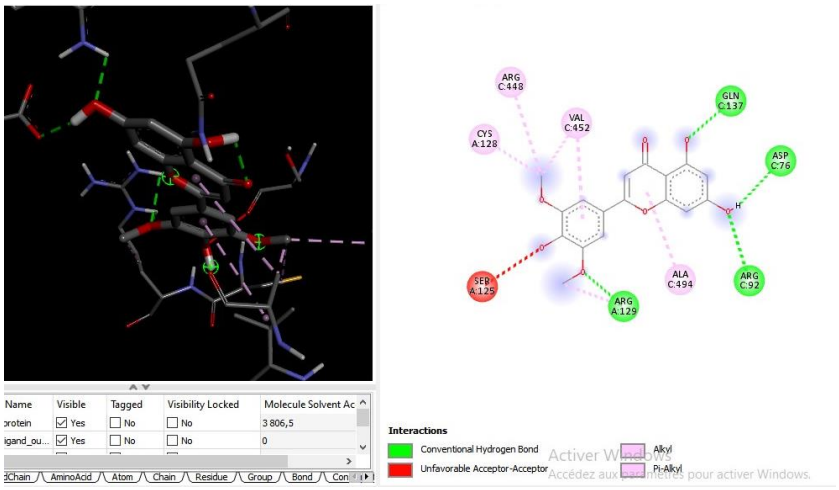

Figure 97: Interaction between the NAE1 enzyme and the ligand Tricin

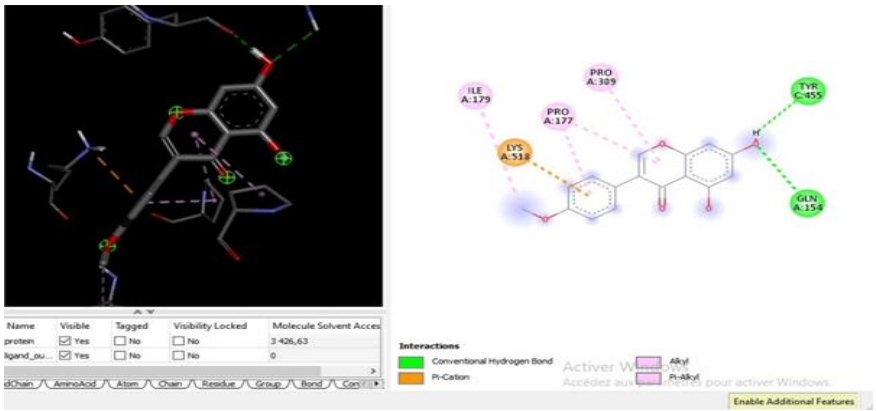

Figure 98: Interaction between theNAE1 enzyme and the ligand Olmelin

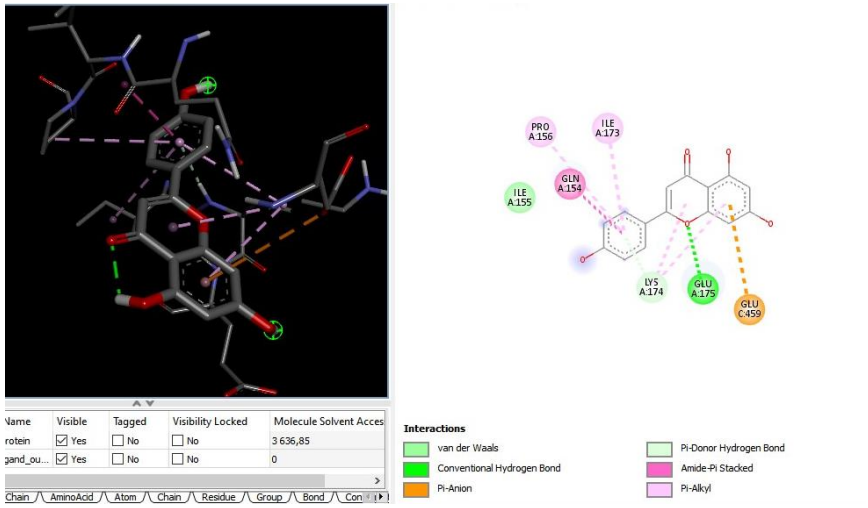

Figure 99: Interaction between the NAE1 enzyme and the ligand Apigenin**.**

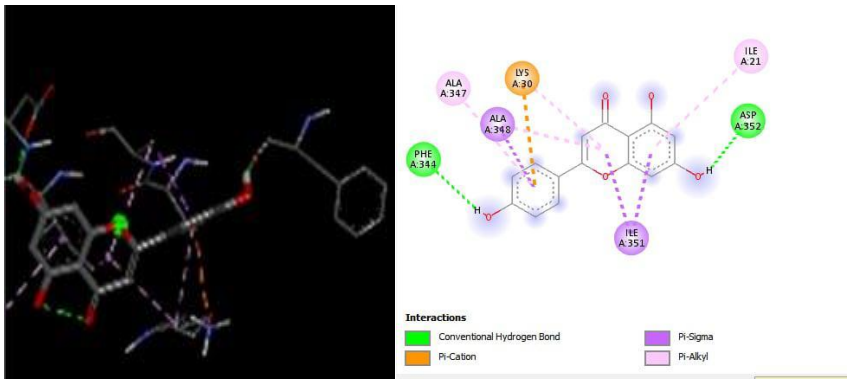

Figure 100: Interaction between the P2X7and the ligand Carnosol**.**

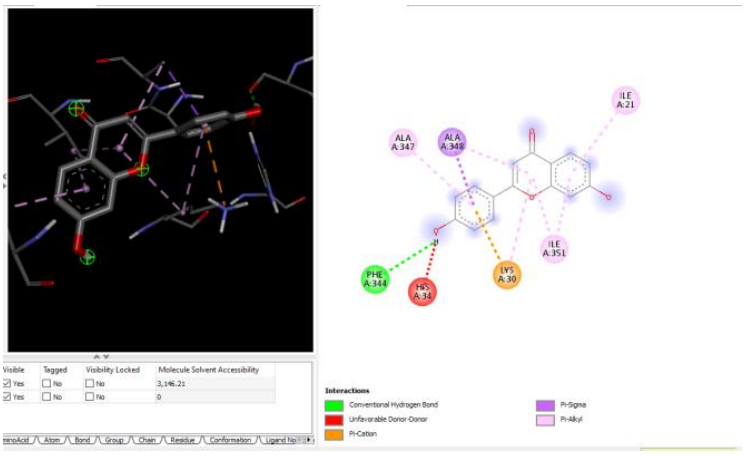

Figure 101: Interaction between the P2X7 and the ligand 7, 4'-dihydroxyflavone

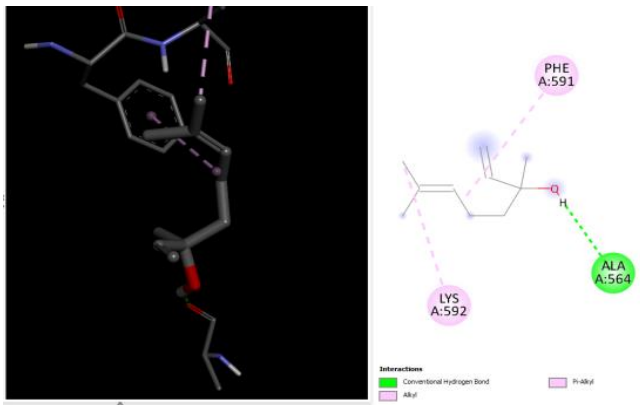

Figure 102: Interaction between the P2X7 and the ligand Linalool

Table 19: The results of all studied interactions.

Receptor	Ligand	Ligand type	Receptor pocket	Interaction Category	Distance (Å)
NAE1	Tricin	ARG C:448	Hydrophobic bond	C==O	4.41686
		CYS A:128	Hydrophobic bond	C==O	3.86795
		VAL C:452	Hydrophobic bond	C==O	3.63411
		SER A:125	Hydrogen bond	H==O	2.15291
		ARG A:129	Hydrogen bond	H==O	2.7642
		ALA C:494	Hydrophobic bond	C==O	5.07074
		ARG C:92	Hydrogen bond	H==O	2.74502
		ASP C:67	Hydrophobic bond	H==O	2.25581
		GLN C:137	Hydrogen bond	H==O	1.91231
	7,4'-dihydroxyflavone	ILE A:172	Hydrogen bond	H==O	2.57983
		GLU A:175	Hydrogen bond	N==O	2.76629
		LYS A:174	Hydrogen bond	N==O	2.30582
		ILE A:155	Hydrogen bond	H==O	2.16971
		TRP A:151	Hydrogen bond	H==O	3.63349
		ILE A:173	Hydrophobic	C==O	5.27877
		GLN A:154	Hydrophobic	C==O	3.57319
		PRO A:156	Hydrophobic	C==O	5.37761
		GLU C:459	Electrostatic	C==O	4.87558
	Olmelin	LYS A:518	Hydrophobic	C==O	3.98755
		ARG A:300	Hydrophobic bond	H==O	2.67884

		GLN A:154	Hydrophobic bond	H==O	3.06005
		PRO A:309	Hydrophobic bond	H==O	5.25139
		PRO A:177	Hydrophobic	C==O	4.72087
		GLU A:175	Hydrophobic bond	H==O	1.9629
		ILE A:179	Hydrophobic	C==O	5.31791
	Apigenin	TRP A:151	Hydrophobic bond	H==O	3.63955
		ILE A:155	Hydrophobic bond	H==O	2.87162
		GLU A:175	Hydrophobic bond	N==O	2.76298
		GLU C:459	Electrostatic	C==O	4.89153
		LYS A:174	Hydrophobic bond	N==O	2.30453
		GLN A:154	Hydrophobic bond	C==O	3.57329
		PRO A:156	Hydrophobic bond	C==O	5.36992
		ILE A:173	Hydrophobic bond	C==O	5.2717
		ILE A:172	Hydrophobic bond	H==O	2.25581
P2X7	7,4'-dihydroxyflavone	HIS A:34	Hydrophobic bond	H==O	3.42136
		PHE A:344	Hydrophobic bond	H==O	3.01621
		LYS A:30	Electrostatic	N==O	4.32351
		ALA A:348	Hydrophobic bond	C==O	3.60179
		ILE A:21	Hydrophobic bond	C==O	4.80362
		ILE A:351	Hydrophobic bond	C==O	4.72151
	Linalool	LEU A:346	Hydrophobic bond	C==O	4.04385
		TYR A:343	Hydrophobic bond	C==O	3.72261
		TYR A:40	Hydrophobic bond	C==O	4.72046
	Carnosol	ASP A:352	Hydrogen bond	H==O	2.11737
		PHE A:344	Hydrogen bond	H==O	2.32568
		ALA A:348	Hydrophobic bond	C==O	3.70686
		LYS A:30	Electrostatic	N==O	4.25803
		ILE A:351	Hydrophobic bond	C==O	3.86210
		ALA A:347	Hydrophobic bond	C==O	4.75495
		ILE A:21	Hydrophobic bond	C==O	5.29221

- In this study, we tested the interaction of the two receptors with several molecules from three different extracts: sage; fenugreek and date seeds. Each extract contain several molecules,

each molecule was hooked up to different amino acids; different types of bond and different distances from one amino acid to another.

- The table :19 shows:

According to the work of Bitam,*et al* 2023 **[177]**:

✓ **NAE1 PROTEIN Interactions:**

- The Tricin exhibited binding affinity of -7.8 kcal/mol towards the NAE1 protein. The compound established four hydrogen bonds with (SER A: 125), (ARG A: 129), (ARG C: 92),and (GLN C:137) residues, and formed **five hydrophobic interactions** with (ARG C:448), (CYS A:128),(VAL C:452),(ALA C:494),and (ASP C:67). These interactions are considered to be essential for the complex's stability and to increase its binding affinity. The docking interactions for the remaining proteins can be found in Figure 94.
- The 7,4'-Dihydroxyflavone exhibited binding affinity of -6.9 kcal/mol towards the NAE1 protein. The compound established five hydrogen bonds with (ILE A: 172), (GLU A: 175), (LYS A: 174), (ILE A:155),and (TRP A:151) residues, and formed **three hydrophobic interactions** with (ILE A:173), (GLN A:154),and (PRO A: 156).These interactions are considered to be essential for the complex's stability and to increase its binding affinity. The docking interactions for the remaining proteins can be found in Figure 93.
- The Olmelin exhibited binding affinity of -7.6 kcal/mol towards the NAE1 protein. The compound established four hydrogen bonds with (ARG A:300), (GLN A:154), (PRO A:309),and (GLU A:175) residues, and formed three **hydrophobic interactions** with (LYS A:518), (PRO A:177),(ILE A:179).These interactions are considered to be essential for the complex's stability and to increase its binding affinity. The docking interactions for the remaining proteins can be found in Figure 95.
- The Apigenin exhibited binding affinity of -9.0 kcal/mol towards the NAE1 protein. The compound established six hydrogen bonds with (ILE A: 155), (GLU A: 175), (LYS A: 174), (GLN A: 154), (TRP A: 151) and (PRO A: 156) residues, and formed **two hydrophobic** interactions with (ILE A: 172), (ILE A: 173).These interactions are considered to be essential for the complex's stability and to increase its binding affinity. The docking interactions for the remaining proteins can be found in Figure 96.

✓ **P2X7 receptor Interactions:**

• The 7, 4'-Dihydroxyflavone exhibited binding affinity of -6.8 kcal/mol towards the P2X7 protein. The compound established five hydrogen bonds with (HIS A: 34), (PHE A: 344), (ALA A: 348), (ILE A: 21) and (ILE A: 351) residues. These interactions are considered to be essential for the complex's stability and to increase its binding affinity. The docking interactions for the remaining proteins can be found in Figure 98.

• The Linalool exhibited binding affinity of -4.6 kcal/mol towards the P2X7 protein. The compound established three **hydrophobic bonds** with (LUE A: 346), (TYR A: 343), (TYR A: 40) residues. These interactions are considered to be essential for the complex's stability and to increase its binding affinity. The docking interactions for the remaining proteins can be found in Figure 99.

• The Carnosol exhibited binding affinity of -6.3 kcal/mol towards the P2X7 protein. The compound established two hydrogen bonds with (ASP A:352), (PHE A:344) and four **hydrophobic bonds** (ALA A:348),(ILE A:351),(ALA A:347),(ILE A:21) residues. These interactions are considered to be essential for the complex's stability and to increase its binding affinity. The docking interactions for the remaining proteins can be found in Figure 97.

This shows that several extracts can inhibit the same receptor at the same time, which validates the work of several inhibitors.

- We are searching in this study to get the best affinity between ligand and receptors with minimization of energy consumption in order to maintain the overall shape of the molecule throughout the docking process.
- The size of atoms is completely fixed, and molecules can only interact by adding more atoms, and this process creates new, different molecules
- Changes in state occur by adding or removing energy from a substance, which affects the way the molecules interact with each other. Molecularly altered molecular switching compounds can be defined as molecular systems that can reversibly change their molecular structure in response to one or more external stimuli, such as radiation, magnetic or electric field, chemicals, gases, light, heat, mechanical effects, or pH.
- A single molecule can take on many different configurations, each with a different energy. Given a starting configuration, geometric optimization changes the atomic coordinates to reduce the energy. In practice, this usually means finding the nearest local minimum; Energy

minimization is a trade-off between the energy gained by forming new local bonds (to get rid of dangling bonds) with the energy lost due to bond stress caused by the new configuration

- the BIOVIA DISCOVRY app work on showing the different bond binding in the interaction shows in previous figures ; bonds been Several : hydrogen bonds (H-H) ; Vander Waals (σ-)-(σ+); alkyl ; carbon hydrogen bond (C-H) and hydrophobic bond (H-O).

III.3.4. Energy of Bonding Orbital and Anti-bonding Orbital (HOMO and LUMO):

- In both physical and organic chemistry, it's important to understand the state of atoms. We learn how atoms bond with each other to form molecules. Knowing the state of these bonds allows us to understand how the synthetic reactions of organic compounds proceed.
- The bonding of molecules is known as HOMO and LUMO. These are also called bonding orbital and anti-bonding orbital: the HOMO is involved in bonding orbitals, and the LUMO is involved in anti-bonding orbitals.
- The HOMO is the highest energy molecular orbital that consists of electrons while the LUMO is the next highest energy orbital that is empty. The LUMO is the lowest energy place to excite an electron. **[178]**
- As Prabhat Gautam in 2014 **[179]** said the energy difference between the HOMO and LUMO or HOMO-LUMO gap is the lowest energy excitation of electrons that exists in a molecule. The smaller a compound's HOMO–LUMO gap, the more stable the compound.so can attract the receptor for maximum time can take.[**179]**
- .HOMO is the orbital that acts mainly as an electron donor and LUMO is the orbital that acts largely as an electron acceptor, and the gap between HOMO and LUMO, known as the HOMO-LUMO gap, characterizes molecular chemical stability. **[178]**

➢ Example of study: **7, 4'-dihydroxyflavone – NAE1**

E GP=LUMO-HOMO

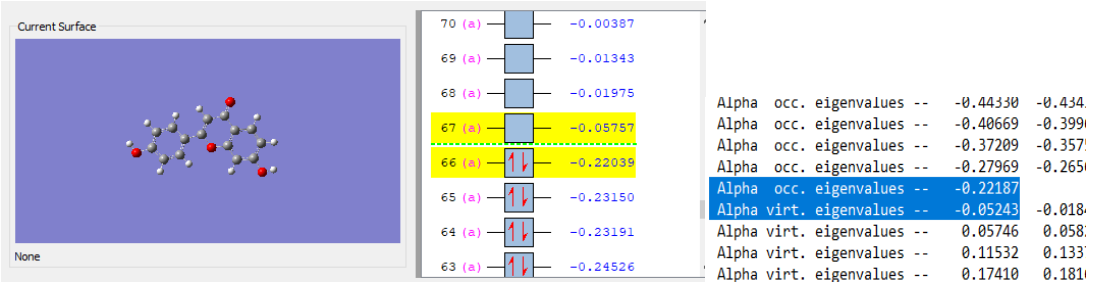

Figure 103: HOMU and LUMO energy orbital

We used excel Microsoft to calculate the energy

				HOMO	LUMO	E gap
				-0.22187	-0.05243	0.16944
Alpha occ. eigenvalues	-0.22187					
Alpha virt. eigenvalues	-0.05243					

Figure 104: Energy of calculation

The Table 19 shows the gap energy of 7, 4'-dihydroxyflavone and Tricin

Table 20: gap Energy of two molecules

Molecule	HOMO	LUMO	E gap (ev)
7, 4'-dihydroxyflavone	-0.22187	-0.05343	3.603988
Tricin	-0.21437	-0.05604	3.367679

III.3.5. Databases

III.3.5.a) Protox III

Table 21: class of toxicity and LD50 of molecules

MOLECULE	LD50 (mg/kg)	Class of toxicity
Tricin	4000	5
Olmelin	2500	5
7,4'-dihydroxyflavone	2500	5
Apigenin	2500	5
Linalool	2200	5
Carnosol	1500	4

III.3.5.b) Protein ligand interaction profiler PLIP

Figure 105: Dashboard for protein –ligand interaction

- **NAE1 Enzyme**

ZN-B-465 **ZN-D-465**

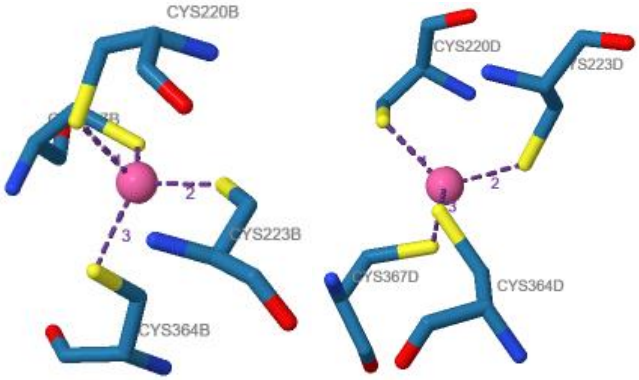

B39-I-464 **B39-J-464**

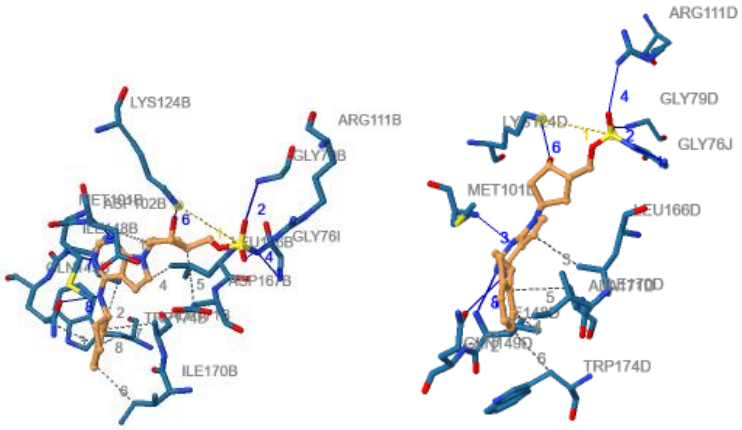

Figure106: Molecular interaction of the best compounds selected from the database NAE1, resulting after an ADME study.

- **P2X7 Receptor**

128 (CHEMBL337395) **128-B-401**

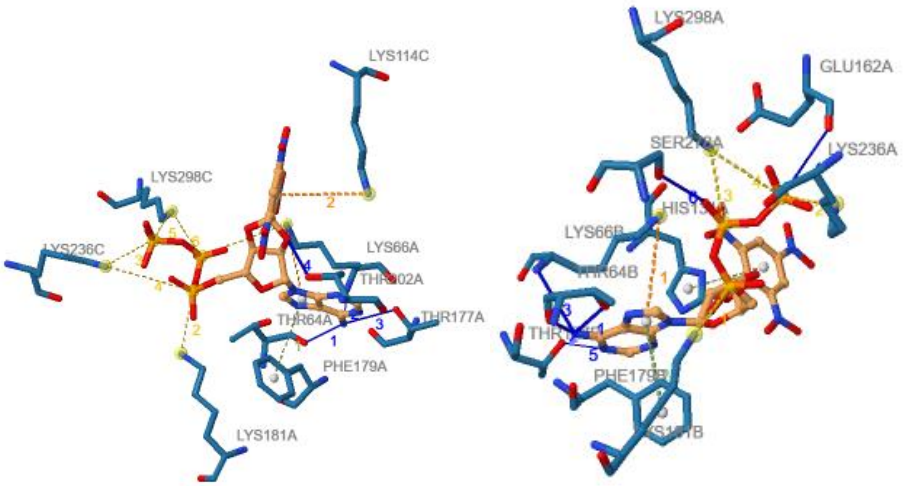

128-C-502 **NAG (Acetyl glucosamine)**

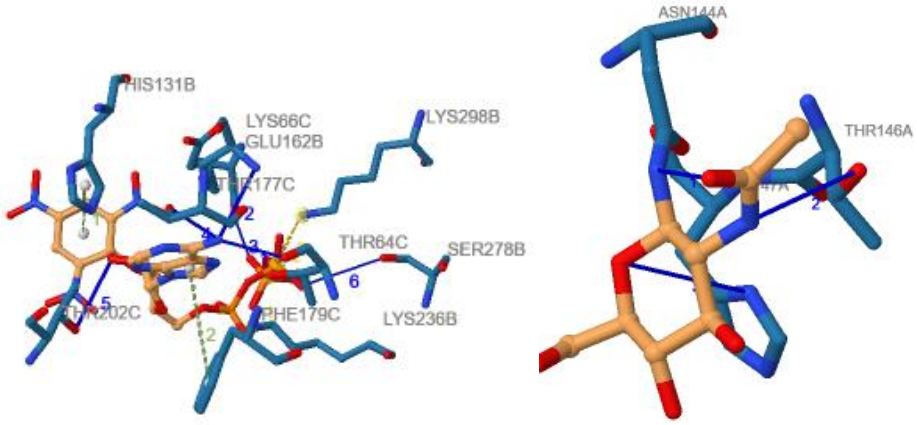

Figure 107: Molecular interaction of the best compounds selected from the database P2X7, resulting after an ADME study

- PLIP, the protein–ligand interaction profiler, detects and visualizes these interactions and provides data in formats suitable for further processing. In our study PLIP has proven very successful in applications ranging from the characterization of docking experiments to the assessment of novel ligand–protein complexes. From the figure above, we can deduce the following :

1. Hydrophobic Atoms: An atom is classified as hydrophobic if it is a carbon and has only carbon or hydrogen atoms as neighbors.

2. Charged Groups: The detection of charged groups is only exhaustive for the binding site, not the ligands. For proteins, positive charges are attributed to the side chain nitrogen's of Arginine, Histidine and Lysine. Negative charged are assigned to the carboxyl groups in Aspartic Acid and Glutamic Acid. In ligands, positive charges are assigned to quaterny ammonium groups, tertiary amines (assuming the nitrogen could pick up hydrogen and thus get charged), sulfonium and guanidine groups. Negative charges are reported for phosphate, sulfonate, sulfonic acid and carboxylate.

3. Halogen bonds donors and acceptors: Assuming that halogen atoms are not present in proteins (unless they are artificially modified), halogen bond donors are searched for only in ligands. Halogen bond acceptors in proteins are all carbon, phosphor or Sulphur atoms connected to oxygen, phosphor, nitrogen or sulfur. **[180]**

III.3.5.c) CB dock :

The table shows some of interactions between ligand and receptor, the table show the simulative amino acids at biovia discovery interaction

Table 22: examples of interactions using CBdock

Receptors	Ligands	CBdock interaction view	Simulative amino acids at biovia discovery interaction
NAE1	Tricin	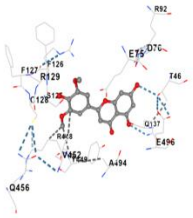	ARG C:448 ;CYS A:128 VAL C:452;SER A:125 ARG A:129 ;ALA C:494 ARG C:92 ;ASP C:67 GLN C:137
	Olmelin	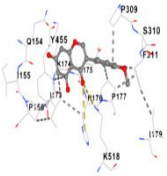	LYS A:518 ;TYR C:455 GLN A:154 ;PRO A:309 PRO A:177 ;ILE A:179
	Apigenin	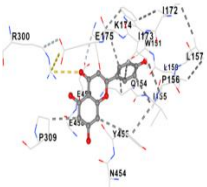	LYS A:174 ;GLN A:154 PRO A:156
	7,4’-dihydroxyflavone	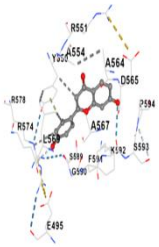	LYS A:174 ;ILE A:155 TRP A:151 ;ILE A:173
P2x7	7,4’-dihydroxyflavone	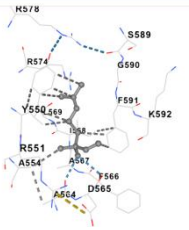	LYS A:30 ;ALA A:348 ILE A:21 ;ILE A:351

	Linalool	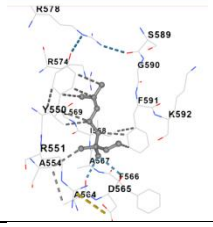	PHE A:591 ; LYS A:592
	Carnosol	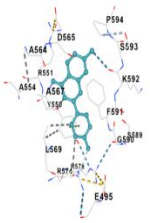	ALA A:348;LYS A:30 ILE A:351 ;ALA A:347

- The advantage of CBdock is facility to establish an interaction without the need of app and spending time; see the structure in 3D form; with of the different positions that the ligand takes to make the best effect.
- CBdock, on the other hand, does not allow us to see the 2D structure of the interaction and the nature of the bonds constructed for the stability of the interaction.

III.3.5.d) Protein-protein interaction:

- Protein-protein interactions are confirmable using the method to detect the change of conditions causing surface Plasmon resonance when another protein binds to a protein that was previously immobilized on a metal surface sensor.
- Protein-protein docking is the prediction of the structure of the complex, given the structures of the individual proteins. In the heart of the docking methodology is the notion of steric and physicochemical complementarity at the protein-protein interface. **[179]**

Figure 108: Dashboard for Protein –protein interaction

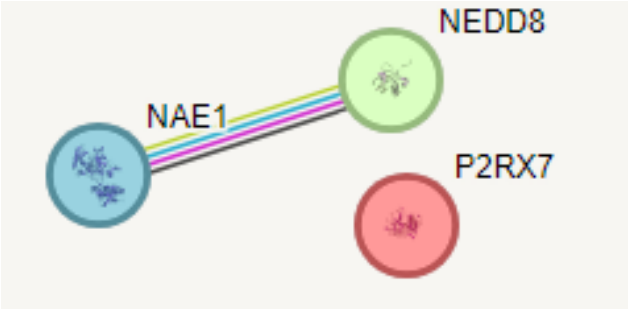

Figure 109: interaction protein-protein between receptors of study NEDD8, NAE1 and P2X7

The result shows that there is interaction between the NEDD8 protein and NAE1 and this prove what we say in the bibliographic study **[75]** (NAE1 is the neddylation activating enzyme).(Figure 109)

While there is no interaction between the NAE1, NEDD8 and the receptor P2X7.

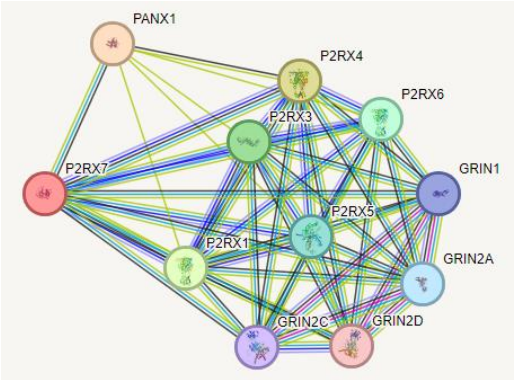

Figure 110: interaction between P2X7 and other proteins

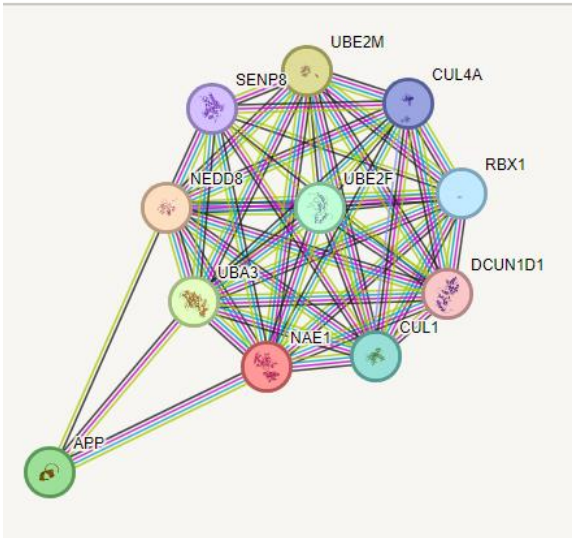

Figure 111: interaction between the NAE1, NEDD8 and other protein

III.3.6.Comparison with commercial drug

III.3.6.1.The commercial treatment (Doxorubicin) and our molecule (Tricin):

We choose the Doxorubicine a chemotherapeutic drug that is widely used for the treatment of advanced esophageal squamous cell carcinoma(ESCC) as a commercial treatment for to compare with the Tricin in targeting the NAE1.

Table 23: comparison Tricin with Doxorubicine

Doxorubicine	Tricin	Similar amino acids
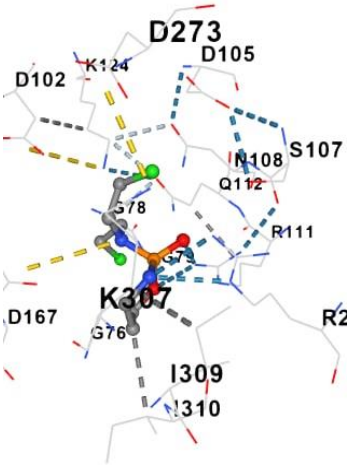	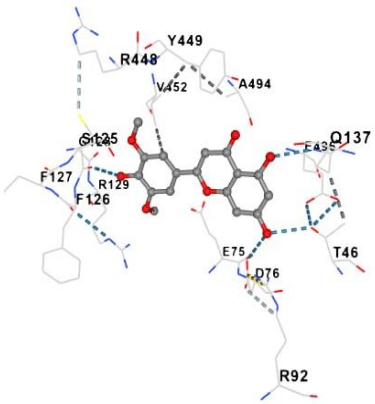	GLU46 ARG47 SER453 ASN454 TYR455 GLN456

The result of discovery shows that the interaction of NAE1 and Tricin was better than the interaction between the Doxorubicine and NAE1.

When studying the active ingredient of Doxorubicine with Cbdock site online , the similar linkages between it and Tricinwith the protein NAE1 are the following amino-acids: (GLU 46, ARG 47, SER 453, ASN 454, TYR 455, GLN 456)

III.3.6.2.Citicoline (Active principal) of Citicoline GL (Pharmaceutical Syrup commercial drug for Alzheimer disease)

We compared the interaction between the molecule 7,4'-dihydroxyflavone and P2X7 receptor with Citicoline active principle of commercial drug.

Table 24: comparison 7, 4'-dihydroxyflavone with Citicoline

Citicoline	7,4'-dihydroxyflavone	Similar amino acids
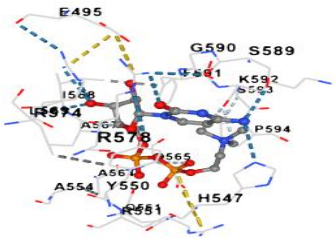	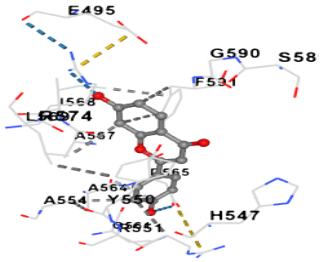	GLU 495 ,HIS 547 ,TYR550 ,ARG551, ALA554, GLN561 , ALA564, ASP565 ,PHE566 , ALA567, ILE568

When studying the active ingredient of Citicoline with Cbdock site online , the similar linkages between it and 7,4'-dihydroxyflavone with the protein P2X7 and are the following amino-acids we have (GLU 495 ,HIS 547 ,TYR550 ,ARG551, ALA554, GLN561 ,ALA564 ,ASP565 ,PHE566 , ALA567, ILE568)

The commercial drug bind with amino acids more than 7,4'-dihydroxyflavone.

Conclusion:

In summary, we have screened 75 phytochemicals from the three plants by molecular docking, in silico ADME and ProTox III, and selected 6 phytochemicals to propose the potential hits against the two therapeutic protein targets (P2X7, NAE1).

The results of the study indicate that the compounds are 7,4'-Dihydroxyflavone ,Tricin ,Olmelin from fenugreek and Linalool , Carnosol are from sage ,and finally Apigenin and7,4'-Dihydroxyflavone from *date seeds* ,they have a potential as drug candidates due to its pharmacokinetic properties and strong binding affinity towards the receptor P2X7 with 7,4'-Dihydroxyflavone with ΔG= -6.8 kcal/mol forming 7 amino acid bonds and Tricin molecule interacts with NAE1, forming 9 amino acid bonds with ΔG = -7.8 kcal/mol. Compliance with Lipinski's rule supports their potential as drug candidates.

General Conclusion

Conclusion

In conclusion, the present study focused on the preparation of emulsuspension utilizing the Tricin and 7,4'-Dihydroxyflavone extracted from *Phoenix dactylifera L* seed and *Trigonella foenum-graecum* (commonly known as Date seeds and Fenugreek) and its potential therapeutic application for Esophageal cancer and Alzheimer's disease. Through an in silico study, we have gained valuable insights into the molecular interactions and potential mechanisms of action of Tricin in targeting the Neddylation activating enzyme NAE1 and 7,4'-Dihydroxyflavone targeting the P2X7 receptor .

During this work, we were interested in the extraction of *Salvia officinalis* , *Trigonella foenum-graecum* and *Phoenix dactylifera L seed* extracts and their associations by maceration, to determine their chemical compositions, to study the antibacterial activity.

Obtaining extracts by maceration using different solvents remains a simple and effective method, and gives interesting yield value of **39.7%, 30.15%** and **25.6%** respectively. The evaluation of the antibacterial activity of the extracts was determined on 3 microbial strains according to the disc diffusion method. This technique has shown that the extracts studied have an inhibitory effect against certain strains tested; the best inhibitory activity was *Staphylococcus aurous* (ATCC6538) with significant zones of inhibition 19 mm these strain showed significant sensitivity to the action of the extracts.

The anti-radical potential of the extract was determined by the DPPH method, the results of which show that the extract has good activity IC50 value was determined with 0.143mg/ml for Fenugreek and 0.193mg/ml for Date seeds and 0.191mg/ml for sage, so this plant contains molecules which are considered to be antioxidant agents.

Our findings indicate that 7,4'-Dihydroxyflavone and Tricin possesses promising pharmacological properties that may contribute to the prevention and treatment of Alzheimer's disease and Esophageal cancer by inhibiting the P2X7 receptor and NAE1 protein . The in silico study demonstrated that 7, 4'-Dihydroxyflavone and Tricin exhibits significant interactions with key molecular targets involved in Alzheimer's pathology and Esophageal cancer , including inhibition of P2X7 receptor , NAE1 protein the main raison of this two diseases in our study . These interactions suggest that Tricin may exert the inhibition of NAE1 leading to the decrease of the hyper-activation of this protein. The same goes on P2X7 receptor which inhibited by 7, 4'-Dihydroxyflavone. Furthermore, the formulation of the two active principals into

emulsuspension offers a convenient and accessible dosage form, potentially enhancing patient compliance and ease of administration.

In summary, our thesis presents a novel approach in the development of an emulsuspension formulation from Tricin and 7, 4'-Dihydroxyflavone derived from, *Phoenix dactylifera L* seed and *Trigonella foenum-graecum* targeting Alzheimer's disease ,Esophageal cancer . The in silico study supports the notion that 7, 4'-Dihydroxyflavone may possess neuro-protective properties against Alzheimer's pathology with strong interaction forming 7 amino acids bond (ALA A:347,ALA A:348,ILE A:21,ILE A:351,LYS A:30,PHE A:344,HIS A:34) with ΔG= -6.8 kcal/mol. And Tricin against Esophageal cancer interact with NAE1 by 10 amino acids (ARG A:129, ASN D:39, GLY D:36, GLU D:35, SER A:37,LYS D:42,ALA A:38, THR A:131,ILE A:516,TYR C:455) with strong binding affinity ΔG = -7.8 kcal/mol. .This research lays the groundwork for future investigations and highlights the potential of Tricin and 7, 4'-Dihydroxyflavone emulsuspension as a therapeutic option for individuals affected by Esophageal cancer and Alzheimer's disease.

In a protein- protein interaction study showed that there was no relationship between P2X7 and NEDD8, unlike the relationship between NEDD8 and NAE1. Inhibiting NAE1 leads to the indirect inhibition of NEDD8.

When we studying the inhibitor reference ligand Citicoline in Cbdock online site, the linkages between it and the protein (P2X7) interaction with inhibitor ligand almost the same with the interaction . we have got 76.92% amino acids with a similarity of this bonds (GLU 495 ,HIS 547 ,TYR550 ,ARG551, ALA554, GLN561 ,ALA564 ,ASP565 ,PHE566 , ALA567, ILE568)

When we studying the inhibitor reference ligand Doxorubicine in Cbdock online site, the linkages between it and the protein (NAE1) the interaction with inhibitor ligand almost the same with the interaction . We have got 47.21% amino acids with a similarity of these bonds (GLU 46, ARG 47, SER 453, ASN 454, TYR 455, GLN 456)

General conclusion

Perspective

Thanks to this thesis it is possible to recognize that much work remains to be done and several parts need to be studied. The preclinical and clinical investigations are necessary to validate the therapeutic potential of Tricin and 7, 4'-Dihydroxyflavone emulsuspension in Alzheimer's disease and Esophageal cancer. Additional studies should focus on evaluating the safety, pharmacokinetics, and efficacy of this formulation in appropriate animal models and human trials.

bibliographic References

[1] Zastrow M. Drug Receptors & Pharmacodynamics. In: Katzung BG. eds. Basic & Clinical Pharmacology, 14e. McGraw-Hill Education; 2017. Accessed May 18, 2024. https://accessmedicine.mhmedical.com/content.aspx?bookid=2249&sectionid=175215570
[2] S. Valera, N. Hussy, R.J. Evans, N. Adami, R.A. North, A. Surprenant, G. Buell Nature, 371 (1994), p. 516
[3] Samways, D. S., Li, Z., and Egan, T. M. (2014). Principles and properties of ion flow in P2X receptors. Front Cell. Neurosci. 8:6. doi: 10.3389/fncel.2014.00006
[4] K.L. Szuhany et al. Assessing BDNF as a mediator of the effects of exercise on depression J. Psychiatr. Res. (2020)
[5] J. Leschik et al. Brain-derived neurotrophic factor expression in serotonergic neurons improves stress resilience and promotes adult hippocampal neurogenesis Prog. Neurobiol. (2022)
[6] Bradley HJ, Browne LE, Yang W, and Jiang LH (2011b) Pharmacological properties of the rhesus macaque monkey P2X7 receptor. Br J Pharmacol 164 (2b):743–754.
[7] Jiang LH, Baldwin JM, Roger S, and Baldwin SA (2013) Insights into the molecular mechanisms underlying mammalian P2X7 receptor functions and contributions in diseases, revealed by structural modeling and single nucleotide polymorphisms. Front Pharmacol 4:55.
[8] Chessell IP, Simon J, Hibell AD, Michel AD, Barnard EA, and Humphrey PPA (1998) Cloning and functional characterisation of the mouse P2X7 receptor. FEBS Lett 439:26–30.
[9] Delarasse, C., Gonnord, P., Galante, M., Auger, R., Daniel, H., Motta, I., et al. (2009). Neural progenitor cell death is induced by extracellular ATP via ligation of P2X7 receptor. J. Neurochem. 109, 846–857. doi: 10.1111/j.1471-4159.2009.06008.x
[10] Origin, distribution, and function of three frequent coding polymorphisms in the gene for the human P2X7 ion channel - Scientific Figure on ResearchGate. Available from: https://www.researchgate.net/figure/D-structure-models-of-wildtype-HHA-and-ancestral-YRT-human-P2X7-A-The-ribbon_fig2_365493905 [accessed 16 May, 2024]
[11] Wiley, J. S. et al. The human P2X7 receptor and its role in innate immunity. Tissue Antigens 78, 321–332 (2011).
[12] Elliott, J. I. et al. Membrane phosphatidylserine distribution as a non-apoptotic signalling mechanism in lymphocytes. Nat .Cell Biol. 7, 808–816 (2005).
[13] Di Virgilio, F., Dal Ben, D., Sarti, A. C., Giuliani, A. L. & Falzoni, S. The P2X7 receptor in infection and inflammation. Immunity 47, 15–31 (2017).
[14] Kaczmarek-Hajek, K. et al. Re-evaluation of neuronal P2X7 expression using novel mouse models and a P2X7-specific nanobody. Elife 7, e36217 (2018).
[15] Sperlágh, B. & Illes, P. P2X7 receptor: an emerging target in central nervous system diseases. Trends Pharm. Sci. 35, 537–547 (2014).
[16] Burnstock, G. P2X ion channel receptors and inflammation. Purinergic Signal 12, 59–67 (2016)
[17] Hardie, D., Ross, F. & Hawley, S. AMPK: a nutrient and energy sensor that maintainsenergy homeostasis. Nat Rev Mol Cell Biol 13, 251–262 (2012). https://doi.org/10.1038/nrm3311
[18] Ortiz, S., Šavikin, K., Massicot, F., Olivier, E., Dutot, M., Rat, P., Deguin, B., Gođevac, D., Menković, N., Živković, J., Zdunić, G., & Boutefnouchet, S. (2023). P2X7-Receptor Pathway Involvement in the Anti-Inflammatory Activity of Medicinal Plants. Chemistry & Biodiversity, 20(8). https://doi.org/10.1002/cbdv.202300427
[19] Wang, X. et al. P2X7 receptor inhibition improves recovery after spinal cord injury. Nat. Med. 10, 821–827 (2004).
[20] Peng, W. et al. Systemic administration of an antagonist of the ATP-sensitive receptor P2X7 improves recovery after spinal cord injury. Proc. Natl Acad. Sci. USA 106, 12489–12493 (2009)

[21] Garré, J. M., Yang, G., Bukauskas, F. F. & Bennett, M. V. FGF-1 triggers pannexin-1 hemichannel opening in spinal astrocytes of rodents and promotes inflammatory responses in acute spinal cord slices. J. Neurosci. 36, 4785–4801 (2016).
[22] Meyer, U. Prenatal poly(i:C) exposure and other developmental immune activation models in rodent systems. Biol. Psychiatry 75, 307–315 (2014).
[23] Huang, Q., Ying, J., Yu, W. et al. P2X7 Receptor: an Emerging Target in Alzheimer's Disease. Mol Neurobiol 61, 2866–2880 (2024). https://doi.org/10.1007/s12035-023-03699-9

[24] Burnstock G and Knight GE (2004) Cellular distribution and functions of P2 receptor subtypes in different systems. Int Rev Cytol 240:31–304.

[25] Sperlágh B, Vizi ES, Wirkner K, and Illes P (2006) P2X7 receptors in the nervous system. Prog Neurobiol 78:327–346

[26] R.E. Sorge, T. Trang, R. Dorfman, S.B. Smith, S. Beggs, J. Ritchie, J.-S. Austin, D.V. Zaykin Nat. Med., 18 (2012), p. 595

[27] I.P. Chessell, J.P. Hatcher, C. Bountra, A.D. Michel, J.P. Hughes, P. Green, J. Egerton, M. Murfin, J. Richardson, W.L. Peck Pain, 114 (2005), p. 386
[28] A. Wesseluis, M. Bours, Z. Henriksen, S. Syberg, S. Petersen, P. Schwarz, N. Jorgensen, S. Van Helden, P. Dagnelie Osteoporosis Int., 24 (2013), p. 1235
[29] S.D. Ohlendorff, C.L. Tofteng, J.-E.B. Jensen, S. Petersen, R. Civitello, M. Fenger, B. Abrahamsen, A.P. Hermann, P. Eiken, N.R. Jorgensen Pharmacogenet. Genom., 17 (2007), p. 555
[30] L. Portales-Cervantes, P. Nino-Moreno, M. Salgado-Bustamante, M.H. Garcia-Hernandez, L. Baranda-Candido, E. Reynaga-Hernandez, C. Barajas-Lopez, R. Gonzalez-Amaro, D. Portales-Perez Cell. Immunol., 276 (2012), p. 168
[31] S. Lucae, D. Salyakina, N. Barden, M. Harvey, B. Gagne, M. Labbe, E.B. Binder, M. Uhr, M. Paez-Pereda, I. Sillaber Hum. Mol. Genet., 15 (2006), p. 2438
[32] A. Erhardt, S. Lucae, P.G. Unschuld, M. Ising, N. Kern, D. Salyakina, R. Lieb, M. Uhr, E.B. Binder, M.E. Keck
[33] E.K. Green, D. Grozeva, R. Raybould, G. Elvidge, S. Macgregor, I. Craig, A. Farner, P. Mcguffin, L. Forty, L. Jones Am. J. Med. Genet., 150 (2009), p. 1063
[34] F. Di Virgiolio Cancer Res., 72 (2012), p. 5441
[35] E. Adinolfi, L. Melchiorri, S. Falzoni, P. Chiozzi, A. Morelli, A. Tieghi, A. Cuneo, G. Castoldi, F. Di Virgilio, O.R. Baricordi Blood, 99 (2002), p. 706
[36]Territo PR, Zarrinmayeh H. P2x7 receptors in neurodegeneration: potential therapeutic applications from basic to clinical approaches. Front Cell Neurosci. 6 avr 2021;15:617036.
[37] P. Honore, D. Donnelly-Roberts, M.T. Namovic, G. Hsieh, C.Z. Zhu, J.P. Mikusa, G. Hernandez, C. Zhong, D.M. Gauvin, P. Chandran J. Pharmacol. Exp. Ther., 319 (2006), p. 1376
[38] I. Mcinnes, S. Cruwys, K. Bowers, M. Braddock Clin. Exp. Rheumatol., 32 (2013), p. 878
[39] J.I. Diaz-Hernandez, R. Gomez-Villafuertes, M. Leon-Otegui, L. Hontecillas-Prieto, A. Del Puerto, J.L. Trejo, J.J. Lucas, J.J. Garrido, J. Gualix, M.T. Miras-Portugal Neurobiol. Ageing, 2012 (1816), p. 33
[40] J.K. Ryu, J.G. Mclarnon NeuroReport, 19 (2008), p. 1715
[41] Beinart, N., Weinman, J., Wade, D., and Brady, R. (2012). Caregiver Burden and Psychoeducational Interventions in Alzheimer's Disease: a review. Dement. Geriatr. Cogn. Dis. Extra 2, 638–648. doi: 10.1159/000345777
[42] Alzheimer's Association (2015). Alzheimer's disease facts and figures. Alzheimer's Dement. 11, 332–384
[43] Goedert, M., and Spillantini, M. G. (2006). A century of Alzheimer's disease. Science 314, 777–781. d oi: 10.1126/science.1132814

[44] De Felice, F. G. (2013). Alzheimer's disease and insulin resistance: translating basic science into clinical applications. J. Clin. Invest. 123, 531–539. doi: 10.1172/JCI64595
[45]Kumar A, Sidhu J, Lui F, Tsao JW. Alzheimer disease. In: StatPearls [Internet]. Treasure Island (FL): StatPearls Publishing; 2024 [cité 21 juin 2024]. Disponible sur: http://www.ncbi.nlm.nih.gov/books/NBK499922/
[46]Boutajangout A, Sigurdsson EM, Krishnamurthy PK. Tau as a therapeutic target for alzheimer's disease. Curr Alzheimer Res. sept 2011;8(6):666-77
[47] Breijyeh Z, Karaman R. Comprehensive Review on Alzheimer's Disease: Causes and Treatment. Molecules. 2020; 25(24):5789. https://doi.org/10.3390/molecules25245789
[48] Zhou, L., Jiang, Y., Luo, Q. et al. Neddylation: a novel modulator of the tumor microenvironment. Mol Cancer 18, 77 (2019). https://doi.org/10.1186/s12943-019-0979-1

[49] Zhou, L., Zhang, W., Sun, Y., & Jia, L. (2018). Protein neddylation and its alterations in human cancers for targeted therapy. Cellular Signalling, 44, 92–102 doi:10.1016/j.cellsig.2018.01.

[50] Sarikas, A., Hartmann, T. & Pan, ZQ. The cullin protein family. Genome Biol 12, 220 (2011). https://doi.org/10.1186/gb-2011-12-4-220

[51] Kim WD, Mathavarajah S, Huber RJ. The cellular and developmental roles of cullins, neddylation, and the cop9 signalosome in dictyostelium discoideum. Front Physiol. 1 mars 2022;13:827435.

[52] Zhou L, Jiang Y, Luo Q, Li L, Jia L. Neddylation: a novel modulator of the tumor microenvironment. Molecular Cancer. 3 avr 2019;18(1):77.

[53] Liu D, Che X, Wu G. Deciphering the role of neddylation in tumor microenvironment modulation: common outcome of multiple signaling pathways. Biomarker Research. 8 janv 2024;12(1):5.

[54] Petroski MD, Deshaies RJ. Function and regulation of cullin–RING ubiquitin ligases. Nat Rev Mol Cell Biol. janv 2005;6(1):9-20.

[55] Structural assembly of cullin-RING ubiquitin ligase complexes. Current Opinion in Structural Biology. 1 déc 2010;20(6):714-21.

[56] Zheng N, Schulman BA, Song L, Miller JJ, Jeffrey PD, Wang P, et al. Structure of the cul1-rbx1-skp1-f boxskp2 scf ubiquitin ligase complex. Nature. 18 avr 2002;416(6882):703-9.

[57] Kleiger G, Saha A, Lewis S, Kuhlman B, Deshaies RJ. Rapid E2-E3 assembly and disassembly enable processive ubiquitylation of cullin-RING ubiquitin ligase substrates. Cell. 25 nov 2009;139(5):957-68.

[58] Pierce NW, Kleiger G, Shan S ou, Deshaies RJ. Detection of sequential polyubiquitylation on a millisecond timescale. Nature. déc 2009;462(7273):615-9.

[59] Gong L, Cui D, Xiong X, Zhao Y. Targeting cullin-ring ubiquitin ligases and the applications in protacs.

[60] Sun Y, Wei W, Jin J, éditeurs. Cullin-RING Ligases and Protein Neddylation: Biology and Therapeutics [Internet]. Singapore: Springer; 2020 [cité 17 mai 2024]. p. 317-47. Disponible sur: https://doi.org/10.1007/978-981-15-1025-0_19

[61] Yoshimura C, Muraoka H, Ochiiwa H, Tsuji S, Hashimoto A, Kazuno H, et al. Tas4464, a highly potent and selective inhibitor of nedd8-activating enzyme, suppresses neddylation and shows antitumor activity in diverse cancer models. Mol Cancer Ther. juill 2019;18(7):1205-16.

[62] Soucy TA, Smith PG, Milhollen MA, Berger AJ, Gavin JM, Adhikari S, et al. An inhibitor of NEDD8-activating enzyme as a new approach to treat cancer. Nature. 9 avr 2009;458(7239):732-6.

[63]Enchev RI, Schulman BA, Peter M. Protein neddylation: beyond cullin-RING ligases. Nat Rev Mol Cell Biol. janv 2015;16(1):30-44.

[64] Cockram PE, Kist M, Prakash S, Chen SH, Wertz IE, Vucic D. Ubiquitination in the regulation of inflammatory cell death and cancer. Cell Death Differ. févr 2021;28(2):591-605.

[65] Bhatia S, Pavlick AC, Boasberg P, Thompson JA, Mulligan G, Pickard MD, et al. A phase I study of the investigational NEDD8-activating enzyme inhibitor pevonedistat (TAK-924/MLN4924) in patients with metastatic melanoma. Invest New Drugs. 2016;34:439-49.

[66] Gatti V, Bernassola F, Talora C, Melino G, Peschiaroli A. The impact of the ubiquitin system in the pathogenesis of squamous cell carcinomas. Cancers (Basel). 16 juin 2020;12(6):1595.

[67] Zou T, Zhang J. Diverse and pivotal roles of neddylation in metabolism and immunity. FEBS J. juill 2021;288(13):3884-912.

[68] Zhou L, Jiang Y, Luo Q, Li L, Jia L. Neddylation: a novel modulator of the tumor microenvironment. Molecular Cancer. 3 avr 2019;18(1):77.

[69] Uniprot [Internet]. [cited 17 mai 2024]. Disponible in: https://www.uniprot.org/uniprotkb/Q15843/entry#function

[70] Yoshimura C, Muraoka H, Ochiiwa H, Tsuji S, Hashimoto A, Kazuno H, et al. Tas4464, a highly potent and selective inhibitor of nedd8-activating enzyme, suppresses neddylation and shows antitumor activity in diverse cancer models. Mol Cancer Ther. juill 2019;18(7):1205-16.

[72] Watson IR, Irwin MS, Ohh M. Nedd8 pathways in cancer, sine Quibus Non. Cancer cell. 15 févr 2011;19(2):168-76.

[73] Qiu Y, Li X, He X, Pu J, Zhang J, Lu S. Computational methods-guided design of modulators targeting protein-protein interactions (Ppis). Eur J Med Chem. 1 déc 2020;207:112764.

[74] SOMCL-19-133, a novel, selective, and orally available inhibitor of NEDD8-activating enzyme (Nae) for cancer therapy. Neoplasia. 1 oct 2022;32:100823.

[75] Identification of the activating and conjugating enzymes of the nedd8 conjugation pathway. Journal of Biological Chemistry. 23 avr 1999;274(17):12036-42.

[76] Whitby FG, Xia G, Pickart CM, Hill CP. Crystal structure of the human ubiquitin-like protein NEDD8 and interactions with ubiquitin pathway enzymes. J Biol Chem. 25 déc 1998;273(52):34983-91.

[77] Role of the nedd8 modification of cul2 in the sequential activation of ecv complex. Neoplasia. 1 nov 2006;8(11):956-63.

[78] The structure of the appbp1-uba3-nedd8-atp complex reveals the basis for selective ubiquitin-like protein activation by an e1. Molecular Cell. 1 déc 2003;12(6):1427-37.

[79] Park HS, Ju UI, Park JW, Song JY, Shin DH, Lee KH, et al. PPARγ neddylation essential for adipogenesis is a potential target for treating obesity. Cell Death Differ. août 2016;23(8):1296-311.

[80] Zhang X, Zhang YL, Qiu G, Pian L, Guo L, Cao H, et al. Hepatic neddylation targets and stabilizes electron transfer flavoproteins to facilitate fatty acid β-oxidation. Proc Natl Acad Sci U S A. 4 févr 2020;117(5):2473-83.

[81] Vogl AM, Brockmann MM, Giusti SA, Maccarrone G, Vercelli CA, Bauder CA, et al. Neddylation inhibition impairs spine development, destabilizes synapses and deteriorates cognition. Nat Neurosci. févr 2015;18(2):239-51.

[82] Zhao Y, Morgan MA, Sun Y. Targeting neddylation pathways to inactivate cullin-ring ligases for anticancer therapy. Antioxid Redox Signal. 10 déc 2014;21(17):2383-400.

[83] Zhang S, Yu Q, Li Z, Zhao Y, Sun Y. Protein neddylation and its role in health and diseases. Sig Transduct Target Ther. 5 avr 2024;9(1):1-36.

[84] Esophageal cancer male to female incidence ratios in Africa: A systematic review and meta-analysis of geographic, time and age trends. Cancer Epidemiology. 1 avr 2018;53:119-28.

[85] Esophageal cancer treatment - nci [Internet]. 2024 [cited18 mai 2024]. Disponible in: https://www.cancer.gov/types/esophageal/patient/esophageal-treatment-pdq

[86] Rustgi AK, El-Serag HB. Esophageal carcinoma. N Engl J Med. 25 déc 2014;371(26):2499-509.

[87] Li L, Wang M, Yu G, Chen P, Li H, Wei D, et al. Overactivated neddylation pathway as a therapeutic target in lung cancer. J Natl Cancer Inst. juin 2014;106(6):dju083.-

[88] Soucy TA, Smith PG, Milhollen MA, Berger AJ, Gavin JM, Adhikari S, et al. An inhibitor of NEDD8-activating enzyme as a new approach to treat cancer. Nature. avr 2009;458(7239):732-6.

[89] Chen P, Hu T, Liang Y, Li P, Chen X, Zhang J, et al. Neddylation inhibition activates the extrinsic apoptosis pathway through atf4-chop-dr5 axis in human esophageal cancer cells. Clin Cancer Res. 15 août 2016;22(16):4145-57.

[90] Heinrich, M.. "phytotherapy." Encyclopedia Britannica, March 12, 2024. https://www.britannica.com/science/phytotherapy.

[91] Altuntas E, Özgöz E, Taser O. Some physical properties of fenugreek (Trigonella foenum-graceum L.) seeds. J Food Eng 2005; 71: 37-43. doi:nhttp://dx.doi.org/10.1016/j.jfoodeng.2004.10.015

[93] Bahmani M, Shirzad H, Mirhosseini M, Mesripour A, Rafieian-Kopaei M. A Review on Ethnobotanical and Therapeutic Uses of Fenugreek (Trigonella foenum-graceum L). Journal of Evidence-Based Complementary & Alternative Medicine. 2016;21(1):53-62. doi:10.1177/2156587215583405

[94] "Trigonella foenum-graecum". Germplasm Resources Information Network. Agricultural Research Service, United States Department of Agriculture. Retrieved 2008-03-13.

[95] Bahmani M, Shirzad H, Mirhosseini M, Mesripour A, Rafieian-Kopaei M. A review on ethnobotanical and therapeutic uses of fenugreek (Trigonella foenum-graceum L.). Evid Based Complement Altern Med 2016; 21:53-62. doi: http:// dx.doi.org/10.1177/2156587215583405

[96] Cowan MM. Plant products as antimicrobial agents. Clin Microbiol Rev1999; 12:564-582. doi: http://dx.doi.org/10.1128/cmr.12.4.564

[97] Roberts KT, Allen-Vercoe E, Williams SA, Graham T, Cui SW. Comparative study of the in vitro fermentative characteristics of fenugreek gum, white bread and bread with fenugreek gum using human faecal microbes. Bioact Carbohydr Diet Fibre 2015; 5:116-124. doi: http://dx.doi. org/10.1016/j.bcdf.2014.09.007

[98] Dixit P, Ghaskadbi S, Mohan H, Devasagayam T. Antioxidant properties of germinated fenugreek seeds. Phytother Res 2005; 19:977-983. doi: http://dx.doi.org/10.1002/ptr.1769

[99] Varshney H, Siddique YH. Pharmacological Attributes of Fenugreek with Special Reference to Alzheimer's Disease. Curr Alzheimer Res. 2023;20(2):71-79. doi: 10.2174/1567205020666230525154300. PMID: 37231762
[100] Morcos SR, Elhawary Z, Gabrial GN. Protein-rich food mixtures for feeding the young in Egypt. 1. Formulation. Z Ernahrungswiss. 1981;20:275–282.
[101] Yoshikawa M, Murakami T, Komatsu H, Murakami N, Yamahara J, Matsuda H. Medicinal foodstuffs. IV. Fenugreek seed. (1): structures of trigoneosides Ia, Ib, IIa, IIb, IIIa, and IIIb, new furostanol saponins from theseeds of Indian Trigonella foenum-graecum L. Chem Pharm Bull. 1997;45:81–87.
[102] Esmaeili A, Rashidi B, Rezazadeh S. Biological Activities of Various Extracts and Chemical Composition of Trigonella monantha C. A. Mey. subsp. monantha Grown in Iran. Iran J Pharm Res. 2012 Fall;11(4):1127-36. PMID: 24250546; PMCID: PMC3813150.
[103] Sharifi-Rad M., Ozcelik B., Altın G., Daşkaya-Dikmen C., Martorell M., Ramírez-Alarcón K., Alarcón-Zapata P., Morais-Braga M.F.B., Carneiro J.N.P., Leal A.L.A.B. Salvia spp. plants-from farm to food applications and phytopharmacotherapy. Trends Food Sci. Technol. 2018;80:242–263. [Google Scholar] [Ref list]
[104] Williams BR, Nazarians A, Gill MA. A review of rivastigmine: a reversible
cholinesterase inhibitor. Clin Ther 2003; 25: 1634-53.
[105] Alvarez A, Opazo C, Alarcón R, Garrido J, Inestrosa NC. Acetylcholinesterase promotes the aggregation of amyloid-b-peptide fragments by forming a complex with the growing fibrils. J Mol Biol 1997; 272: 348-61
[106] Khedher M.R.B., Khedher S.B., Chaieb I., Tounsi S., Hammami M. Chemical composition and biological activities of Salvia officinalis essential oil from Tunisia. EXCLI J. 2017;16:160. [PMC free article] [PubMed] [Google Scholar] [Ref list]
[107] Ghorbani A., Esmaeilizadeh M. Pharmacological properties of Salvia officinalis and its components. J. Tradit. Complement. Med. 2017;7:433–440. [PMC free article] [PubMed] [Google Scholar] [Ref list]
[108]Adams M., Gmünder F., Hamburger M. Plants traditionally used in age-related brain disorders—A survey of ethnobotanical literature. J. Ethnopharmacol. 2007;113:363–381. [PubMed] [Google Scholar] [Ref list]
[109] Perry E.K., Pickering A.T., Wang W.W., Houghton P.J., Perry N.S.L. Medicinal plants and Alzheimer’s disease: From ethnobotany to phytotherapy. J. Pharm. Pharmacol. 1999;51:527–534. [PubMed] [Google Scholar] [Ref list]
[110] Eidi M., Eidi A., Zamanizadeh H. Effect of Salvia officinalis L. leaves on serum glucose and insulin in healthy and streptozotocin-induced diabetic rats. J. Ethnopharmacol. 2005;100:310–313. [PubMed] [Google Scholar] [Ref list]
[111] S Akhondzadeh, M Noroozian, M Mohammadi, S Ohadinia, A Jamshidi, M Khani. J Clin Pharm Ther. 2003;28(1):53-9
[112] Ahmad Reza Golparvar1,*,Amin Hadipanah2, Identification of the Components of Sage (Salvia officinalisL.) and Thyme (Thymus vulgarisL.) Cultivated in Isfahan Climatic Conditions, Electrinic Jornal of Biology
[113] 42- "Phoenix dactylifera". Germplasm Resources Information Network. Agricultural Research Service, United States Department of Agriculture. Retrieved 10 December 2017.

[114] "Phoenix dactylifera L." Plants of the World Online | Kew Science. 2024. Retrieved 1 May 2024.

[115] Biota of North America Project, Phoenix dactylifera". Archived from the original on 20 April 2014. Retrieved 19 April 2014.

[116] Phoenix dactylifera in Flora of China @ efloras.org". eFloras, Flora of China. Archived from the original on 20 April 2014. Retrieved 19 April 2014.

[117] Krueger RR. "Date Palm Genetic Resource Conservation, Breeding, Genetics, And Genomics In California" (PDF). The Conference Exchange. Archived (PDF) from the original on 8 April 2023. Retrieved 26 March 2018.

[118] Date fruit classification using a wide range of classifiers | ieee conference publication | ieee xplore [Internet]. [cited18 mai 2024]. Disponible in: https://ieeexplore.ieee.org/document/10180302

[119] Date_palm [Internet]. [cité 18 mai 2024]. Disponible in : https://www.bionity.com/en/encyclopedia/Date_Palm.html

[120] Qadir A, Aqil M, Ahmad U, Khan N, Warsi MH, Akhtar J, et al. Date seed extract-loaded oil-in-water nanoemulsion: Development, characterization, and antioxidant activity as a delivery model for rheumatoid arthritis. J Pharm Bioallied Sci. 2020;12(3):308-16.

[121] Ataei D, hamidi-Esfahani Z, Ahmadi-Gavlighi H. Enzymatic production of xylooligosaccharide from date (Phoenix dactylifera L.) seed. Food Sci Nutr. 3 nov 2020;8(12):6699-707.

[122] The effect of date seed (Phoenix dactylifera) supplementation on inflammation, oxidative stress biomarkers, and performance in active people: A blinded randomized controlled trial protocol. Contemporary Clinical Trials Communications. 1 août 2022;28:100951.

[123] Saryono, Warsinah, Isworo A, Sarmoko. Anti-inflammatory activity of date palm seed by downregulating interleukin-1β, TGF-β, cyclooxygenase-1 and -2: A study among middle age women. Saudi Pharm. J. 2020;28:1014–1018.

[124] Hilary S, Kizhakkayil J, Souka U, Al-Meqbaali F, Ibrahim W, Platat C. In-vitro investigation of polyphenol-rich date (Phoenix dactylifera L.) seed extract bioactivity. Front Nutr. 23 août 2021;8:667514.

[125] Tang ZX, Shi LE, Aleid SM. Date fruit: chemical composition, nutritional and medicinal values, products. J Sci Food Agric. 15 août 2013;93(10):2351-61.

[126] Hong YJ, Tomas-Barberan FA, Kader AA, Mitchell AE. The flavonoid glycosides and procyanidin composition of Deglet Noor dates (Phoenix dactylifera). J Agric Food Chem. 22 mars 2006;54(6):2405-11.

[127] Shafiei M, Karimi K, Taherzadeh MJ. Palm date fibers: analysis and enzymatic hydrolysis. Int J Mol Sci. 1 nov 2010; 11(11):4285-96.

[128] Golshan Tafti A. Solaimani Dahdivan N. Yasini Ardakani S A. Physicochemical properties and applications of date seed and its oil. International Food Research Journal . (August 2017) ;24(4): 1399-1406.

[129] Besbes S. Blecker C. Deroanne C. Drira N. Attia H. Date seeds: Chemical composition and characteristic profiles of the lipid fraction. Food Chem. 2004, 84, 577–584.

[130] Assirey E A. Nutritional composition of fruit of 10 date palm (Phoenix dactylifera L.) cultivars grown in Saudi Arabia. J. Taibah Univ. Sci. 2015 ;9;75–79.

[131] Ogungbenle H. Chemical and fatty acid compositions of date palm fruit (Phoenix dactylifera L) flour. Bangladesh Journal of Scientific and Industrial Research [Internet]. 2011 [cité 19 mai 2024]; Disponible sur: https://www.semanticscholar.org/paper/Chemical-and-Fatty-Acid-Compositions-of-Date-Palm

[132] Al-Shahib W, Marshall RJ. The fruit of the date palm: its possible use as the best food for the future? Int J Food Sci Nutr. juill 2003;54(4):247-59.

[133] Mrabet A, Jiménez-Araujo A, Guillén-Bejarano R, Rodríguez-Arcos R, Sindic M. Date seeds: a promising source of oil with functional properties. Foods. 16 juin 2020;9(6):787.

[134] Alharbi KL, Raman J, Shin HJ. Date fruit and seed in nutricosmetics. Cosmetics. sept 2021;8(3):59.

[135] N. Echegaray, M. Pateiro, B. Gullón, R. Amarowicz, J. M. Misihairabgwi, and J. M. Lorenzo, "Phoenix dactylifera products in human health - a review," Trends in Food Science & Technology, vol. 105, pp. 238–250, 2020.

[136] A. Younas, S. A. Naqvi, M. R. Khan et al., "Functional food and nutra-pharmaceutical perspectives of date (Phoenix dactylifera L.) fruit," Journal of Food Biochemistry, vol. 44, no. 9, article e13332, 2020

[137] S. A. Ali, N. Parveen, and A. S. Ali, "Links between the prophet Muhammad (PBUH) recommended foods and disease management: a review in the light of modern superfoods," International Journal of Health Sciences, vol. 12, no. 2, pp. 61–69, 2018.

[138] Molecular Docking: Concept and Application. (2023).35-48. doi: 10.9734/bpi/napr/v1/6049a

[139] Molecular Docking: Methodological Approaches of Risk Assessment. Разработка и регистрация лекарственных средств, (2023).;12(2):206-210. doi: 10.33380/2305-2066-

2023-12-2-206-210

[140] Pablo, Machado. Molecular Docking in the Study of Ligand-Protein Recognition: An Overview. Biomedical engineering, (2023). doi: 10.5772/intechopen.106583

[141] Molecular Docking - Recent Advances [Working Title]. Biomedical engineering, (2023). doi: 10.5772/intechopen.100665

[142] Molecular Docking: Metamorphosis in Drug Discovery. Biomedical engineering, (2023). doi: 10.5772/intechopen.105972

[143] T. Schulz-Gasch, M. Stahl, "Scoring Functions for Protein-ligand Interactions: A Critical Perspective", Drug Discovery Today: Technologies, 2004, 1, 231-239.

[144] BOUCHERIT H. Theoretical study of the interactions involved in the inhibition of methionine aminopeptidase of mycobacteriumtuberculosis by various molecules. Master's thesis in biochemistry. Constantine: Mentouri Constantine University. Algeria. 2012. 71p

[145] R. Wang, Y. Lu, X. Fang, S. Wang, "An Extensive Test of 14 Scoring Functions Using the PDBbind Refined Set of 800 Protein-ligand Complexes", J. Chem. Inf. Comp. Sci., 2004, 44, 2114-2125

[146] Leach A.R. Molecular modelling: Principles and application. Pearson Education Canada.2001.582. 10-6p

[147] El Hadji Said K. Contribution à l'étude de l'inhibition d'enzyme par des Tripodes pyrazoliques par modélisation moléculaire. These de Master d'université de TLEMCEN Faculté des Sciences Département de Chimie. Tlemcen. Algérie. 2016. 50P

[148] Copyright 2012 - 2018 Avada | All Rights Reserved | Powered by WordPress | Theme Fusion a 2022

[149] O. Trott and A. J. Olson. AutodockVina: improving the speedand accuracy of docking with a new scoring function, efficientoptimization, and multithreading. Journal of Computational Chemistry, 31(2):455–461, 2010.

[150] Optimization | Gaussian.com [Internet]. [cited 8 juin 2024]. Disponible in: https://gaussian.com/opt/

[151] G09w: preferences [Internet]. [Cited 8 juin 2024]. Disponible in: http://thiele.ruc.dk/~spanget/help/g09/g09w_prefs.htm

[152] Bálint D, Jäntschi L. Comparison of molecular geometry optimization methods based on molecular descriptors. Mathematics. janv 2021;9(22):2855.

[153]Optimization | Gaussian.com [Internet]. [cited 8 juin 2024]. Disponible in: https://gaussian.com/opt/
[157] O. Trott and A. J. Olson. Autodock Vina: improving the speed and accuracy of docking with a new scoring function, efficient optimization, and multithreading. Journal of Computational Chemistry, 31(2):455–461, 2010
[158] G09w: preferences [Internet]. [Cited 8 juin 2024]. Disponible in: http://thiele.ruc.dk/~spanget/help/g09/g09w_prefs.htm
[159] Bálint D, Jäntschi L. Comparison of molecular geometry optimization methods based on molecular descriptors. Mathematics. janv 2021;9(22):2855.
[160] Copyright 2012 - 2018 Avada | All Rights Reserved | Powered by WordPress | Theme Fusion a 2022
[161] The UniProt Consortium , UniProt: the universal protein knowledgebase in 2021, Nucleic Acids Research, Volume 49, Issue D1, 8 January 2021, Pages D480–D489, https://doi.org/10.1093/nar/gkaa1100
[162] Alessandra Neis Oct 21, 2019 ,5 min read , a 2022
[163] Hay, M., Thomas, D. W., Craighead, J. L., Economides, C. & Rosenthal, J. Clinical development success rates for investigational drugs. Nature Biotechnol. 32, 40–51 (2014).
[164] Priyanka Banerjee, Emanuel Kemmler, Mathias Dunkel, Robert Preissner, ProTox 3.0: a webserver for the prediction of toxicity of chemicals, Nucleic Acids Research, 2024;, gkae303, https://doi.org/10.1093/nar/gkae303
[165] Szklarczyk D, Kirsch R, Koutrouli M, et al. The STRING database in 2023: protein-protein association networks and functional enrichment analyses for any sequenced genome of interest. Nucleic Acids Res. 2023;51(D1):D638-D646. doi:10.1093/nar/gkac1000
[166] Szklarczyk D, Gable AL, Lyon D, et al. STRING v11: protein-protein association networks with increased coverage, supporting functional discovery in genome-wide experimental datasets. Nucleic Acids Res. 2019;47(D1):D607-D613.doi:10.1093/nar/gky1131
[167] Salentin S, Schreiber S, Haupt VJ, Adasme MF, Schroeder M. PLIP: fully automated protein-ligand interaction profiler. Nucleic Acids Res. 2015;43(W1):W443-W447. doi:10.1093/nar/gkv315
[168]Yang, Liu., Xiao-Chun, Yang., Jianhong, Gan., Shuang, Chen., Zhi-Xiong, Xiao., Yang, Cao. CB-Dock2: improved protein–ligand blind docking by integrating cavity detection, docking and homologous template fitting. Nucleic Acids Research, (2022).;50(W1):W159-W164. doi: 10.1093/nar/gkac394
[169] Blind docking of 4-Amino-7-Chloroquinoline analogs as potential dengue virus protease inhibitor using CB Dock a web server. Indian Journal of Biochemistry & Biophysics, (2023). doi: 10.56042/ijbb.v60i1.64604
[170] Yang, Liu., Maximilian, Grimm., Wentao, Dai., Mu-Chun, Hou., Zhi-Xiong, Xiao., Yang, Cao. CB-Dock: a web server for cavity detection-guided protein-ligand blind docking.. Acta Pharmacologica Sinica, (2020).;41(1):138-144. doi: 10.1038/S41401-019-0228-6
[171] Mateusz, Kurcinski., Michał, H., Jamróz., Maciej, Blaszczyk., Andrzej, Kolinski., Sebastian, Kmiecik. CABS-dock web server for the flexible docking of peptides to proteins without prior knowledge of the binding site. Nucleic Acids Research, (2015).;43 doi: 10.1093/NAR/GKV456
[172] Bickerton, G.R., *et al.* (2012) Quantifying the chemical beauty of drugs. *Nat. Chem.*, **4**, 90-98.
[173] M.J. Frisch, et al., Gaussian 09W, Revision A.1, Gaussian Incorp, Wallingford, CT, 2009.
[174] LIBIOS 83 rue Edmond Michelet 69490 Vindry Sur Turdine France, info@libios.fr ,REFERENCE : KF01007.
[175] Benet LZ, Hosey CM, Ursu O, Oprea TI. Bddcs, the rule of 5 and drugability. Adv Drug Deliv Rev. 1 juin 2016;101:89-98
[176] Bitam S, Hamadache M, Hanini S. Targeting bladder cancer with Trigonella foenum-graecum: a computational study using network pharmacology and molecular docking. Journal of Biomolecular Structure and Dynamics. 12 avr 2024;42(6):3286-93.
[177] Zhou HX, Pang X. Electrostatic Interactions in Protein Structure, Folding, Binding, and

Condensation. Chem Rev. 2018 Feb 28;118(4):1691-1741. doi: 10.1021/acs.chemrev.7b00305. Epub 2018 Jan 10. PMID: 29319301; PMCID: PMC5831536.
[178] Prabhat Gautam, Ramesh Maragani, Rajneesh Misra,Tuning the HOMO–LUMO gap of donor-substituted benzothiazoles,Tetrahedron Letters,Volume 55, Issue 50,2014, Pages 6827-6830.
[179]Ames BN, Durston WE, Yamasaki E, Lee FD. Carcinogens are mutagens: a simple test system combining liver homogenates for activation and bacteria for detection. Proc Natl Acad Sci USA. août 1973;70(8):2281-5.

bibliographic References

Annexes

Toxicity Prediction of 7,4'-Dihydroxyflavone

Classification	Target	Shorthand	Prediction	Probability
Organ toxicity	Hepatotoxicity	dili	Inactive	0.68
Organ toxicity	Neurotoxicity	neuro	Inactive	0.86
Organ toxicity	Nephrotoxicity	nephro	Active	0.55
Organ toxicity	Respiratory toxicity	respi	Active	0.74
Organ toxicity	Cardiotoxicity	cardio	Inactive	0.59
Toxicity end points	Carcinogenicity	carcino	Inactive	0.51
Toxicity end points	Immunotoxicity	immuno	Inactive	0.93
Toxicity end points	Mutagenicity	mutagen	Inactive	0.64
Toxicity end points	Cytotoxicity	cyto	Inactive	0.82
Toxicity end points	BBB-barrier	bbb	Inactive	0.52
Toxicity end points	Ecotoxicity	eco	Active	0.50
Toxicity end points	Clinical toxicity	clinical	Inactive	0.55
Toxicity end points	Nutritional toxicity	nutri	Inactive	0.52
Tox21-Nuclear receptor signalling pathways	Aryl hydrocarbon Receptor (AhR)	nr_ahr	Active	0.95
Tox21-Nuclear receptor signalling pathways	Androgen Receptor (AR)	nr_ar	Inactive	0.99
Tox21-Nuclear receptor signalling pathways	Androgen Receptor Ligand Binding Domain (AR-LBD)	nr_ar_lbd	Inactive	0.97
Tox21-Nuclear receptor signalling pathways	Aromatase	nr_aromatase	Active	0.57
Tox21-Nuclear receptor signalling pathways	Estrogen Receptor Alpha (ER)	nr_er	Active	0.94
Tox21-Nuclear receptor signalling pathways	Estrogen Receptor Ligand Binding Domain (ER-LBD)	nr_er_lbd	Active	0.88
Tox21-Nuclear receptor signalling pathways	Peroxisome Proliferator Activated Receptor Gamma (PPAR-Gamma)	nr_ppar_gamma	Active	0.65
Tox21-Stress response pathways	Nuclear factor (erythroid-derived 2)-like 2/ antioxidant responsive element (nrf2/ARE)	sr_are	Inactive	0.98
Tox21-Stress response pathways	Heat shock factor response element (HSE)	sr_hse	Inactive	0.98
Tox21-Stress response pathways	Mitochondrial Membrane Potential (MMP)	sr_mmp	Active	0.88
Tox21-Stress response pathways	Phosphoprotein (Tumor Supressor) p53	sr_p53	Active	0.66
Tox21-Stress response pathways	ATPase family AAA domain-containing protein 5 (ATAD5)	sr_atad5	Active	0.94
Molecular Initiating Events	Thyroid hormone receptor alpha (THRα)	mie_thr_alpha	Inactive	0.90
Molecular Initiating Events	Thyroid hormone receptor beta (THRβ)	mie_thr_beta	Inactive	0.78
Molecular Initiating Events	Transtyretrin (TTR)	mie_ttr	Inactive	0.97
Molecular Initiating Events	Ryanodine receptor (RYR)	mie_ryr	Inactive	0.98
Molecular Initiating Events	GABA receptor (GABAR)	mie_gabar	Inactive	0.96
Molecular Initiating Events	Glutamate N-methyl-D-aspartate receptor (NMDAR)	mie_nmdar	Inactive	0.92
Molecular Initiating	alpha-amino-3-hydroxy-5-methyl-4-	mie_ampar	Inactive	0.97

Classification	Target	Shorthand	Prediction	Probability
Events	isoxazolepropionate receptor (AMPAR)			
Molecular Initiating Events	Kainate receptor (KAR)	mie_kar	Inactive	0.99
Molecular Initiating Events	Achetylcholinesterase (AChE)	mie_ache	Inactive	0.68
Molecular Initiating Events	Constitutive androstane receptor (CAR)	mie_car	Inactive	0.98
Molecular Initiating Events	Pregnane X receptor (PXR)	mie_pxr	Inactive	0.92
Molecular Initiating Events	NADH-quinone oxidoreductase (NADHOX)	mie_nadhox	Inactive	0.97
Molecular Initiating Events	Voltage gated sodium channel (VGSC)	mie_vgsc	Inactive	0.95
Molecular Initiating Events	Na+/I- symporter (NIS)	mie_nis	Inactive	0.98
Metabolism	Cytochrome CYP1A2	CYP1A2	Active	0.98
Metabolism	Cytochrome CYP2C19	CYP2C19	Inactive	0.63
Metabolism	Cytochrome CYP2C9	CYP2C9	Active	0.77
Metabolism	Cytochrome CYP2D6	CYP2D6	Inactive	0.93
Metabolism	Cytochrome CYP3A4	CYP3A4	Active	0.94
Metabolism	Cytochrome CYP2E1	CYP2E1	Inactive	0.98

Toxicity Prediction of Olmelin

Classification	Target	Shorthand	Prediction	Probability
Organ toxicity	Hepatotoxicity	dili	Inactive	0.73
Organ toxicity	Neurotoxicity	neuro	Inactive	0.83
Organ toxicity	Nephrotoxicity	nephro	Active	0.65
Organ toxicity	Respiratory toxicity	respi	Active	0.84
Organ toxicity	Cardiotoxicity	cardio	Active	0.62
Toxicity end points	Carcinogenicity	carcino	Inactive	0.65
Toxicity end points	Immunotoxicity	immuno	Inactive	0.75
Toxicity end points	Mutagenicity	mutagen	Inactive	0.94
Toxicity end points	Cytotoxicity	cyto	Inactive	0.90
Toxicity end points	BBB-barrier	bbb	Active	0.52
Toxicity end points	Ecotoxicity	eco	Inactive	0.50
Toxicity end points	Clinical toxicity	clinical	Active	0.50
Toxicity end points	Nutritional toxicity	nutri	Active	0.58
Tox21-Nuclear receptor signalling pathways	Aryl hydrocarbon Receptor (AhR)	nr_ahr	Active	1.0
Tox21-Nuclear receptor signalling pathways	Androgen Receptor (AR)	nr_ar	Inactive	0.99
Tox21-Nuclear receptor signalling pathways	Androgen Receptor Ligand Binding Domain (AR-LBD)	nr_ar_lbd	Inactive	0.99
Tox21-Nuclear receptor signalling pathways	Aromatase	nr_aromatase	Active	0.52
Tox21-Nuclear receptor signalling pathways	Estrogen Receptor Alpha (ER)	nr_er	Active	1.0
Tox21-Nuclear receptor signalling pathways	Estrogen Receptor Ligand Binding Domain (ER-LBD)	nr_er_lbd	Active	1.0
Tox21-Nuclear receptor signalling pathways	Peroxisome Proliferator Activated Receptor Gamma (PPAR-Gamma)	nr_ppar_gamma	Inactive	0.88
Tox21-Stress response pathways	Nuclear factor (erythroid-derived 2)-like 2/ antioxidant responsive element (nrf2/ARE)	sr_are	Inactive	0.98
Tox21-Stress response pathways	Heat shock factor response element (HSE)	sr_hse	Inactive	0.98
Tox21-Stress response pathways	Mitochondrial Membrane Potential (MMP)	sr_mmp	Active	0.96
Tox21-Stress response pathways	Phosphoprotein (Tumor Supressor) p53	sr_p53	Active	0.53
Tox21-Stress response pathways	ATPase family AAA domain-containing protein 5 (ATAD5)	sr_atad5	Active	1.0
Molecular Initiating Events	Thyroid hormone receptor alpha (THRα)	mie_thr_alpha	Inactive	0.90
Molecular Initiating Events	Thyroid hormone receptor beta (THRβ)	mie_thr_beta	Inactive	0.78
Molecular Initiating Events	Transtyretrin (TTR)	mie_ttr	Inactive	0.97
Molecular Initiating Events	Ryanodine receptor (RYR)	mie_ryr	Inactive	0.98
Molecular Initiating Events	GABA receptor (GABAR)	mie_gabar	Inactive	0.96
Molecular Initiating Events	Glutamate N-methyl-D-aspartate receptor (NMDAR)	mie_nmdar	Inactive	0.92
Molecular Initiating	alpha-amino-3-hydroxy-5-methyl-4-	mie_ampar	Inactive	0.97

Classification	Target	Shorthand	Prediction	Probability
Events	isoxazolepropionate receptor (AMPAR)			
Molecular Initiating Events	Kainate receptor (KAR)	mie_kar	Inactive	0.99
Molecular Initiating Events	Achetylcholinesterase (AChE)	mie_ache	Inactive	0.73
Molecular Initiating Events	Constitutive androstane receptor (CAR)	mie_car	Inactive	0.98
Molecular Initiating Events	Pregnane X receptor (PXR)	mie_pxr	Inactive	0.92
Molecular Initiating Events	NADH-quinone oxidoreductase (NADHOX)	mie_nadhox	Inactive	0.97
Molecular Initiating Events	Voltage gated sodium channel (VGSC)	mie_vgsc	Inactive	0.95
Molecular Initiating Events	Na+/I- symporter (NIS)	mie_nis	Inactive	0.98
Metabolism	Cytochrome CYP1A2	CYP1A2	Active	0.95
Metabolism	Cytochrome CYP2C19	CYP2C19	Active	0.98
Metabolism	Cytochrome CYP2C9	CYP2C9	Active	0.60
Metabolism	Cytochrome CYP2D6	CYP2D6	Inactive	0.78
Metabolism	Cytochrome CYP3A4	CYP3A4	Inactive	0.95
Metabolism	Cytochrome CYP2E1	CYP2E1	Inactive	0.99

Toxicity Prediction of Apigenin

Classification	Target	Shorthand	Prediction	Probability
Organ toxicity	Hepatotoxicity	dili	Inactive	0.68
Organ toxicity	Neurotoxicity	neuro	Inactive	0.86
Organ toxicity	Nephrotoxicity	nephro	Active	0.60
Organ toxicity	Respiratory toxicity	respi	Active	0.75
Organ toxicity	Cardiotoxicity	cardio	Inactive	0.63
Toxicity end points	Carcinogenicity	carcino	Inactive	0.62
Toxicity end points	Immunotoxicity	immuno	Inactive	0.99
Toxicity end points	Mutagenicity	mutagen	Inactive	0.57
Toxicity end points	Cytotoxicity	cyto	Inactive	0.87
Toxicity end points	BBB-barrier	bbb	Inactive	0.51
Toxicity end points	Ecotoxicity	eco	Active	0.51
Toxicity end points	Clinical toxicity	clinical	Inactive	0.54
Toxicity end points	Nutritional toxicity	nutri	Inactive	0.55
Tox21-Nuclear receptor signalling pathways	Aryl hydrocarbon Receptor (AhR)	nr_ahr	Active	1.0
Tox21-Nuclear receptor signalling pathways	Androgen Receptor (AR)	nr_ar	Inactive	0.99
Tox21-Nuclear receptor signalling pathways	Androgen Receptor Ligand Binding Domain (AR-LBD)	nr_ar_lbd	Inactive	1.0
Tox21-Nuclear receptor signalling pathways	Aromatase	nr_aromatase	Active	0.61
Tox21-Nuclear receptor signalling pathways	Estrogen Receptor Alpha (ER)	nr_er	Active	1.0
Tox21-Nuclear receptor signalling pathways	Estrogen Receptor Ligand Binding Domain (ER-LBD)	nr_er_lbd	Active	1.0
Tox21-Nuclear receptor signalling pathways	Peroxisome Proliferator Activated Receptor Gamma (PPAR-Gamma)	nr_ppar_gamma	Active	1.0
Tox21-Stress response pathways	Nuclear factor (erythroid-derived 2)-like 2/ antioxidant responsive element (nrf2/ARE)	sr_are	Inactive	0.99
Tox21-Stress response pathways	Heat shock factor response element (HSE)	sr_hse	Inactive	0.99
Tox21-Stress response pathways	Mitochondrial Membrane Potential (MMP)	sr_mmp	Active	1.0
Tox21-Stress response pathways	Phosphoprotein (Tumor Supressor) p53	sr_p53	Active	1.0
Tox21-Stress response pathways	ATPase family AAA domain-containing protein 5 (ATAD5)	sr_atad5	Active	0.96
Molecular Initiating Events	Thyroid hormone receptor alpha (THRα)	mie_thr_alpha	Inactive	0.90
Molecular Initiating Events	Thyroid hormone receptor beta (THRβ)	mie_thr_beta	Inactive	0.78
Molecular Initiating Events	Transtyretrin (TTR)	mie_ttr	Inactive	0.97
Molecular Initiating Events	Ryanodine receptor (RYR)	mie_ryr	Inactive	0.98
Molecular Initiating Events	GABA receptor (GABAR)	mie_gabar	Inactive	0.96
Molecular Initiating Events	Glutamate N-methyl-D-aspartate receptor (NMDAR)	mie_nmdar	Inactive	0.92
Molecular Initiating	alpha-amino-3-hydroxy-5-methyl-4-	mie_ampar	Inactive	0.97

Classification	Target	Shorthand	Prediction	Probability
Events	isoxazolepropionate receptor (AMPAR)			
Molecular Initiating Events	Kainate receptor (KAR)	mie_kar	Inactive	0.99
Molecular Initiating Events	Achetylcholinesterase (AChE)	mie_ache	Inactive	0.68
Molecular Initiating Events	Constitutive androstane receptor (CAR)	mie_car	Inactive	0.98
Molecular Initiating Events	Pregnane X receptor (PXR)	mie_pxr	Inactive	0.92
Molecular Initiating Events	NADH-quinone oxidoreductase (NADHOX)	mie_nadhox	Inactive	0.97
Molecular Initiating Events	Voltage gated sodium channel (VGSC)	mie_vgsc	Inactive	0.95
Molecular Initiating Events	Na+/I- symporter (NIS)	mie_nis	Inactive	0.98
Metabolism	Cytochrome CYP1A2	CYP1A2	Active	1.0
Metabolism	Cytochrome CYP2C19	CYP2C19	Active	0.99
Metabolism	Cytochrome CYP2C9	CYP2C9	Active	0.81
Metabolism	Cytochrome CYP2D6	CYP2D6	Inactive	0.89
Metabolism	Cytochrome CYP3A4	CYP3A4	Active	0.99
Metabolism	Cytochrome CYP2E1	CYP2E1	Inactive	0.98

Toxicity Prediction of Linalool

Classification	Target	Shorthand	Prediction	Probability
Organ toxicity	Hepatotoxicity	dili	Inactive	0.76
Organ toxicity	Neurotoxicity	neuro	Inactive	0.62
Organ toxicity	Nephrotoxicity	nephro	Inactive	0.87
Organ toxicity	Respiratory toxicity	respi	Inactive	0.99
Organ toxicity	Cardiotoxicity	cardio	Inactive	0.75
Toxicity end points	Carcinogenicity	carcino	Inactive	0.64
Toxicity end points	Immunotoxicity	immuno	Inactive	0.99
Toxicity end points	Mutagenicity	mutagen	Inactive	0.95
Toxicity end points	Cytotoxicity	cyto	Inactive	0.82
Toxicity end points	BBB-barrier	bbb	Active	0.92
Toxicity end points	Ecotoxicity	eco	Active	0.56
Toxicity end points	Clinical toxicity	clinical	Inactive	0.63
Toxicity end points	Nutritional toxicity	nutri	Inactive	0.70
Tox21-Nuclear receptor signalling pathways	Aryl hydrocarbon Receptor (AhR)	nr_ahr	Inactive	1.0
Tox21-Nuclear receptor signalling pathways	Androgen Receptor (AR)	nr_ar	Inactive	1.0
Tox21-Nuclear receptor signalling pathways	Androgen Receptor Ligand Binding Domain (AR-LBD)	nr_ar_lbd	Inactive	1.0
Tox21-Nuclear receptor signalling pathways	Aromatase	nr_aromatase	Inactive	0.99
Tox21-Nuclear receptor signalling pathways	Estrogen Receptor Alpha (ER)	nr_er	Inactive	0.99
Tox21-Nuclear receptor signalling pathways	Estrogen Receptor Ligand Binding Domain (ER-LBD)	nr_er_lbd	Inactive	0.99
Tox21-Nuclear receptor signalling pathways	Peroxisome Proliferator Activated Receptor Gamma (PPAR-Gamma)	nr_ppar_gamma	Inactive	1.0
Tox21-Stress response pathways	Nuclear factor (erythroid-derived 2)-like 2/ antioxidant responsive element (nrf2/ARE)	sr_are	Inactive	0.99
Tox21-Stress response pathways	Heat shock factor response element (HSE)	sr_hse	Inactive	0.99
Tox21-Stress response pathways	Mitochondrial Membrane Potential (MMP)	sr_mmp	Inactive	0.86
Tox21-Stress response pathways	Phosphoprotein (Tumor Supressor) p53	sr_p53	Inactive	1.0
Tox21-Stress response pathways	ATPase family AAA domain-containing protein 5 (ATAD5)	sr_atad5	Inactive	1.0
Molecular Initiating Events	Thyroid hormone receptor alpha (THRα)	mie_thr_alpha	Inactive	0.90
Molecular Initiating Events	Thyroid hormone receptor beta (THRβ)	mie_thr_beta	Inactive	0.78
Molecular Initiating Events	Transtyretrin (TTR)	mie_ttr	Inactive	0.97
Molecular Initiating Events	Ryanodine receptor (RYR)	mie_ryr	Inactive	0.98
Molecular Initiating Events	GABA receptor (GABAR)	mie_gabar	Inactive	0.96
Molecular Initiating Events	Glutamate N-methyl-D-aspartate receptor (NMDAR)	mie_nmdar	Inactive	0.92
Molecular Initiating	alpha-amino-3-hydroxy-5-methyl-4-	mie_ampar	Inactive	0.97

Classification	Target	Shorthand	Prediction	Probability
Events	isoxazolepropionate receptor (AMPAR)			
Molecular Initiating Events	Kainate receptor (KAR)	mie_kar	Inactive	0.99
Molecular Initiating Events	Achetylcholinesterase (AChE)	mie_ache	Inactive	0.76
Molecular Initiating Events	Constitutive androstane receptor (CAR)	mie_car	Inactive	0.98
Molecular Initiating Events	Pregnane X receptor (PXR)	mie_pxr	Inactive	0.92
Molecular Initiating Events	NADH-quinone oxidoreductase (NADHOX)	mie_nadhox	Inactive	0.97
Molecular Initiating Events	Voltage gated sodium channel (VGSC)	mie_vgsc	Inactive	0.95
Molecular Initiating Events	Na+/I- symporter (NIS)	mie_nis	Inactive	0.98
Metabolism	Cytochrome CYP1A2	CYP1A2	Inactive	0.97
Metabolism	Cytochrome CYP2C19	CYP2C19	Inactive	0.90
Metabolism	Cytochrome CYP2C9	CYP2C9	Active	0.59
Metabolism	Cytochrome CYP2D6	CYP2D6	Inactive	0.87
Metabolism	Cytochrome CYP3A4	CYP3A4	Inactive	0.98
Metabolism	Cytochrome CYP2E1	CYP2E1	Inactive	0.97

Toxicity Prediction of Carnosol

Classification	Target	Shorthand	Prediction	Probability
Organ toxicity	Hepatotoxicity	dili	Inactive	0.76
Organ toxicity	Neurotoxicity	neuro	Inactive	0.83
Organ toxicity	Nephrotoxicity	nephro	Inactive	0.53
Organ toxicity	Respiratory toxicity	respi	Active	0.56
Organ toxicity	Cardiotoxicity	cardio	Inactive	0.54
Toxicity end points	Carcinogenicity	carcino	Inactive	0.62
Toxicity end points	Immunotoxicity	immuno	Active	0.99
Toxicity end points	Mutagenicity	mutagen	Inactive	0.88
Toxicity end points	Cytotoxicity	cyto	Inactive	0.83
Toxicity end points	BBB-barrier	bbb	Active	0.67
Toxicity end points	Ecotoxicity	eco	Inactive	0.53
Toxicity end points	Clinical toxicity	clinical	Inactive	0.6
Toxicity end points	Nutritional toxicity	nutri	Inactive	0.51
Tox21-Nuclear receptor signalling pathways	Aryl hydrocarbon Receptor (AhR)	nr_ahr	Inactive	0.96
Tox21-Nuclear receptor signalling pathways	Androgen Receptor (AR)	nr_ar	Inactive	0.91
Tox21-Nuclear receptor signalling pathways	Androgen Receptor Ligand Binding Domain (AR-LBD)	nr_ar_lbd	Inactive	0.86
Tox21-Nuclear receptor signalling pathways	Aromatase	nr_aromatase	Inactive	0.84
Tox21-Nuclear receptor signalling pathways	Estrogen Receptor Alpha (ER)	nr_er	Inactive	0.74
Tox21-Nuclear receptor signalling pathways	Estrogen Receptor Ligand Binding Domain (ER-LBD)	nr_er_lbd	Inactive	0.84
Tox21-Nuclear receptor signalling pathways	Peroxisome Proliferator Activated Receptor Gamma (PPAR-Gamma)	nr_ppar_gamma	Inactive	0.94
Tox21-Stress response pathways	Nuclear factor (erythroid-derived 2)-like 2/ antioxidant responsive element (nrf2/ARE)	sr_are	Inactive	0.81
Tox21-Stress response pathways	Heat shock factor response element (HSE)	sr_hse	Inactive	0.81
Tox21-Stress response pathways	Mitochondrial Membrane Potential (MMP)	sr_mmp	Inactive	0.60
Tox21-Stress response pathways	Phosphoprotein (Tumor Supressor) p53	sr_p53	Inactive	0.78
Tox21-Stress response pathways	ATPase family AAA domain-containing protein 5 (ATAD5)	sr_atad5	Inactive	0.93
Molecular Initiating Events	Thyroid hormone receptor alpha (THRα)	mie_thr_alpha	Inactive	0.90
Molecular Initiating Events	Thyroid hormone receptor beta (THRβ)	mie_thr_beta	Inactive	0.78
Molecular Initiating Events	Transtyretrin (TTR)	mie_ttr	Inactive	0.97
Molecular Initiating Events	Ryanodine receptor (RYR)	mie_ryr	Inactive	0.98
Molecular Initiating Events	GABA receptor (GABAR)	mie_gabar	Inactive	0.96
Molecular Initiating Events	Glutamate N-methyl-D-aspartate receptor (NMDAR)	mie_nmdar	Inactive	0.92
Molecular Initiating	alpha-amino-3-hydroxy-5-methyl-4-	mie_ampar	Inactive	0.97

Classification	Target	Shorthand	Prediction	Probability
Events	isoxazolepropionate receptor (AMPAR)			
Molecular Initiating Events	Kainate receptor (KAR)	mie_kar	Inactive	0.99
Molecular Initiating Events	Achetylcholinesterase (AChE)	mie_ache	Inactive	0.76
Molecular Initiating Events	Constitutive androstane receptor (CAR)	mie_car	Inactive	0.98
Molecular Initiating Events	Pregnane X receptor (PXR)	mie_pxr	Inactive	0.92
Molecular Initiating Events	NADH-quinone oxidoreductase (NADHOX)	mie_nadhox	Inactive	0.97
Molecular Initiating Events	Voltage gated sodium channel (VGSC)	mie_vgsc	Inactive	0.95
Molecular Initiating Events	Na+/I- symporter (NIS)	mie_nis	Inactive	0.98
Metabolism	Cytochrome CYP1A2	CYP1A2	Inactive	0.86
Metabolism	Cytochrome CYP2C19	CYP2C19	Inactive	0.87
Metabolism	Cytochrome CYP2C9	CYP2C9	Inactive	0.57
Metabolism	Cytochrome CYP2D6	CYP2D6	Inactive	0.87
Metabolism	Cytochrome CYP3A4	CYP3A4	Inactive	0.65
Metabolism	Cytochrome CYP2E1	CYP2E1	Inactive	1.0

Tricin

The toxicity radar chart is intended to quickly illustrate the confidence of positive toxicity results compared to the average of its class.

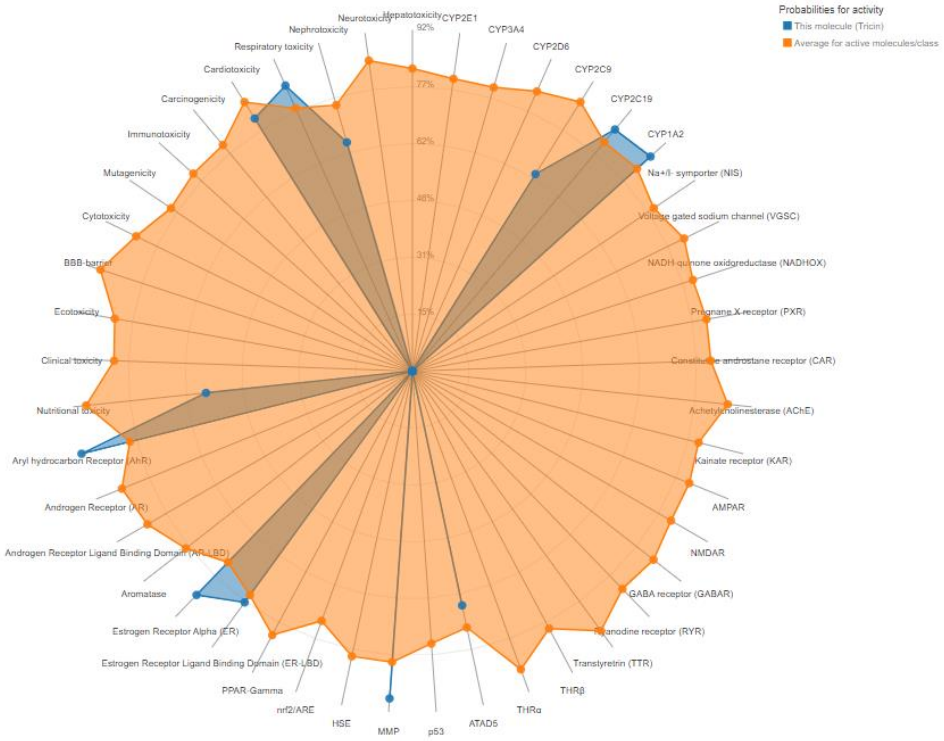

The network chart is intended to quickly illustrate the connection between the selected compound and predicted activities

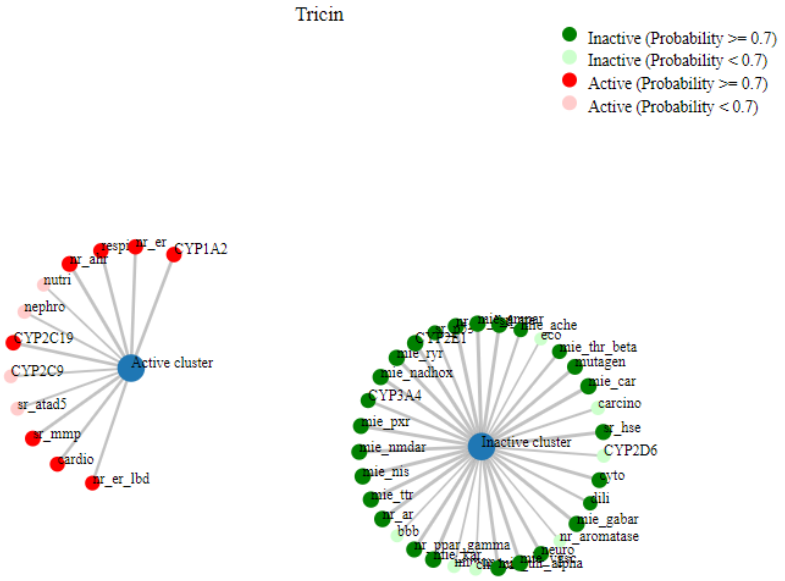

7,4'-Dihydroxyflavone

The toxicity radar chart

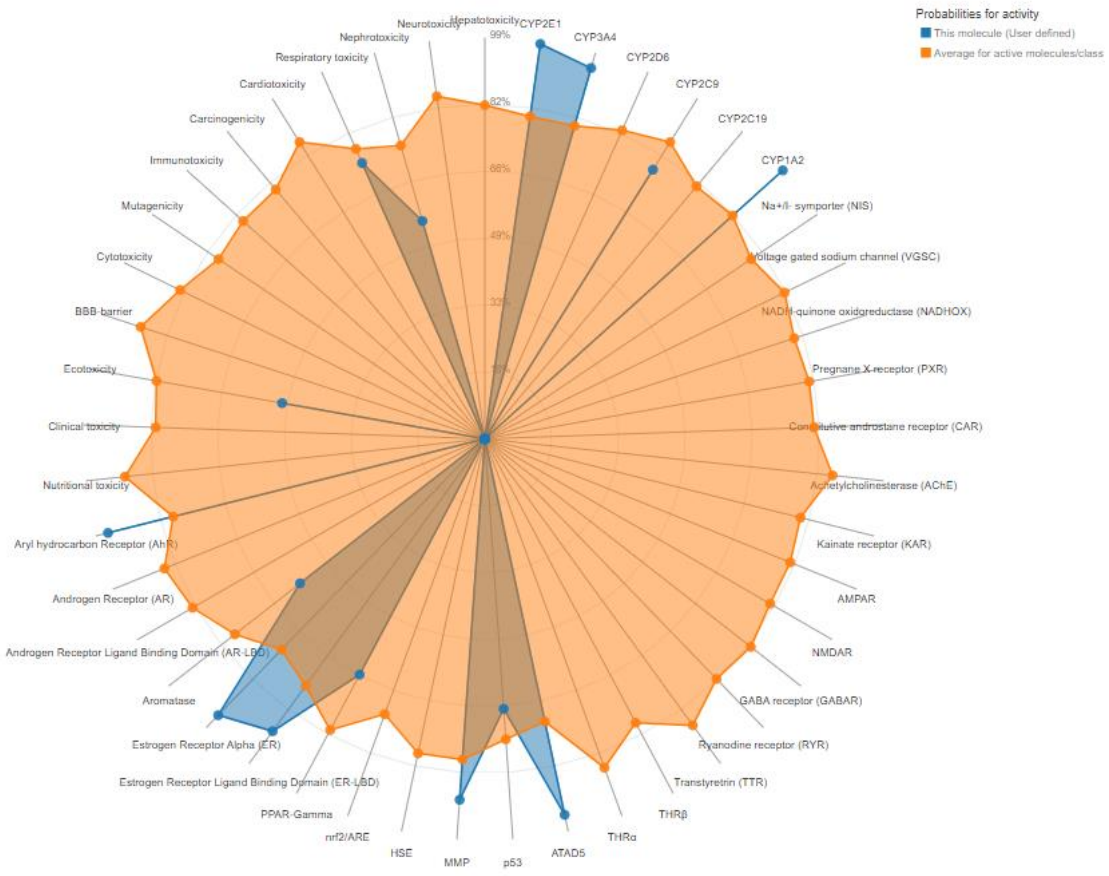

The network card

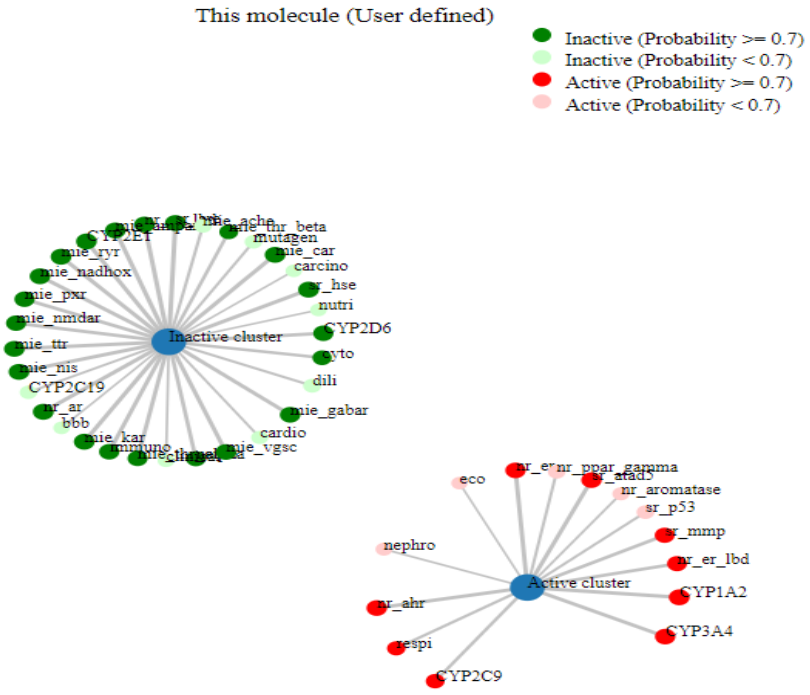
This molecule (User defined)
Inactive (Probability >= 0.7)
Inactive (Probability < 0.7)
Active (Probability >= 0.7)
Active (Probability < 0.7)
Inactive cluster
mie_ache
mutagen
mie_car
carcino
nr_hse
nutri
CYP2D6
cyto
dili
mie_gabar
cardio
mie_vgsc
mie_ryr
mie_nadhox
mie_pxr
mie_nmdar
mie_ttr
mie_nis
CYP2C19
nr_ar
bbb
mie_kar
Active cluster
nr_ppar_gamma
nr_aromatase
nr_p53
nr_mmp
nr_er_lbd
CYP1A2
CYP3A4
CYP2C9
respi
nr_ahr
nephro
eco